Analysis of Walking and Balancing Models Actuated and Controlled by Ankles

by

Jooeun Ahn

B.S. Mechanical Engineering
Seoul National University, 2001

Submitted to the Department of Mechanical Engineering
in Partial Fulfillment of the Requirement for the Degree of
Master of Science in Mechanical Engineering

at the

Massachusetts Institute of Technology

September 2006

Signature of Author . . . . . .
Department of Mechanical Engineering
August 7, 2006

Certified by. . . . . .
Neville Hogan
Professor of Mechanical Engineering and Professor of Brain and Cognitive Sciences
Thesis Supervisor

Accepted by. . . . . .
Lallit Anand
Chairman, Department Committee on Graduate Students

Analysis of Walking and Balancing Models Actuated and Controlled by Ankles

by

Jooeun Ahn

Submitted to the Department of Mechanical Engineering
on August 11 2006, in partial fulfillment of the requirements
for the degree of Master of Science in Mechanical Engineering

Abstract

Experimental data show that ankle torque is the most important actuator in normal human locomotion. I investigate the dynamics of simple models actuated by ankles alone. To assess the contribution of ankle actuation to locomotion, I first analyze the dynamics of some passive walkers without any joint torque. These passive walkers include a rimless wheel model and springy-legged models with and without a double stance phase. I analyze the stability of the period-one gait of each passive walker to compare it with the stability of the period-one gait of an ankle actuated model. Subsequently, I investigate whether balancing of a double inverted pendulum model whose shape and mass distribution are similar to a human can be achieved by control of ankle torque in a frontal plane. I study the dynamics of the model and design a controller that makes the model balance with biologically realistic ankle torque and a reasonable foot-floor friction coefficient. I conclude that an ankle-actuated model can make a stable period-one gait in a sagittal plane. Also, I deduce that the ankle torque control in a frontal plane can stabilize a double inverted pendulum model whose shape and mechanical properties are similar to those of humans.

Thesis Supervisor: Neville Hogan
Title: Professor of Mechanical Engineering and Professor of Brain and Cognitive Sciences

Acknowledgements

First and foremost, I express my deepest gratitude to my advisor, Professor Neville Hogan. He has given me key advice on how to start my own study. He has also given me detailed advice to improve the way how I develop my argument. All his advice has made it possible for me to make the first step in my field.

Much thanks also to everyone in the Newman Laboratory. In particular, I would like to express a lot of thanks to Doctor Hermano Igo Krebs. He has pointed out important questions to be clarified and encouraged me to do my work with great pleasure. I also owe much thanks to Steven Knight Charles who helped me most to accustom myself to the new environment. Also, my thanks go to Anindo Roy, Josh Young and Laura DiPietro who supported me by giving advice or encouragement. I also want to mention Shelly Levy-Tzedek, Ryan A Griffin, Nevan Hanumara, Lorenzo Masia, and Marjorie A. Joss who helped me kindly to join the amazing laboratory.

I must mention two friends of mine. Jaehyung and Yoonhwan's friendship during the last winter has supported me so that I can regenerate myself to make my first step. I give my thanks to them for being my constant supporters.

Last, but definitely not least, my family has been the most significant source of love and encouragement. I thank my parents, my lovely wife and my sister for their incredible support. Also, warm hearted affections from my father in law and mother in law have supported me. Words cannot begin to explain my gratitude and love for all of my family.

Contents

List of Figures

List of Tables

1. Introduction

1.1. Motivation and Goals

Some recent developments in rehabilitation techniques in locomotion have turned out to be effective [1]. However, some rehabilitation techniques can be not only effective but also efficient in terms of price or efforts. Efficiency may be achieved by focusing on the recovery of the movement of a specific joint rather than trying to improve the movement of all the joints participating in locomotion. One good starting point is the ankle joint because the ankle is known as the most important actuator in propulsion, in terms of the amount of torque [2]. In this thesis, I establish models actuated or controlled by ankles to provide theoretical fundamentals to assess the effectiveness of rehabilitation therapy focusing on ankles.

Many aspects of bipedal locomotion have been widely studied. Some researchers have analyzed normal gait by solving inverse dynamics [3]. They have measured joint angles and ground reaction forces, so the amount of torque of each joint can be estimated from the measured data. A robot might generate generic human bipedal locomotion by following the command of the solved torque at each joint. Other researchers have studied human locomotion by designing and testing simple walking machines compared to humans in terms of morphology, gait appearance and energy use [4]. These simple machines fundamentally depend on passive dynamics. Only very simple control is used compared to bipedal walking robots following the solved inverse dynamics of a human gait. The former approach, which uses inverse dynamics, might generate more humanlike or elaborated bipedal walking. In contrast, the latter approach provides more clues to what dynamics bipedal walking involves.

However, the contribution of each joint torque in terms of forward dynamics has not been

fully studied. Particularly, related to rehabilitation therapy, though some groups have developed therapeutic robots for locomotion by imposing kinematic patterns of leg motion [1], this approach ignores the probable role of dynamics in human locomotion.

The Newman Laboratory for Biomechanics and Human Rehabilitation at the Massachusetts Institute of Technology (MIT) has shown the value of therapeutic robots for upper-extremity rehabilitation [5-9]. Recently, the Newman Laboratory has also developed a two-degree of freedom therapy robot module for the ankle [10]. My analysis in this thesis can provide a basis to assess whether and how such a robot module for the ankle may be used for locomotor rehabilitation by investigating the dynamics of a simple model actuated and controlled by ankles.

My study in this thesis consists of two parts—locomotion in a sagittal plane and balancing in a frontal plane. The main motivation of the analysis of the ankle actuated walking model in a sagittal plane is based on two aspects. On the one hand, experimental data show that ankle torque is larger than knee torque or hip torque during walking [2]. On the other hand, some totally passive walkers can generate stable bipedal gait on a slight slope [11], but they cannot make a stable gait on a horizontal floor. If the ankle torque is the most significant contributor to locomotion not only in terms of the amount of torque but also in terms of dynamical behavior, one can expect the existence of a stable gait even on a horizontal floor with only ankle actuation.

In particular, I confine my analysis to the existence of a stable period-one gait with actuation of ankles alone. Period-one gaits are the gaits in which a walker recovers its state exactly after one step. There can also be multi-period gaits that show periodicity with the period of two or more steps. In locomotion of animals including humans, these multi-period asymmetric gaits are also common and physically meaningful. However, at this stage, I focus only on the period-one gait that is the most common, basic, and therefore most important mode of normal periodic gait.

Analyzing the contribution of ankle torque in a frontal plane to balancing with one foot or walking is another important problem. One way to assess the role of ankle torque in a frontal plane is to investigate the dynamics of a model controlled by a single joint alone. If a model whose shape and mechanical properties are similar to those of humans succeeds to balance with one foot using ankle torque control alone, it can support the idea that human balancing in a frontal plane can be achieved with some ankle control and negligible hip control. Accordingly, the success of the model can support rehabilitation strategies focusing on ankle torque in a frontal plane rather than other strategies involving both hip and ankles. With this motivation, I establish a double inverted pendulum model controlled by ankle torque and investigate the controllability and dynamics of the model.

In summary, this study can provide a theoretical basis on which one can develop or improve hardware or algorithms for assistance at the ankle to help recovery of locomotion or balancing after neurological or orthopedic injury. Considering efficiency, rehabilitation therapy focusing on ankles may be less expensive than prior therapies treating all the joints participating in walking or balancing. More basically, apart from efficiency of the therapy, this research can provide a further understanding of the dynamics of bipedal walking. Particularly, the contribution of ankle actuation to bipedal locomotion in a sagittal plane is evaluated through this study. Additionally, the contribution of ankle torque control to balancing in a frontal plane is studied.

1.2. Thesis Organization by Chapters

I describe my analysis of the dynamics of passive walkers in a sagittal plane in chapter 2, 3 and 4: analysis of the motion of a rimless wheel is described in chapter 2; analysis of the motion of a springy legged model without double stance phase is described in chapter 3; and, analysis of the

motion of a springy legged model with double stance phase is described in chapter 4.

Subsequently, I present my analysis of the ankle actuated model in chapter 5. With the understanding of the dynamics of the preceding passive walkers in chapter 2, 3 and 4, I establish a simple model with actuated ankles and analyze the dynamics of the model in a sagittal plane.

In addition, I analyze balancing in a frontal plane with one foot using ankle torque in chapter 6. I make a double inverted pendulum model whose mechanical properties and geometries are similar to those of a human and study the dynamics of the model controlled by one joint representing an ankle.

Finally, I summarize the results and discuss the conclusions and implications in chapter 7. Future directions of the research are also discussed. For readers' information, the source codes that I used and other supplementary contents are attached in the Appendix.

1.3. Terminology and Notation

Throughout the rest of this thesis, I use the terminology of a ***stride function*** and the following notation for expression of vectors, time, evolution rules and discrete maps.

1.3.1. A Stride Function and a Poincaré Map

Tad McGeer introduced the ***stride function*** whose input and output are the state variables such as angles of joints and their derivatives at the beginning of one step and at the beginning of the next step respectively. I extend the concept of the stride function suggested by McGeer by including leg length and their derivatives in the input and output of the stride function for springy legged models. The motion of a walking model can be expressed as a set of equations of motion,

which usually take the form of differential equations. The solution of the equations can provide a map whose input and output are the state vectors of the beginning of one step and the end of the step respectively. Separated from the set of equations of motion, there is another map whose input and output are the state vectors of the end of one step and the beginning of the following step respectively. The combination of two maps can be considered as a kind of stride function **f**. In the language of dynamical systems, the stride function can be considered as a discrete Poincaré map.

1.3.2. Vector Notation

I use bold print to describe a vector. In addition, without specific definition, **i**, **j** and **k** represent the unit vectors in positive x, y and z direction respectively. For example,

$$\mathbf{a} = \vec{a} = a_x\vec{i} + a_y\vec{j} + a_z\vec{k} = a_x\mathbf{i} + a_y\mathbf{j} + a_z\mathbf{k} \,. \qquad \text{Eq 1-1}$$

Also, without specific definition, the same character that is not written in bold print represents the magnitude of the vector that is indicated by the bold print of the character. For example, a means the magnitude of the vector **a**. In particular, without specific definitions, the characters with subscript x, y and z indicate the magnitudes of components of the corresponding vector in positive x, y and z directions respectively. For example, $a_x = \vec{a} \bullet \mathbf{i}$ in Eq 1-1.

1.3.3. Time Notation

Without specific definition, T_- and T_+ represent the time just before and right after time T respectively. T_- and T_+ are infinitesimally close to time T when an event occurs.

1.3.4. Notation for Maps and Evolution Rules

Without specific definition, italic print such as f, for example, represents an evolution rule of a continuous dynamical system, which might be another expression of a set of equations of motion. Sometimes, italic print such as f, for example, can also represent a simple scalar function. On the other hand, bold print such as **f**, for example, represents a discrete mapping.

1.4. Method of Stability Analysis

Stability of the gait of each model is of great importance in this study. As explained in 1.3.1, each step can be considered as a stride function or a Poincaré map whose input and output are some of the state variables at the beginning of one step and the beginning of the following step respectively. A proper set of state variables generating the period-one gait becomes a fixed point of the stride function. To analyze stability of the period-one gaits, if any, I perform stability analyses by following three steps: (1) I find the fixed points of the Poincaré map, if any, which generate the period-one gaits; (2) I analyze the stability by investigating the eigenvalues of the derivative matrix of the Poincaré map at the fixed points; and, (3) I visualize the stability or instability by showing the behavior of the small neighborhood of each fixed point.

1.4.1. Poincaré Section and the Reduced State Vector

A Poincaré map can be constructed by choosing a proper Poincaré section [12]. A Poincaré section is a local cross section in the state space. The dimension of the Poincaré section is reduced by one from the original dimension of the state space. A simple visualization is introduced by an example shown in Figure 1-1. Generally, the Poincaré section could be any

section, not necessarily aligned with the state space axes. Furthermore, the Poincaré section needs not to be planar as long as every flow generated by the evolution rule is transverse to it. In the special cases of my study, I set the Poincaré section by simply fixing one state variable for each model as in Figure 1-1.

In this study, the selection of the Poincaré section is crucial because the Poincaré section acts as an anchor indicating a completion of a step. For example, if I choose the angle between the legs as a state variable fixed at the Poincaré section, which indicates the end of one step for a springy legged model, a problem occurs; if the leg length does not recover its initial value at the moment when the angle recovers its initial value, the initial leg length of the following step becomes different from the initial leg length of the preceding step. Then, the energy stored in springy legs can be different at the beginning of each step, which is not desirable.

Hereafter, without specific definition, I define the state vector with reduced dimension that is restricted to the Poincaré section as the ***reduced state vector*** and express it as a vector with hat. Please see Figure 1-1. With a Poincaré section Σ, I can define a Poincaré map $\mathbf{f}$ as $\mathbf{f}: \Sigma \to \Sigma$; $\hat{\mathbf{x}}_{k+1} = \mathbf{f}(\hat{\mathbf{x}}_k)$, where $\hat{\mathbf{x}} \in \Sigma$.

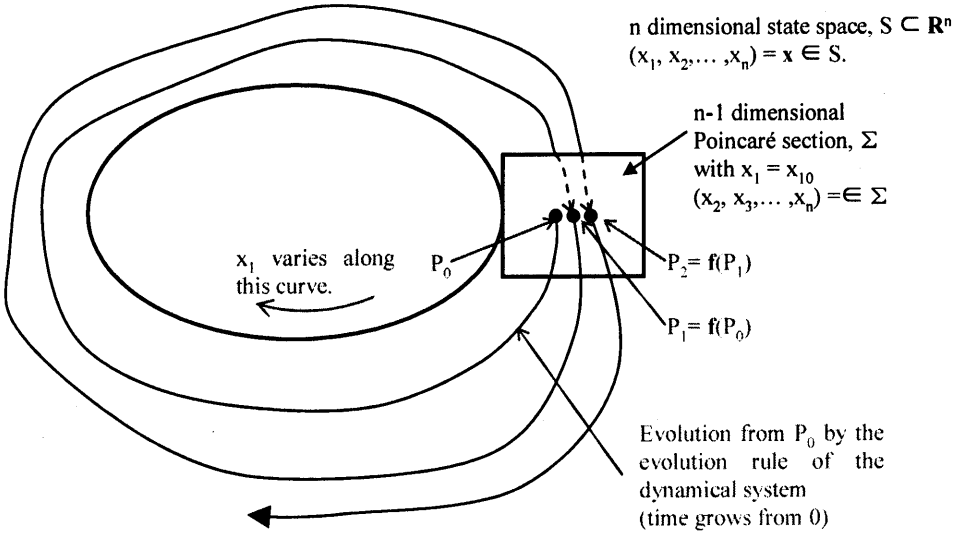

Figure 1-1: A schematic explanation of Poincaré section

1.4.2. Stability and Asymptotic Stability

Stability and asymptotic stability of a fixed point of a discrete map can be defined as the following:

Definition 1 Let $\hat{\mathbf{x}} = \hat{\mathbf{x}}_{eq}$ be a fixed point of a discrete map $\hat{\mathbf{x}}_{k+1} = \mathbf{f}(\hat{\mathbf{x}}_k)$. In other words, $\hat{\mathbf{x}}_{eq} = \mathbf{f}(\hat{\mathbf{x}}_{eq})$. The fixed point $\hat{\mathbf{x}} = \hat{\mathbf{x}}_{eq}$ is ***stable*** when for $\forall \varepsilon > 0$ and $\forall n \in \mathbf{N}$, which is the set of positive integers, $\exists\ \delta = \delta(\varepsilon) > 0$, such that for $\forall\ \hat{\mathbf{x}}_0$, $\left|\hat{\mathbf{x}}_0 - \hat{\mathbf{x}}_{eq}\right| < \delta$, we have $\left|\mathbf{f}^n(\hat{\mathbf{x}}_0) - \hat{\mathbf{x}}_{eq}\right| < \varepsilon$.

Definition 2 Let $\hat{\mathbf{x}} = \hat{\mathbf{x}}_{eq}$ be a fixed point of a discrete map $\hat{\mathbf{x}}_{k+1} = \mathbf{f}(\hat{\mathbf{x}}_k)$. The fixed point $\hat{\mathbf{x}} = \hat{\mathbf{x}}_{eq}$ is ***asymptotically stable*** when $\hat{\mathbf{x}} = \hat{\mathbf{x}}_{eq}$ is stable and $\exists\ \delta = \delta(\varepsilon) > 0$ such that for $\forall\ \hat{\mathbf{x}}_0$, $\left|\hat{\mathbf{x}}_0 - \hat{\mathbf{x}}_{eq}\right| < \delta$, we have $\left|\mathbf{f}^n(\hat{\mathbf{x}}_0) - \hat{\mathbf{x}}_{eq}\right|$ go to zero as n goes to ∞.

1.4.3. Stability Analysis Using Linearization

Once I consider each step as a Poincaré map whose input and output are the reduced state vectors, $\hat{\mathbf{x}}$'s, at the beginning of one step and the following step respectively, the dynamical system corresponding to each model becomes a discrete dynamical system or a discrete map.

One way to investigate the stability of a fixed point of a map is using linearization, which is conclusive for ***hyperbolic*** fixed points [12]. Let $\hat{\mathbf{x}} = \hat{\mathbf{x}}_{eq} + \xi$, where $\hat{\mathbf{x}}_{eq}$ is a fixed point of a map $\mathbf{f}$, and ξ be a vector indicating a very small error. If (1) the derivative matrix of the map $\mathbf{f}$ exists, and (2) the fixed point is hyperbolic, then,

$$\mathbf{f}(\hat{\mathbf{x}}) = \mathbf{f}(\hat{\mathbf{x}}_{eq} + \xi) = \mathbf{f}(\hat{\mathbf{x}}_{eq}) + \frac{\partial \mathbf{f}}{\partial \hat{\mathbf{x}}}\xi + O(\xi^2)$$

$$\Rightarrow \mathbf{f}(\hat{\mathbf{x}}) - \mathbf{f}(\hat{\mathbf{x}}_{eq}) \cong \frac{\partial \mathbf{f}}{\partial \hat{\mathbf{x}}}\xi.$$

Hence, in cases that (1) and (2) above are met, stability analysis can be performed by investigating eigenvalues of the derivative matrix $\mathbf{J}(\hat{\mathbf{x}})$ at the fixed point, where $\mathbf{J} = \frac{\partial \mathbf{f}}{\partial \hat{\mathbf{x}}}$. If all the eigenvalues of this derivative matrix are located within a unit circle in a complex plane, the system is asymptotically stable. If there is at least one eigenvalue outside the unit circle, the system is unstable. If the largest magnitude of the eigenvalues is equal to one, the system is non-hyperbolic and the stability analysis by linearization is no longer conclusive.

In each of the models I analyze, the derivative matrix of the Poincaré map exists and the investigated fixed point is hyperbolic. Therefore, stability analysis using linearization is conclusive in the cases of models I analyze in this thesis. A brief proof of the existence of the derivative matrices of the Poincaré maps of the analyzed models is derived in Appendix A. The analyses in Chapters 2-5 will help readers to fully understand the proof in Appendix A.

2. A Rimless Wheel Model in a Vertical Plane

To understand the dynamics of a passive walker, I select a rimless spoked wheel model that is constrained in a vertical plane as a starting point. This model is considered as a proper starting point not only because it is simple but also because it captures many of the essential behaviors of bipedal walking. This model imitates foot collision due to foot placement and the inverted-pendulum motion of the single stance phase of bipedal walking. Some prior work has been done analyzing this model in several ways [11, 13].

I analyze the dynamics of the model on a horizontal floor and on a slight slope. I show that the rimless wheel loses kinetic energy with a constant reduction ratio per collision, and the rimless wheel on a slight slope can make a stable period-one gait with some proper initial condition and selected parameter values.

2.1. Analysis of the Model on a Horizontal Floor

2.1.1. Assumptions and Definitions of Parameters

A point mass moves in a vertical plane under the influence of gravity, restrained by a rigid massless leg that rests on the ground but can instantaneously be moved in front of the mass. One way to visualize this model is to imagine a wheel with radial spokes and no rim. The spokes have no mass and wheel has mass but no moment of inertia.

For the definitions of parameters and the coordinate axes, see Figure 2-1. The angle θ is defined by the orientation of the stance leg.

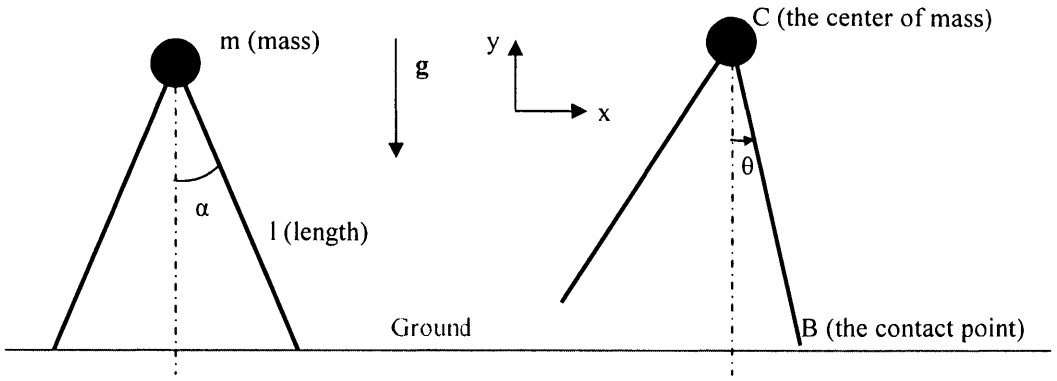

Figure 2-1: A rimless wheel model on a horizontal floor; α is the initial value of θ

2.1.2. Analysis of Speed of the Point Mass

Let the vector forms of **H, M, r,** v and **P** indicate angular momentum, applied torque about a specific point, a position vector from one point to another, a velocity vector and linear momentum respectively.

Figure 2-2 shows the motion of the rimless wheel. The point mass moves as an inverted pendulum, and the leg collides with the ground at point B at time $t = t_0$. For the analysis, I divide the dynamic process into two parts: the collision and the phase between collisions.

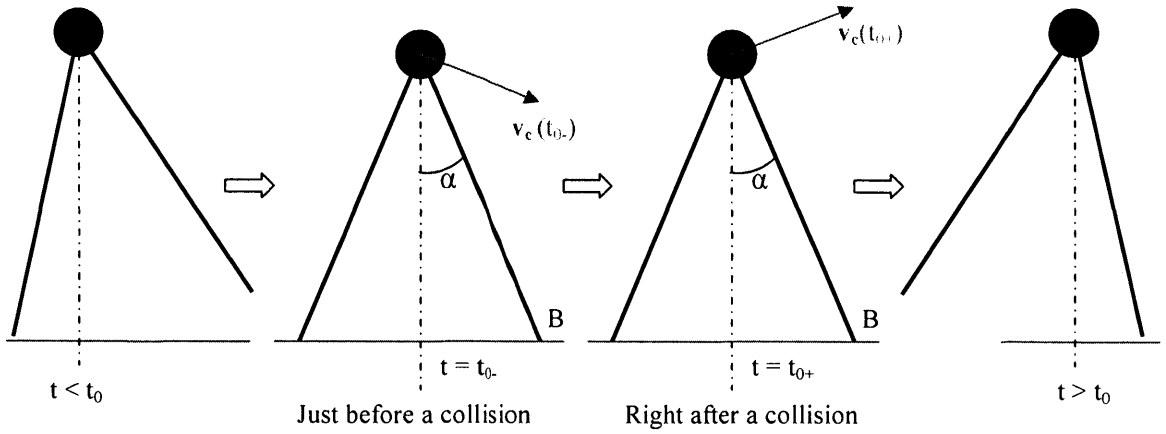

Figure 2-2 : The motion of the rimless wheel; a collision occurs at point B

Part 1 – The Collision ($t_{0-} \rightarrow t_{0+}$)

The free body diagram (FBD) of the system is shown in Figure 2-3. The impulsive ground reaction force (GRF) is the only contact force. To avoid considering this impulsive force, which is relatively difficult to characterize, I apply the angular momentum principle about point B in Figure 2-3 so that the torque due to the impulsive force is zero. By the angular momentum principle about B,

$$\frac{d}{dt}\overrightarrow{H_B} + \vec{v}_B \times \vec{P} = \overrightarrow{M_B} = \overrightarrow{r_{BC}} \times m\vec{g} \,. \qquad \text{Eq 2-1}$$

Because the velocity of point B is zero, the second term on the left hand side of Eq 2-1 vanishes, and

$$\overrightarrow{H_B}(t_{0+}) - \overrightarrow{H_B}(t_{0-}) = \int_{0-}^{t_{0+}} (\overrightarrow{r_{BC}} \times m\vec{g})dt \,. \qquad \text{Eq 2-2}$$

The right hand side of Eq 2-2 equals zero because the time gap between t_{0+} and t_{0-} goes to zero, and the integrated term is not impulsive. Therefore, the angular momentum about point B is conserved during the collision, and

$$\overrightarrow{H_B}(t_{0+}) = \overrightarrow{H_B}(t_{0-}) \,. \qquad \text{Eq 2-3}$$

With the assumption that the model finishes its inverted pendulum motion at t_{0-} and starts a new inverted pendulum motion about B at t_{0+}, the velocity $\mathbf{v}_c$ at $t = t_0$ can be written

$$\overrightarrow{v_c}(t_{0-}) = \overrightarrow{v_0} = (v_o \cos\alpha)\vec{i} - (v_o \sin\alpha)\vec{j} \,, \text{ and}$$

$$\overrightarrow{v_c}(t_{0+}) = \overrightarrow{v_1} = (v_1 \cos\alpha)\vec{i} + (v_1 \sin\alpha)\vec{j} \,, \qquad \text{Eq 2-4}$$

where $\vec{i}$ and $\vec{j}$ are the unit vectors directing +x axis and +y axis respectively. From Eq 2-3 and Eq 2-4,

$$\overrightarrow{r_{BC}} \times \overrightarrow{mv_1} = \overrightarrow{H_B(t_{0+})} = \overrightarrow{H_B(t_{0-})} = \overrightarrow{r_{BC}} \times \overrightarrow{mv_0}, \text{ or}$$

$$-(mlv_1)\vec{k} = mlv_0(\sin^2\alpha - \cos^2\alpha)\vec{k} = -(mlv_0\cos 2\alpha)\vec{k}, \qquad \text{Eq 2-5}$$

where $\vec{k}$ is the unit vector in the direction of +z axis. Finally, by comparing the magnitude of the left hand side and the right hand side of Eq 2-5,

$$v_1 = v_0\cos 2\alpha. \qquad \text{Eq 2-6}$$

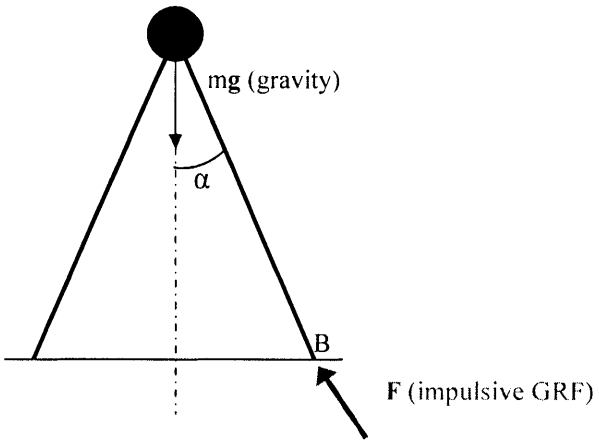

Figure 2-3: The free body diagram of the rimless wheel at a collision

Part 2 – The Phase between Collisions

The free body diagram (FBD) of the system is shown in Figure 2-4. By the assumption of massless legs, force **F**, which is the ground reaction force (GRF), must be directed toward point C in Figure 2-4. In other words, force **F** is always parallel with the position vector $\mathbf{r}_{BC}$. The consequence of the parallel direction of **F** with $\mathbf{r}_{BC}$ is this: when I analyze the motion of the inverted pendulum by decomposing it into the tangential and normal directions, there is no contact force applied in the tangential direction. Hereafter, I refer to this fact as ⓐ. Also, force F does no

work during the inverted pendulum motion because point B, as shown in Figure 2-4, does not move. I refer to this fact as ⓑ. I will depend on facts ⓐ and ⓑ to find the critical values of the initial speed.

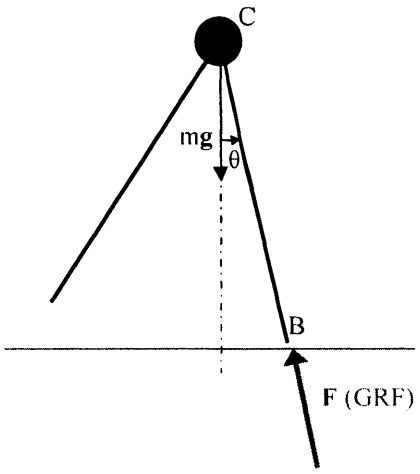

Figure 2-4: The free body diagram of the rimless wheel between collisions

Minimum Speed for the System to Make the Next Step

I investigate the critical speed v_{1Cr} or v_{0Cr} that makes the velocity zero at the apex ($\theta = 0$) after the collision. If the initial speed is less than this critical value, the rimless wheel cannot vault over and cannot make the next step.

Because of ⓑ, the only working force applied to the system is gravity, which is a conservative force. Therefore, the total mechanical energy of the system is conserved between collisions. If $v_1 = v_{1Cr}$, the total mechanical energy becomes $\frac{1}{2}mv_{1Cr}^2 + 0 = 0 + mgl(1-\cos\alpha)$, and v_{1Cr} is obtained as

$$v_{1Cr} = \sqrt{2gl(1-\cos\alpha)}\,. \qquad \text{Eq 2-7}$$

In terms of v_0, the minimum speed that makes the model vault over is

$$v_{0Cr} = \frac{\sqrt{2gl(1-\cos\alpha)}}{\cos 2\alpha}. \qquad \text{Eq 2-8}$$

Maximum Speed for the System Not to Leave the Floor

With the assumption that the model starts a new inverted pendulum motion about point B in Figure 2-4, I establish the equation of motion in the normal and the tangential components; see Figure 2-5. For any motion, the acceleration can be decomposed into two components: one is the tangential component, and the other is the normal component. If I define the radius of curvature as ρ, then,

$$\frac{d}{dt}\vec{v} = \frac{dv}{dt}\vec{e_t} + \frac{v^2}{\rho}\vec{e_n}. \qquad \text{Eq 2-9}$$

Hence, the equation of motion of the rimless wheel becomes

$$\begin{aligned} m\frac{d}{dt}\vec{v} &= m\frac{dv}{dt}\vec{e_t} + m\frac{v^2}{l}\vec{e_n} \\ &= m\vec{g} + \vec{F} = mg\cos\theta\vec{e_n} - mg\sin\theta\vec{e_t} - F\vec{e_n} \\ &= -mg\sin\theta\vec{e_t} + (mg\cos\theta - F)\vec{e_n}. \end{aligned} \qquad \text{Eq 2-10}$$

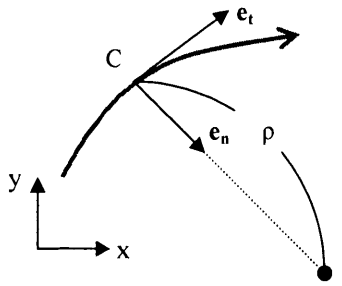

Figure 2-5: The vector components in the normal and the tangential directions

To investigate the maximum speed for the system not to leave the floor, I confine my interest to the normal component only. Extracting the normal components from Eq 2-10,

$$m\frac{v^2}{l} = mg\cos\theta - F \Rightarrow F = mg\cos\theta - m\frac{v^2}{l} = f(\theta). \qquad \text{Eq 2-11}$$

Let the right hand side of Eq 2-11 be $f(\theta)$. Physically, leaving the floor indicates zero magnitude of **F** (GRF) in Figure 2-4. Hence, to keep the model attached on the floor, I must keep the minimum of $f(\theta)$ above zero.

By conservation of mechanical energy during the inverted pendulum motion, the kinetic energy reaches the maximum when the point mass is at the lowest position in y. Therefore, v^2 reaches the maximum when $\theta = -\alpha$ or $+\alpha$. Also, $\cos\theta$ becomes the minimum when $\theta = -\alpha$ or $+\alpha$ ($-\pi/2 < -\alpha < \theta < \alpha < \pi/2$). As a result, $f(\theta)$ becomes the minimum when $\theta = -\alpha$ or $+\alpha$, and I need

$$\min(F) = mg\cos\alpha - m\frac{v_1^2}{l} = mg\cos\alpha - m\frac{(\cos^2 2\alpha)v_0^2}{l} \geq 0, \text{ or}$$

$$v_0 \leq \frac{\sqrt{gl\cos\alpha}}{\cos 2\alpha}. \qquad \text{Eq 2-12}$$

Considering that the speed is reduced by the factor of $\cos2\alpha$ due to the collision, it is more meaningful to find the maximum initial speed in pure x direction that keeps the wheel from flying off. The maximum initial speed can be obtained by the same procedure, resulting in

$$v_0 \leq \frac{\sqrt{gl\cos\alpha}}{\cos\alpha} = \sqrt{\frac{gl}{\cos\alpha}}. \qquad \text{Eq 2-13}$$

2.1.3. Further Analysis

The Range of α

Eq 2-8 implies that if $\alpha = \pi/4$, the model can never vault over regardless of the initial speed. This result makes sense physically. If $\alpha = \pi/4$, the direction of the ground reaction force is exactly

opposite to the direction of the momentum. Therefore, the point mass cannot use its momentum to vault over; see Figure 2-6.

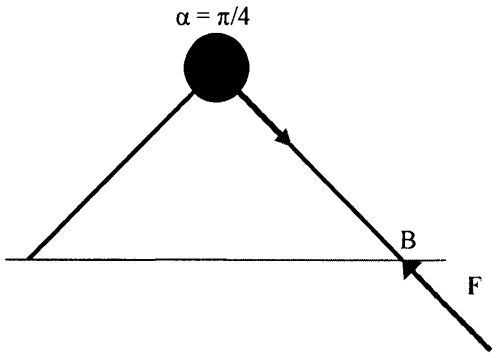

Figure 2-6: The rimless wheel model with $\alpha = \pi/4$

If $\alpha > \pi/4$, Eq 2-8 yields a meaningless result, indicating that there exists some negative speed that can make the model vault over. By confining the range of α to $(0, \pi/4)$, which is also reasonable for human bipedal walking, I can preclude such misleading solutions.

From Eq 2-8 and Eq 2-12, it is suggested that the initial speed v_0 must satisfy $\frac{\sqrt{2gl(1-\cos\alpha)}}{\cos 2\alpha} < v_0 < \frac{\sqrt{gl\cos\alpha}}{\cos 2\alpha}$ for the model to generate a reasonable gait. This inequality has meaning only when $\sqrt{2gl(1-\cos\alpha)} < \sqrt{gl\cos\alpha}$, or $\cos\alpha > 2/3$, which means $0<\alpha<0.84$. This range includes $(0, \pi/4)$. Therefore, I can confine my interest to the case of $\alpha \in (0, \pi/4)$.

Mechanical Energy Loss per Step

Eq 2-6 implies that the kinetic energy of the system, which is proportional to v^2, is reduced by a factor of $\cos^2 2\alpha$ per collision. Therefore, energy loss at a collision increases as the angle α

increases. In contrast, mechanical energy is conserved during the inverted pendulum motion.

Consequently, the energy is lost per step, and there is no way to compensate for the lost energy. Therefore, any periodic gaits cannot be observed in this model. After finite steps, the rimless wheel on a horizontal floor cannot vault over, and it fails to make the next step.

2.2. Analysis of the Model on a Slight Slope

2.2.1. Assumptions and Definitions of Parameters

A point mass moves in a vertical plane under the influence of gravity, restrained by a rigid massless leg that rests on the ground but can instantaneously be moved in front of the mass. The model is placed on a slight slope so that gravity can do work on each step. For the definitions of parameters and the coordinate axes, see Figure 2-7. I assume that α is greater than γ. The angle θ is defined by the orientation of the stance leg.

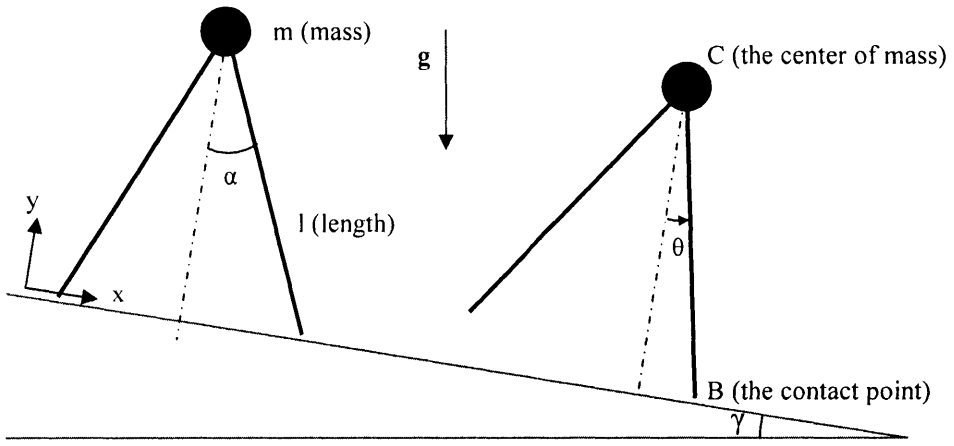

Figure 2-7: A rimless wheel model on a slight slope; γ is the slope angle

2.2.2. Analysis of Speed of the Point Mass

The meaning of **H, M, r, v** and **P** is consistent with the meaning of **H, M, r, v** and **P** in 2.1.2. See Figure 2-7. The point mass moves as an inverted pendulum, and the leg collides with the ground at point B at time $t = t_0$. For the analysis, I divide the dynamic process into two parts: the collision and the phase between collisions.

Part 1 – The Collision ($t_{0-} \rightarrow t_{0+}$)

By the same procedure as in 2.1.2,

$$\overrightarrow{H_B}(t_{0+}) = \overrightarrow{H_B}(t_{0-}). \qquad \text{Eq 2-14}$$

In other words, the angular momentum about point B in Figure 2-7 is conserved during the collision.

With the assumption that the model finishes its inverted pendulum motion at $t_{0-}$and starts a new inverted pendulum motion about point B in Figure 2-7 at t_{0+}, the velocity v_c at $t = t_0$ can be written

$$\overrightarrow{v_c}(t_{0-}) = \overrightarrow{v_0} = (v_o \cos\alpha)\vec{i} - (v_o \sin\alpha)\vec{j}, \text{ and}$$

$$\overrightarrow{v_c}(t_{0+}) = \overrightarrow{v_1} = (v_1 \cos\alpha)\vec{i} + (v_1 \sin\alpha)\vec{j}, \qquad \text{Eq 2-15}$$

where $\vec{i}$ and $\vec{j}$ are the unit vectors directing +x axis and +y axis respectively. From Eq 2-14 and Eq 2-15,

$$\overrightarrow{r_{BC}} \times m\overrightarrow{v_1} = \overrightarrow{H_B}(t_{0+}) = \overrightarrow{H_B}(t_{0-}) = \overrightarrow{r_{BC}} \times m\overrightarrow{v_0}, \text{ or}$$

$$-(mlv_1)\vec{k} = mlv_0(\sin^2\alpha - \cos^2\alpha)\vec{k} = -(mlv_0 \cos 2\alpha)\vec{k}, \qquad \text{Eq 2-16}$$

where $\vec{k}$ is the unit vector directed along the +z axis. Finally, by comparing the magnitude of the left hand side and the right hand side of Eq 2-16,

$$v_1 = v_0 \cos 2\alpha \,. \qquad \text{Eq 2-17}$$

This is the same result as Eq 2-6 of 2.1.2 .

Part 2 – The Phase between Collisions

The free body diagram (FBD) of the system is shown in Figure 2-8. Note that gravity applies in an oblique direction because the x axis in Figure 2-8 is parallel with the surface of the slope. As mentioned in 2.1.2, **F** (GRF) must be directed toward C all the time. In other words, force **F** is always parallel with the position vector $\mathbf{r}_{BC}$. Also, point B does not move during the phase between collisions. Therefore, ⓐ and ⓑ in 2.1.2 still hold.

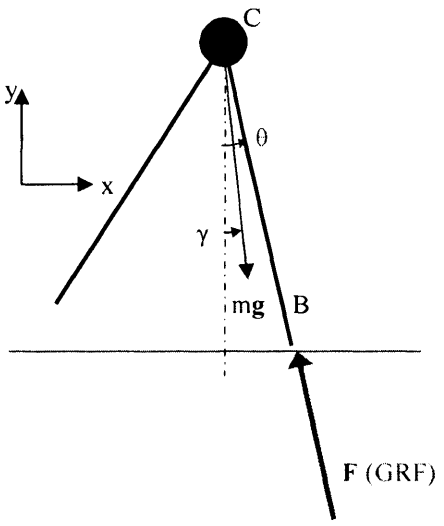

Figure 2-8: The free body diagram of the rimless wheel on a slope between collisions

Minimum Speed for the System to Make the Next Step

I investigate the critical speed v_{1Cr} or v_{0Cr} that makes the velocity zero at the apex ($\theta = 0$) after the collision. If the initial speed is less than this critical value, the rimless wheel cannot vault over and cannot make the next step. Due to ⓑ, the only working force applied to the system is

gravity, which is a conservative force. Therefore, the total mechanical energy of the system is conserved between collisions.

If $v_1 = v_{1Cr}$, the total mechanical energy becomes $\frac{1}{2}mv_{1Cr}^2 + 0 = 0 + mgl\{1-\cos(\alpha-\gamma)\}$,

and v_{1Cr} is obtained as

$$v_{1Cr} = \sqrt{2gl\{1-\cos(\alpha-\gamma)\}}\,. \qquad \text{Eq 2-18}$$

In terms of v_0, the minimum speed that makes the model vault over is

$$v_{0Cr} = \frac{\sqrt{2gl\{1-\cos(\alpha-\gamma)\}}}{\cos 2\alpha}. \qquad \text{Eq 2-19}$$

Maximum Speed for the System Not to Leave the Floor

I establish the equation of motion in the normal and the tangential components. The equation of motion becomes

$$\begin{aligned} m\frac{d}{dt}\vec{v} &= m\frac{dv}{dt}\vec{e_t} + m\frac{v^2}{l}\vec{e_n} \\ &= m\vec{g} + \vec{F} = mg\cos(\theta-\gamma)\vec{e_n} - mg\sin(\theta-\gamma)\vec{e_t} - F\vec{e_n} \\ &= -mg\sin(\theta-\gamma)\vec{e_t} + \{mg\cos(\theta-\gamma) - F\}\vec{e_n}. \end{aligned} \qquad \text{Eq 2-20}$$

To investigate the maximum speed for the system not to leave the floor, I confine my interest to the normal component only. Extracting the normal components from Eq 2-20,

$$m\frac{v^2}{l} = mg\cos(\theta-\gamma) - F \Rightarrow F = mg\cos(\theta-\gamma) - m\frac{v^2}{l} = h(\theta)\,. \qquad \text{Eq 2-21}$$

As explained in 2.1.2, to keep the model attached on the floor, I need to keep the minimum of $h(\theta)$ above zero.

By conservation of mechanical energy during the inverted pendulum motion between two specific collisions, the kinetic energy reaches the maximum at the moment of $\theta = -\alpha$ when the

potential energy becomes its minimum. Therefore, v^2 reaches the maximum when $\theta = -\alpha$. Also, assuming that $0 < \alpha < \pi/2$ and $0 < \gamma < \pi$, $\cos(\theta - \gamma)$ becomes the minimum when $\theta = -\alpha$. As a result, $h(\theta)$ becomes the minimum when $\theta = -\alpha$, and I need

$$\min(F) = mg\cos(\alpha+\gamma) - \frac{mv^2}{l}_{(\theta=-\alpha)} \geq 0. \qquad \text{Eq 2-22}$$

Because of ⓑ in 2.1.2, I can apply conservation of mechanical energy to find v^2 when $\theta = -\alpha$. Figure 2-9 shows that the work done by gravity per step can be written

$$W_{1\to 2} = m\vec{g} \bullet \overrightarrow{r_{12}} = 2mgl\sin\alpha\sin\gamma \quad . \qquad \text{Eq 2-23}$$

Then, from $\Delta\frac{1}{2}mv^2 = 2mgl\sin\alpha\sin\gamma$, Eq 2-22 and Eq 2-23,

$$\min(F) = mg\cos(\alpha+\gamma) - \frac{mv^2}{l}_{(\theta=-\alpha)} = mg\cos(\alpha+\gamma) - m\frac{(\cos^2 2\alpha)v_0^2 + 4gl\sin\alpha\sin\gamma}{l} \geq 0. \quad \text{Eq 2-24}$$

Therefore,

$$v_0 \leq \frac{\sqrt{gl\{\cos(\alpha+\gamma) - 4\sin\alpha\sin\gamma\}}}{\cos 2\alpha}. \qquad \text{Eq 2-25}$$

The maximum speed in the pure x direction that keeps the wheel from flying off can be obtained by the same procedures, resulting in

$$v_0 \leq \frac{\sqrt{gl\{\cos(\alpha+\gamma) - 4\sin\alpha\sin\gamma\}}}{\cos\alpha}. \qquad \text{Eq 2-26}$$

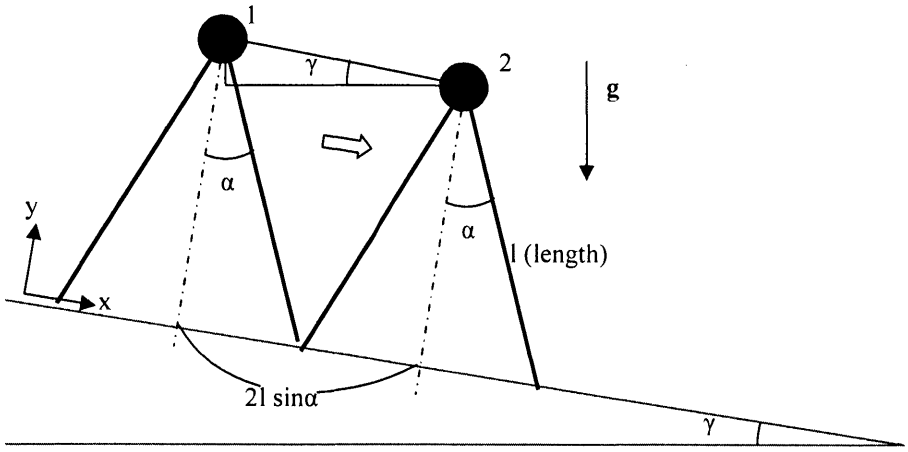

Figure 2-9: The rimless wheel on a slope at the beginning and at the ending of a step

The Range of α

From Eq 2-19 and Eq 2-25, it is suggested that the initial speed v_0 must satisfy

$$\frac{\sqrt{2gl\{1-\cos(\alpha-\gamma)\}}}{\cos 2\alpha} < v_0 < \frac{\sqrt{gl\{\cos(\alpha+\gamma)-4\sin\alpha\sin\gamma\}}}{\cos 2\alpha}.$$

This inequality has meaning only when $\sqrt{2gl\{1-\cos(\alpha-\gamma)\}} < \sqrt{gl\{\cos(\alpha+\gamma)-4\sin\alpha\sin\gamma\}}$, or $0 < 2-2\cos(\alpha-\gamma) < \cos(\alpha+\gamma)-4\sin\alpha\sin\gamma$. I confine my interest to the range of α in which α satisfies this inequality.

2.2.3. Existence of a Period-One Gait

The kinetic energy of the system, which is proportional to v^2, is reduced by the factor of $\cos^2 2\alpha$ per collision. However, it regains some kinetic energy during the inverted pendulum motion because gravity does non-zero work per step. Therefore, the kinetic energy may either increase or decrease throughout one step. Furthermore, it is possible that there exists a critical

case in which the kinetic energy at the end of one step is same as the kinetic energy at the end of the next step. The work done by gravity is obtained from Eq 2-23. To compensate for the loss of kinetic energy due to collision by the work done by gravity, I need

$$2mgl\sin\alpha\sin\gamma = \frac{1}{2}mv_0{}^2(1-\cos^2 2\alpha)\text{, or}$$

$$v_0{}^2 = \frac{4gl\sin\alpha\sin\gamma}{1-\cos^2 2\alpha} \quad . \qquad \text{Eq 2-27}$$

Therefore, some elaborately tuned initial velocity can make a period-one gait.

Each step can be considered as a stride function or a Poincaré map, and the state vector generating the period-one gait becomes a fixed point of the stride function. In this case, there exists a unique fixed point. One important issue is the stability of the fixed point. In the following sections, I investigate the stability of the fixed point in a qualitative and quantitative way.

2.2.4. Stability Analysis of the Period-One Gait

Qualitative Analysis

The period-one gait of the rimless wheel is expected to be stable. With enough but not excessive initial speed v_0, which is suggested in 2.2.2, the system obtains either increased or decreased speed at the end of an inverted pendulum motion; see Figure 2-9. Let KE1 be the kinetic energy at position 1 (just before the collision), and KE2 be the kinetic energy at position 2 (just before the collision). Suppose that KE1 is larger than the kinetic energy of the period-one gait at the same moment. Then, at the following collision, the system suffers greater loss than the case of the period-one gait because the reduction ratio is always $\cos^2 2\alpha$. Then, it becomes impossible for the work done by gravity to compensate for the loss of kinetic energy. Therefore,

KE2 becomes smaller than KE1. After repeating such progress for several steps, KE(n) becomes small enough that work done by gravity can compensate for the loss of kinetic energy. Then, the kinetic energy settles down at the kinetic energy of the period-one gait. Similar argument applies to the case in which KE1 is smaller than the initial kinetic energy of the period-one gait.

However, the asymptotic stability of the fixed point can be observed only when this system is guaranteed to vault over and not to fly off the slope at every step. In other words, at every collision, the speed just before the collision must be between the maximum and minimum speeds discussed in 2.2.2. For example, if the initial speed is so small that the system fails to vault over, it cannot show the stable period-one gait.

Quantitative Analysis

As mentioned in 1.4, I treat the stride function of each step as a Poincaré map and analyze the stability of the fixed point of the map. To construct the Poincaré map, I need to obtain the equation of motion of the system and express the dynamical system in state space representation. After constructing Poincaré map, I perform stability analysis by following three steps: (1) I find the fixed point of the Poincaré map that generates the period-one gait, which is already done in 2.2.3; (2) I confirm the asymptotic stability by investigating the eigenvalues of the derivative matrix of the Poincaré map at the fixed point; and, (3) I visualize the asymptotic stability by showing the behavior of the small neighborhood of the fixed point.

Equation of Motion

Please consult Figure 2-7 and Figure 2-8. As explained in 2.2.2, the speed reduces by the factor of $\cos 2\alpha$ during the collision. For the phase between collisions I can derive equations of motion using the Lagrangian approach. Note that the only constraint force is the ground reaction

force (GRF) that does no work by the assumption of fixed B. Therefore, the constraint is ideal. Also, the active force, gravity, is a conservative force. As a result, all non-potential generalized forces are zero.

Let L, T and V be the Lagrangian, kinetic energy and potential energy respectively.

$$L = T - V = \frac{1}{2} m(l\dot{\theta})^2 - mgl\cos(\theta - \gamma), \text{ and}$$

$$\frac{d}{dt}\frac{\partial L}{\partial \dot{\theta}} - \frac{\partial L}{\partial \theta} = 0 \Rightarrow \ddot{\theta} - \frac{g}{l}\sin(\theta - \gamma) = 0. \qquad \text{Eq 2-28}$$

Eq 2-28 is the equation of motion during the phase between collisions

Poincaré Section

Please see Figure 2-7. The angle θ is a generalized coordinate of this dynamical system. From Eq 2-28, the equation of motion is expressed in a second-order ordinary differential equation, and I need two state variables θ and dθ/dt to describe this dynamical system in state space. For this system, a completion of one step can be indicated by the value of θ; a step is regarded as completed when θ goes from α to -α. In other words, a proper Poincaré section is anchored at the sub-state space where θ becomes $\pm\alpha$. In conclusion, the Poincaré map corresponding to the stride function of this model is defined in the one dimensional Poincaré section Σ, which is

$$\Sigma = \{(\theta, \dot{\theta}) \,|\, \theta = \pm\alpha \quad \text{and} \quad \dot{\theta} \in \mathbf{R}\}.$$

Fixed Points of a Poincaré Map

As mentioned in 2.2.3, there is a unique fixed point of the rimless wheel on a slope with the initial speed of $v_0 = \sqrt{\frac{4gl\sin\alpha\sin\gamma}{1-\cos^2 2\alpha}}$. This initial speed makes constant kinetic energy at

every moment just before a collision, and the fixed point of the Poincaré map can be directly obtained from this initial speed.

Stability Analysis Using the Derivative Matrix of the Poincaré Map

I prove the existence of the derivative matrix of the the Poincaré map in Appendix A.1. Then, rigorous proof of asymptotic stability can be achieved by showing that all the eigenvalues of the derivative matrix of the Poincaré map stay inside a unit circle. With the selected Poincaré section, I construct the Poincaré map and its derivative matrix both analytically and numerically. Then, I investigate the eigenvalues of the derivative matrix at the fixed point both analytically and numerically.

With the definitions of $\mathbf{x} = \begin{pmatrix} x_1 \\ x_2 \end{pmatrix} = \begin{pmatrix} \theta \\ \dot{\theta} \end{pmatrix}$ and $\hat{\mathbf{x}} = (x_2) = (\dot{\theta})$, the numerical construction of the Poincaré map is performed as the following:

Step 1 Solve the obtained equation of motion (Eq 2-28) with a given initial condition.

Step 2 Find the minimal positive time when θ becomes -α, and define the time as T_f. T_f is the time when the collision occurs.

Step 4 Find the reduced state vector $\hat{\mathbf{X}} = (x_2) = (d\theta/dt)$ at T_{f-}, which is the time just before the collision

Step 5 Find the reduced state vector $\hat{\mathbf{X}} = (x_2) = (d\theta/dt)$ at T_{f+}, which is the time right after the collision. Using the result of analysis of the collision in 2.2.2, $\dot{\theta}\big|_{t=Tf+} = (\cos 2\alpha)\dot{\theta}\big|_{t=Tf-}$.

As a result, the Poincaré map, **f** is summarized schematically as the following:

$$\mathbf{f} : (\hat{\mathbf{x}}_0, t = 0_+) \xrightarrow{\dot{\mathbf{x}}=f(\mathbf{x})} (\hat{\mathbf{x}}, t = T_{f-}) \xrightarrow{Collision} (\hat{\mathbf{x}}, t = T_{f+}), \text{ where}$$

$$f(\mathbf{x}) = \begin{pmatrix} x_2 \\ \frac{g}{l}\sin(x_1 - \gamma) \end{pmatrix}, \text{ and}$$

$$\mathbf{x}\big|_{t=Tf+} = \begin{pmatrix} \theta \\ \dot{\theta} \end{pmatrix}\Bigg|_{t=Tf+} = \begin{pmatrix} -\theta \\ (\cos 2\alpha)\dot{\theta} \end{pmatrix}\Bigg|_{t=Tf-} = \begin{pmatrix} \alpha \\ (\cos 2\alpha)\dot{\theta} \end{pmatrix}\Bigg|_{t=Tf-}.$$

Once I construct the Poincaré map, I can also construct the derivative matrix of the Poincaré map. In this case, the only varying state variable is the initial angular speed, dθ/dt, so the reduced state vector $\hat{\mathbf{x}}$ and the derivative matrix become a scalar and a one-by-one matrix respectively. With parameter values of m = 10 (kg), g = 9.81 (m/s^2), l = 1 (m), α = 22.5 (deg) (π/8 rad) and γ = 5.73 (deg) (0.1π rad), the eigenvalue of the derivative matrix of the Poincaré map at the fixed point is found to be 0.5, which is located inside the unit circle. This guarantees the asymptotic stability of the fixed point of the map.

On the other hand, I can also construct the Poincaré map analytically using a work-energy principle. Using a work-energy principle and following the argument in Appendix A.1, the Poincaré map becomes

$$\dot{\theta}(t = T_{f+}) = -\frac{\cos 2\alpha}{l}\sqrt{l^2\dot{\theta}_{0+}{}^2 + \frac{4mgl\sin\alpha\sin\gamma}{m}} = \mathbf{f}(\hat{\mathbf{x}}_0, t = 0_+) = \mathbf{f}(\dot{\theta}_0), \text{ and}$$

the derivative matrix of the map becomes

$$\frac{\partial \mathbf{f}(\hat{\mathbf{x}}_0)}{\partial \hat{\mathbf{x}}_0} = -\cos 2\alpha \frac{\dot{\theta}_{0+}}{\sqrt{\dot{\theta}_{0+}{}^2 + \frac{4mgl\sin\alpha\sin\gamma}{ml^2}}}, \text{ where } \dot{\theta}_{0+} = \dot{\theta}(t = 0_+).$$

The fixed point of the Poincaré map can be obtained from energy balance or from Eq 2-27. Considering Eq 2-27 solves the speed just before the collision when the system is at the fixed point, $\dot{\theta}(t = 0_+)$ at the fixed point becomes $\dot{\theta}(t = 0_+)_{\text{fixed}} = -\frac{\cos 2\alpha}{l}\sqrt{\frac{4gl\sin\alpha\sin\gamma}{1-\cos^2 2\alpha}}$. Therefore, the

derivative matrix of the Poincaré map at the fixed point becomes

$$\left.\frac{\partial \mathbf{f}(\hat{\mathbf{x}}_0)}{\partial \hat{\mathbf{x}}_0}\right|_{\text{fixed}} = -\cos 2\alpha \left.\frac{\dot{\theta}_{0+}}{\sqrt{\dot{\theta}_{0+}^2 + \frac{4mgl\sin\alpha\sin\gamma}{ml^2}}}\right|_{\dot{\theta}_{0+}=-\frac{\cos\alpha}{l}\sqrt{\frac{4gl\sin\alpha\sin\gamma}{1-\cos^2 2\alpha}}} = \cos^2 2\alpha .$$

With parameter value of $\alpha = 22.5$ (deg) ($\pi/8$ rad), the eigenvalue of the derivative matrix of the Poincaré map at the fixed point is obtained analytically to be 0.5, which is the same result of the numerical work.

Both Analytical and numerical analysis guarantees the asymptotic stability of the fixed point. However, it is important to note that as explained already, the asymptotically stable fixed point can be observed only when this system is guaranteed to vault over and not to fly off the slope at every step. In other words, at every collision, the speed just before the collision must be between the maximum and minimum speeds discussed in 2.2.2.

Visualization of Asymptotic Stability

I first check if the analytically obtained fixed point behaves like a fixed point of the Poincaré map that is numerically constructed. Then, I investigate the behavior of the small neighborhood of this fixed point. Please consult Figure 2-7. With parameter values of m = 10 (kg), g = 9.81 (m/s^2), l = 1 (m), $\alpha = 22.5$ (deg) ($\pi/8$ rad) and $\gamma = 5.73$ (deg) (0.1π rad), the speed just before a collision when the system is at the fixed point is obtained as 1.73 (m/s) from Eq 2-27. The corresponding angular speed is 1.73 (rad/s) and angular speed of investigated neighborhood varies from 1.43 (rad/s) to 2.03 (rad/s). This investigated neighborhood is totally included in the speed range whose upper limit and lower limit are the marginal value for the system to fly off and vault over respectively. Asymptotic stability is found in this small neighborhood as Figure 2-10 shows.

In Figure 2-10, $(d\theta/dt)_0$ is $d\theta/dt$ just before a collision when the system is at the fixed point, and ε is the difference between the investigated angular speed just before a collision and $(d\theta/dt)_0$. For example, $\varepsilon = 0.3$ corresponds to the angular speed of 2.03 (rad/s). The green line with $\varepsilon = 0$, which indicates the angular speed of 1.73 (rad/s), shows the behavior of the fixed point obtained analytically. The constant zero deviation means that this point is truly a fixed point of the Poincaré map that does not change its state variables with increasing numbers of mapping. The various angular speeds in [1.43, 2.03] (rad/s) converge to $(d\theta/dt)_0$ of the fixed point as the numbers of mapping increases. This convergence indicates that the fixed point is asymptotically stable. However, the convergence is not a global behavior but a local behavior because it can be observed only when the system vaults over and does not fly off the slope.

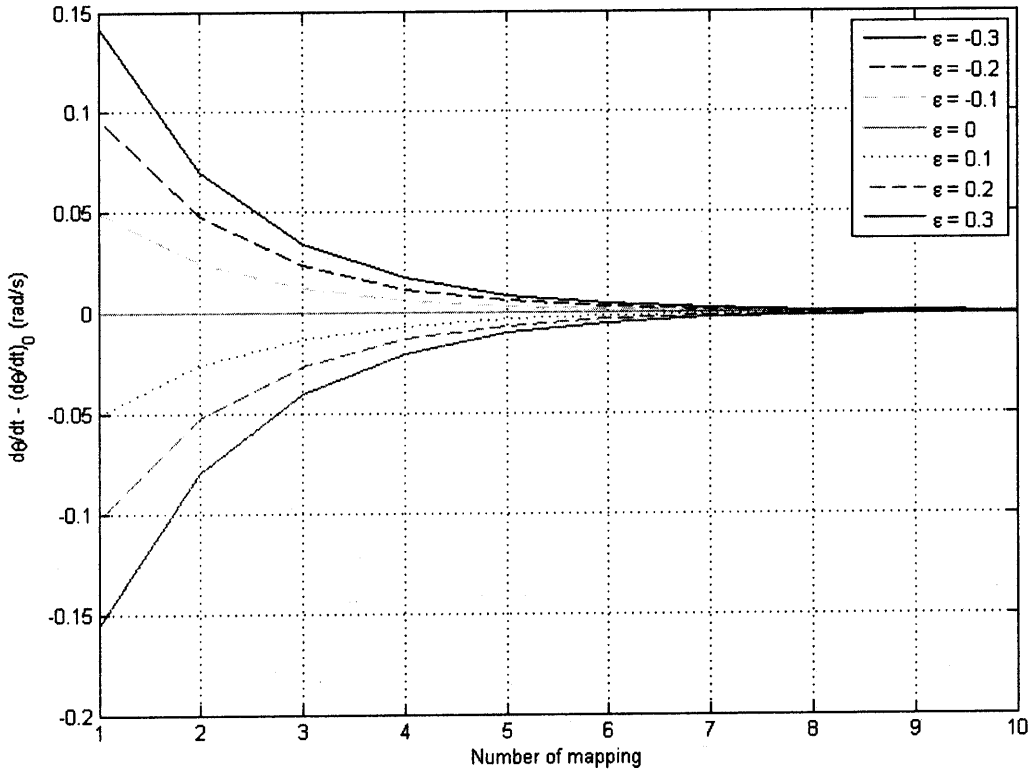

Figure 2-10: Asymptotic stability of the period-one gait of the rimless wheel on a slight slope

2.3. Summary and Discussion

The rimless wheel model investigated in this chapter can generate a stable period-one gait on a slight slope though it fails to make a period-one gait on a horizontal ground. The stability of the period-one gait is due to the two facts: one is that a collision dissipates kinetic energy by a fixed ratio determined by the geometry of the model; and, the other is that the work done by gravity is constant per step. A constant work done by an external force on each step can make a stable period-one gait if the kinetic energy is lost by a constant reduction ratio due to collisions

Another thing to note is that the eigenvalue of the derivative matrix of the Poincaré map representing the stride function of the rimless wheel on a slight slope at the fixed point is a function of the geometry of the model only. Without being influenced by other parameter values such as mass, leg length and the angle of slope, only the angle between two legs determines the eigenvalue and establishes the stability of the fixed point as long as the system vaults over and does not fly off the slope.

The result of the analysis can suggest that training on a slight downhill slope might be an effective way to assist gait rehabilitation. On a slight slope, a patient suffering from neurological or orthopedic injury might generate a stable periodic gait more easily by virtue of the passive dynamics that the rimless wheel model uses. This may accelerate motor learning of the lower extremities and assist gait rehabilitation.

3. A Springy Legged Model without Double Stance

The rimless wheel model studied in the previous chapter fails to make a stable periodic gait on level ground because kinetic energy is dissipated while there is no way to compensate for the lost energy. The energy loss of a rimless wheel on level ground is due to the reduction of speed by each collision. Therefore, an energy-lossless gait might be achieved by letting a model make a step in a collisionless manner. One way to make a collisionless step is letting a model have springy legs. As the first step of studying a passive walker that walks in a collisionless manner, I analyze the motion of a springy legged model without a double stance phase in this chapter.

3.1. Assumptions and Definitions of Parameters

A point mass moves on a horizontal floor in a vertical plane under the influence of gravity, restrained by a springy massless leg. A double stance phase is not allowed, and each leg is allowed only to be compressed and can not be stretched. For definitions of the parameters and coordinate axes, please see Figure 3-1 and Table 3-1.

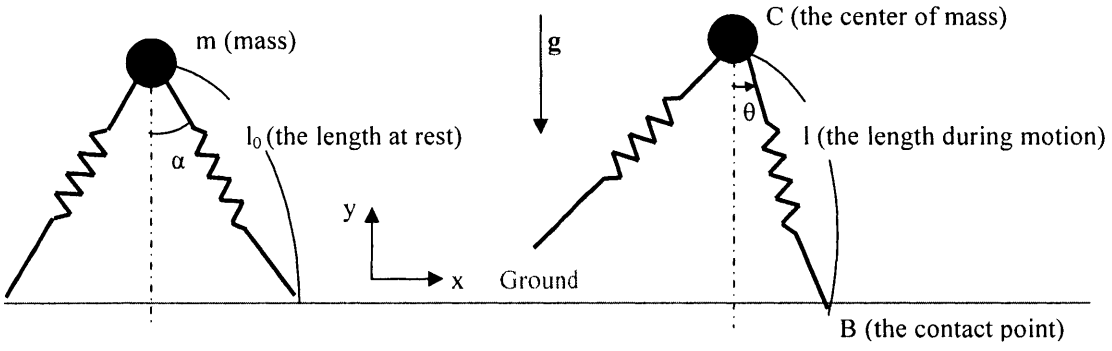

Figure 3-1: A springy legged model without double stance phase on a horizontal floor

Table 3-1: The meaning of parameters of a springy legged model without double stance phase

Parameter	Meaning
m	The mass of the inverted pendulum
k	The spring constant of a leg
l	The length of stance leg during the inverted pendulum motion
l_0	The unloaded length of a spring leg
θ	An angle of a stance leg during the inverted pendulum motion
α	The half of the angle between two legs; α is the initial value of θ

3.2. Equations of Motion and Initial Conditions

I derive equations of motion using the Lagrangian approach. The free body diagram (FBD) of the system is shown in Figure 3-2. Note that the only constraint force is the ground reaction force (GRF) that does no work due to the assumption of a fixed contact point B. Therefore, the constraint is ideal, and all the active forces are conservative forces. As a result, all non potential generalized forces are zero.

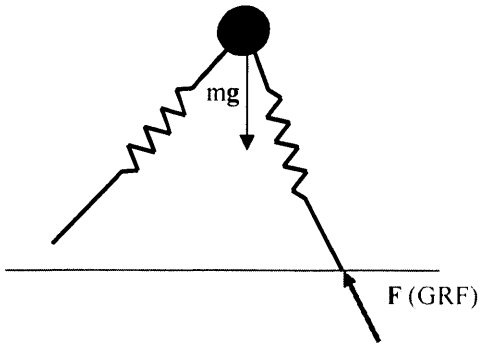

Figure 3-2: The free body diagram of the springy legged model without double stance

Let the generalized coordinates be (l, θ), and Lagrangian be L.

$$L = T - V \text{, where}$$

$$T = \frac{1}{2}m\{\dot{l}^2 + (l\dot{\theta})^2\}, \text{ and } V = \frac{1}{2}k(l - l_0)^2 + mgl\cos\theta .$$

$$\Rightarrow L = \frac{1}{2}m\{\dot{l}^2 + (l\dot{\theta})^2\} - \frac{1}{2}k(l - l_0)^2 - mgl\cos\theta .$$

Because non potential generalized forces are zero in this case, and $\frac{d}{dt}\frac{\partial L}{\partial \dot{q}} - \frac{\partial L}{\partial q} = Q = 0$,

$$\frac{d}{dt}\frac{\partial L}{\partial \dot{l}} - \frac{\partial L}{\partial l} = 0 \Rightarrow \ddot{l} - \dot{\theta}^2 l + \frac{k}{m}(l - l_0) + g\cos\theta = 0 \text{, and} \qquad \text{Eq 3-1}$$

$$\frac{d}{dt}\frac{\partial L}{\partial \dot{\theta}} - \frac{\partial L}{\partial \theta} = 0 \Rightarrow l\ddot{\theta} + 2\dot{l}\dot{\theta} - g\sin\theta = 0 . \qquad \text{Eq 3-2}$$

The equations of motion are expressed by two coupled second-order ordinary differential equations. Let the state variables be l, dl/dt, θ and dθ/dt, and let (l, dl/dt, θ, dθ/dt) = (x_1, x_2, x_3, x_4). Then, Eq 3-1 and 3-2 can be expressed as

$$\frac{d}{dt}\begin{pmatrix} x_1 \\ x_2 \\ x_3 \\ x_4 \end{pmatrix} = \begin{pmatrix} x_2 \\ x_1 x_4^2 - g\cos x_3 - \frac{k}{m}(x_1 - l_0) \\ x_4 \\ -\frac{2}{x_1}(x_2 x_4) + \frac{g}{x_1}\sin x_3 \end{pmatrix} . \qquad \text{Eq 3-3}$$

To solve this set of ODEs, I need four initial conditions. See Figure 3-3. The initial conditions can be divided into the initial conditions for position and the initial conditions for velocity. To initiate the motion from the exact moment when the leg begins to touch the ground, I define the initial position as $x_1 = l_0$ and $x_3 = \alpha$ at $t = t_0 = 0$. The initial velocity is given by its magnitude of v_0 and the direction angle of β. To find the corresponding initial values of x_2 and x_4, I use the kinematics shown in Figure 3-4, which expresses the position vector with radial and

transverse components. It can be easily shown that

$$\vec{v} = \frac{d}{dt}\vec{r} = \dot{r}\vec{e_r} + r\dot{\theta}\vec{e_\theta}.$$

By taking B as origin O in Figure 3-4 and comparing the components of radial and transverse directions, the initial value of x_2 (dl/dt) and x_4 (dθ/dt) can be expressed in terms of v_0 and β.

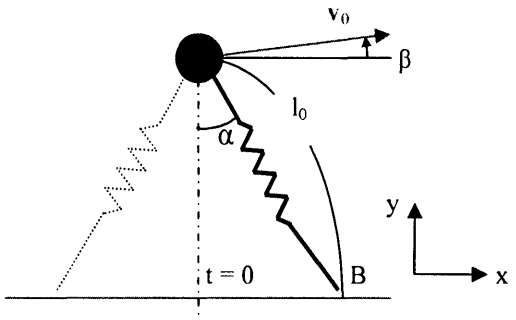

Figure 3-3: The initial position and velocity of the springy legged model without double stance

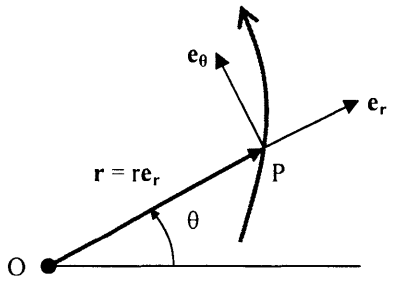

Figure 3-4: A position vector expressed in radial and transverse components

As a result, the initial conditions are obtained as

$$\left.\begin{pmatrix} x_1 \\ x_2 \\ x_3 \\ x_4 \end{pmatrix}\right|_{t=0} = \begin{pmatrix} l_0 \\ -v_0\sin(\alpha-\beta) \\ \alpha \\ -\frac{v_0}{l_0}\cos(\alpha-\beta) \end{pmatrix}. \qquad \text{Eq 3-4}$$

Eq 3-3 and Eq 3-4 provide the set of ODEs and initial conditions

3.3. The Existence of a Period-One Gait

I define $\mathbf{x}$ and f as the following:

$$\mathbf{x} = \begin{pmatrix} x_1 \\ x_2 \\ x_3 \\ x_4 \end{pmatrix} = \begin{pmatrix} l \\ \dot{l} \\ \theta \\ \dot{\theta} \end{pmatrix}, \mathbf{x}_0 = \begin{pmatrix} x_1 \\ x_2 \\ x_3 \\ x_4 \end{pmatrix}\Bigg|_{t=0}, \text{ and } f(\mathbf{x}) = \begin{pmatrix} x_2 \\ x_1 x_4^2 - g\cos x_3 - \frac{k}{m}(x_1 - l_0) \\ x_4 \\ -\frac{2}{x_1}(x_2 x_4) + \frac{g}{x_1}\sin x_3 \end{pmatrix}.$$

The dynamical system representing the motion of the springy legged model without double stance phase obeys the evolution rule, $\dot{\mathbf{x}} = f(\mathbf{x})$. In other words, the state vector $\mathbf{x}$ evolves from $\mathbf{x}_0$ as; $(\mathbf{x}_0, t=0) \xrightarrow{\dot{\mathbf{x}}=f(\mathbf{x})} (\mathbf{x}, t)$. When I confine my interest to the case in which the model vaults over and makes the next step, one of the crucial steps in finding a period-one gait is to find out the initial condition that recovers its value at the beginning of the following step. As mentioned before, to initiate the motion from the exact moment when the leg begins to touch the ground, I confine my analysis to the case of $x_1(t=0) = l_0$ and $x_3(t=0) = \alpha$. This set of initial condition captures the behavior of the ground reaction force that is zero before the touch down of the foot but becomes positive after touch down of the foot. Note that the initial conditions for position are replaced with parameter values, which are l_0 and α, and the only variables in initial conditions are x_2 and x_4, which are related only to initial velocity.

In terms of a dynamical system, the period-one gait is equivalent to the fixed point of the Poincaré map. To find the fixed point of the Poincaré map, I need to select a proper Poincaré section and investigate the existence of fixed points. With some selected parameter values and initial speed with which the model does neither fail to vault over nor fly off, I find a fixed point of the Poincaré map.

3.3.1. The Poincaré Section

It is important to select a proper state variable acting as an anchor of the Poincaré section. For example, if I choose the angle between the stance leg and the vertical axis as a fixed state variable indicating the end of one step, the potential energy stored in the springy legs can vary at the beginning of each step. Suppose that the leg length does not recover its initial value of unloaded length when the angle recovers its initial value. This length is possibly less than the unloaded length, and then, the energy stored in springy legs can be different at each beginning of a step. Therefore, if I want to select a Poincaré section so that the energy stored in springy legs is same at every beginning of a step, a completion of one step must be indicated by the leg length. In conclusion, I select a Poincaré section so that the Poincaré map corresponding to the stride function of this model is defined in the three dimensional state space Σ, which is

$$\Sigma = \{(l,\dot{l},\theta,\dot{\theta}) \mid l = l_0 \wedge \dot{l} \in \mathbf{R} \wedge -\pi < \theta < \pi \wedge \dot{\theta} \in \mathbf{R}\}, \text{ where "} \wedge \text{" means "AND."}$$

3.3.2. Algorithm for Finding Fixed Points of the Poincaré Map

Please see Figure 3-3. Considering that the initial conditions for position are replaced with parameter values l_0 and α, the only variable initial conditions are v_0 and β, which are related to the initial velocity. Therefore, the fixed point can be expressed in terms of these two variables. With the Poincaré section that I selected in 3.3.1, I can evaluate the existence of the period-one gait by investigating whether the velocity vector recovers its initial value, and the angular displacement θ becomes the negative of its initial value when x_1 recovers its value of l_0. With the definitions of

$\hat{\mathbf{x}} = \begin{pmatrix} x_2 \\ x_3 \\ x_4 \end{pmatrix} = \begin{pmatrix} \dot{l} \\ \theta \\ \dot{\theta} \end{pmatrix}$, my algorithm for finding such an initial condition is the following:

Step 1 Assume an arbitrary initial velocity.

Step 2 Solve the evolution rule obtained in 3.2 with that initial velocity.

Step 3 Find the minimal positive time when x_1 becomes the unloaded length l_0, and define the time as T_f.

Step 4 Find the desirable (x_2, x_3, x_4) at T_f to make a period-one gait and define the transpose of this vector as $\hat{\mathbf{X}}\mathbf{f} = (x_{f2}, x_{f3}, x_{f4})^T$

Step 5 Let $((x_2(T_f)/ x_{f2} - 1), (x_3(T_f)/ x_{f3} - 1), (x_4(T_f)/ x_{f4} - 1))^T$ be the vector ξ. Note that I do not include $(x_1(T_f)/ l_0 - 1)$ so that ξ is in three-dimensional state space instead of four-dimensional state space because x_1 is the variable that acts as an anchor of the Poincaré section, and $(x_1(T_f)/ l_0 - 1)$ should be zero at every step.

Step 6 Minimize the cost function that is the norm of the normalized vector ξ with the initial conditions as variables. The minimum of the cost function should be zero if any period-one gait exists.

Step 7 Check if this optimal initial condition actually yields a periodic gait that keeps the springy leg from stretching; check the existence of a period-one gait.

In step 4, desirable state variables at $t = T_f$ can be calculated by decomposing the velocity vector into radial and transverse components. Please see Figure 3-5. In terms of state variables, to achieve a period-one gait with the initial velocity whose magnitude and the angle of direction are v_0 and β respectively, the system must satisfy

$$\left.\begin{pmatrix} x_1 \\ x_2 \\ x_3 \\ x_4 \end{pmatrix}\right|_{t=T_f} = \begin{pmatrix} l_0 \\ v_0 \sin(\alpha+\beta) \\ -\alpha \\ -\frac{v_0}{l_0}\cos(\alpha+\beta) \end{pmatrix} = \mathbf{x_f} = \begin{pmatrix} l_0 \\ \hat{\mathbf{x}}\mathbf{f} \end{pmatrix}. \qquad \text{Eq 3-5}$$

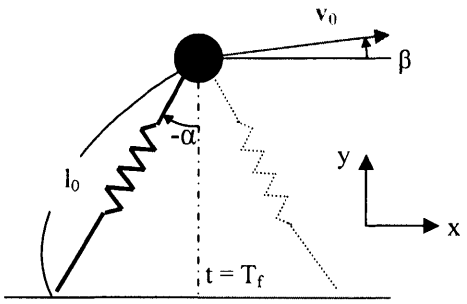

Figure 3-5: The state of the springy legged model at $t = T_f$ for a period-one gait

To optimize the norm in step 6, I use the command "Fminsearch" in MATLAB. This command finds a local minimum of a scalar function of several variables, starting at an initial estimate. I can find an initial condition for a fixed point by changing the initial estimate over the range where the model does neither fail to vault over nor fly off. The detailed source codes are attached in Appendix B.

3.3.3. The Fixed Point of the Poincaré Map

The parameter values of the springy legged model I analyzed are shown in Table 3-2.

Table 3-2: Parameter values of the springy legged model without double stance phase

Parameter	Value
m	10 kg
k	1000 N/m
g	9.81 m/s^2
l_0	1 m
α (θ at t=0)	π/8

With the parameter values in Table 3-2, the fixed point of the Poincaré map that makes the

norm of ξ zero corresponds to the initial velocity of $v_0 = 1.7375$ (m/s) and $\beta = 0$ (rad). The state variables with this initial condition are shown in Figure 3-6. All the state variables remain in a physically reasonable domain, and, particularly, the stance leg is kept compressed throughout the whole step. Therefore, I can conclude the existence of a period-one gait. This model conserves not only the kinetic energy but also the linear momentum in x direction with this set of initial conditions. Please note that in Figure 3-6, l and $d\theta/dt$ are symmetric while dl/dt and θ are anti-symmetric. These behaviors can be explained by the continuity of the velocity at the end of one step and the definition of positive direction of θ. For example, considering the positive direction of the θ, during one step, θ should go from positive to negative, while $d\theta/dt$ should be kept positive. Also, at the end of a step, the stance leg is replaced with the other leg, and stretching of the previous stance leg will be the compressing of the next stance leg, which explains the anti-symmetry of dl/dt.

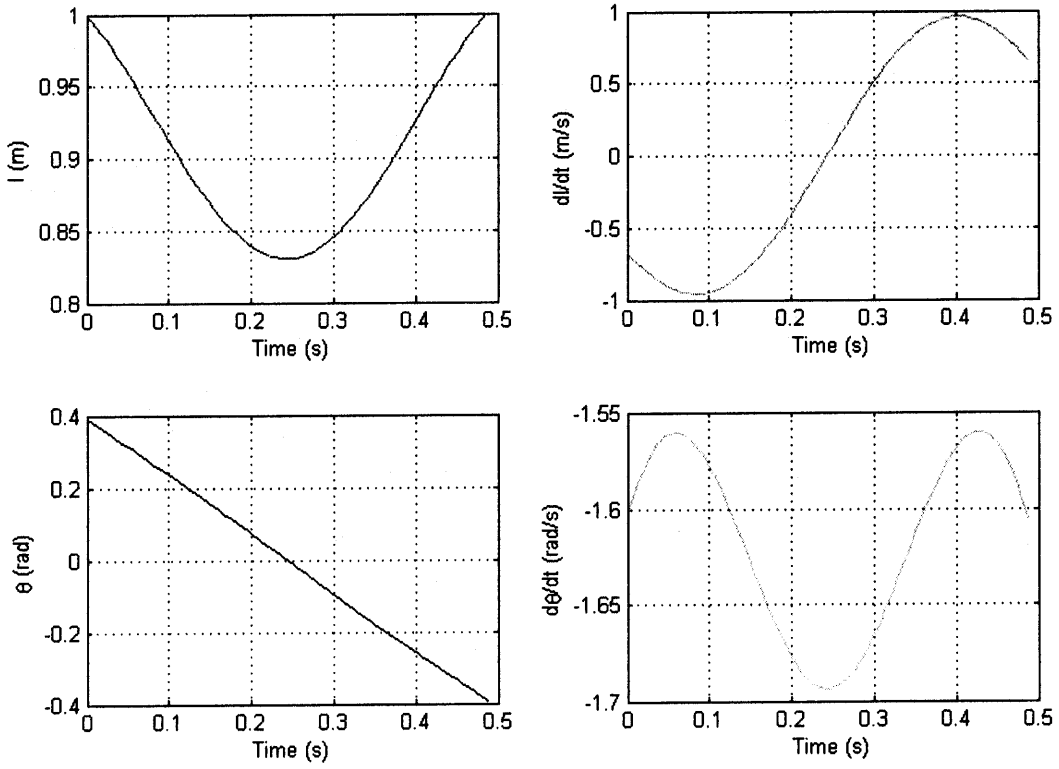

Figure 3-6: The state variables during one step with $v_0 = 1.7375$ (m/s) and $\beta = 0$ (rad)

If I confine my interest to the case of zero β, I can plot the norm of ξ with various initial speeds. Figure 3-7 shows the plot, and Figure 3-8 shows the magnified view of the Figure 3-7 near the initial velocity of $v_0 = 1.7375$ (m/s), which makes ξ zero with the parameter values in Table 3-2. The range of speed investigated in Figure 3-7 is up to 31.5 (m/s). Increasing speed over 31.5 (m/s) makes the norm of ξ approach to zero asymptotically. With the parameter values, the model cannot vault over if the initial speed is below 1.156 (m/s). On the other hand, opposed to the case of rimless wheel model, there is no upper limit of the speed that makes the model fly off with these parameter values. No matter how fast the speed is, the spring is kept compressed with the given parameter values. Instead, the asymptotic behavior shown in Figure 3-7 provides that no matter how high the speed is, it cannot yield an exact fixed point. This result implies that for the initial velocity with zero β, there exists only one fixed point of the Poincaré map. Therefore, I can conclude that the solved period-one gait with $v_0 = 1.7375$ (m/s) is the unique fixed point of the Poincaré map with a horizontal initial velocity and the parameter values in Table 3-2.

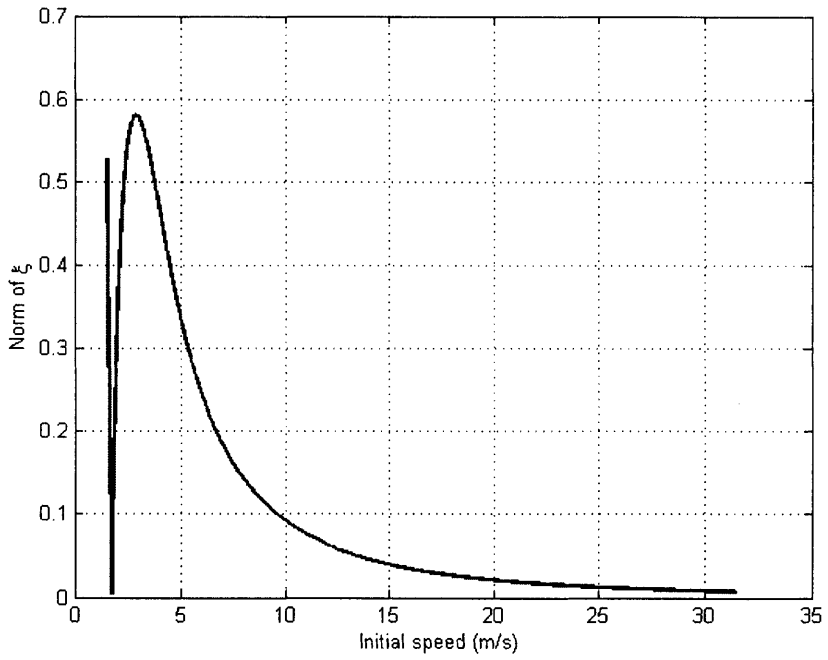

Figure 3-7: The norm of ξ with various initial speeds; initial speed varies from 1.5 to 31.5 (m/s).

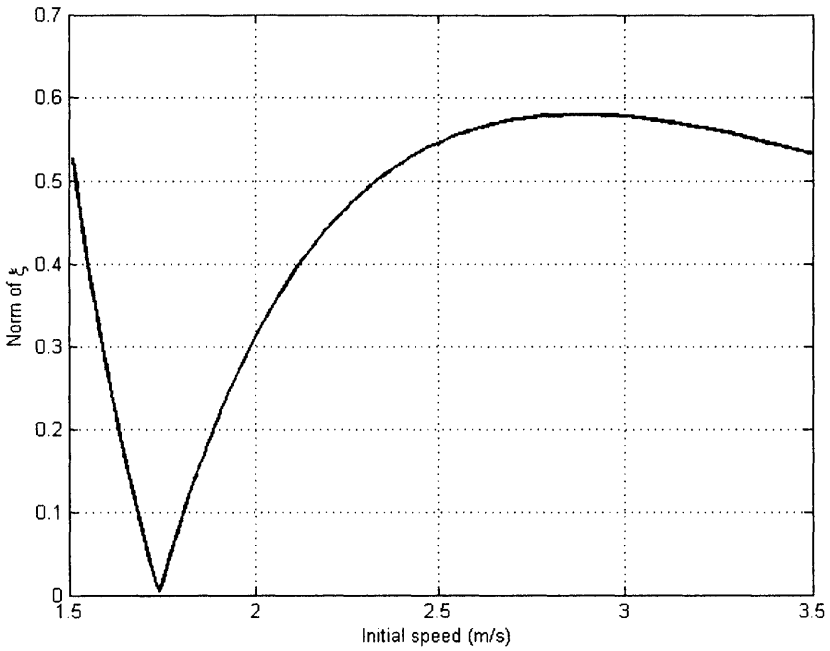

Figure 3-8: The norm of ξ with various initial speeds; magnified view around $v_0 = 1.7375$ (m/s)

3.4. Stability of the Fixed Point of Period-One Gait

As mentioned in 1.4, I treat the stride function of each step as a Poincaré map and analyze the stability of the fixed point of the map. To construct the Poincaré map, I need to combine (A) the map whose input and output are the reduced state vectors at the beginning of a step and the end of a step respectively with (B) the map whose input and output are the reduced state vectors of the end of one step and the beginning of the following step respectively. After constructing Poincaré map, I perform stability analysis by following three steps: (1) I find the fixed point of the Poincaré map that generates the period-one gait, which was already done in 3.3; (2) I assess the stability by investigating the eigenvalues of the derivative matrix of the Poincaré map at the fixed point; and, (3) I visualize the stability or instability by showing the behavior of the small neighborhood of the

fixed point. Definitions of state vector $\mathbf{x}$, reduced state vector $\hat{\mathbf{x}}$, state variable x_i, vector ξ and evolution rule f, which were established in 3.3, are still valid throughout this section.

3.4.1. Constructing the Poincaré Map

As mentioned in 3.3.1, I select the length of a springy leg as an indicator of the completion of a step and define the Poincaré section accordingly. I reuse the definition of T_f introduced in 3.3.2; T_f is the minimal time when the stance leg recovers its initial unloaded length. I also define T_{f-} and T_{f+} as the time just before and right after T_f respectively. If I solve the ODE established in 3.2, I can obtain a state vector at any time including T_{f-}. Therefore, I can construct a map whose input and output are the reduced state vectors at $t = 0_+$ and $t = T_{f-}$ respectively. Let this map be $\mathbf{f}_1$.

$$\mathbf{f}_1 : (\hat{\mathbf{x}}_0, t = 0_+) \xrightarrow{\dot{\mathbf{x}} = f(\mathbf{x})} (\hat{\mathbf{x}}, t = T_{f-}).$$

I need to complete the whole map by adding the map whose input and output are the reduced state vectors at $t = T_{f-}$ and $t = T_{f+}$ respectively. Let this map be $\mathbf{f}_2$. Because this model does not involve any collision or impulsive force, the acceleration is finite all the time, which means the velocity vector is continuous. The map $\mathbf{f}_2$ can be considered as the transition of a state vector describing the state of the point mass in terms of the corresponding stance leg and can be obtained using the continuity of velocity.

$$\mathbf{f}_2 : (\hat{\mathbf{x}}, t = T_{f-}) \xrightarrow{\textit{continuity of velocity}} (\hat{\mathbf{x}}, t = T_{f+}).$$

The combination of $\mathbf{f}_1$ and $\mathbf{f}_2$ makes the whole map corresponding to the Poincaré map whose input and output are the reduced state vectors at $t = 0_+$ and $t = T_{f+}$ respectively. Let the whole map be $\mathbf{f}$.

$$\mathbf{f} = \mathbf{f}_2 \circ \mathbf{f}_1 : (\hat{\mathbf{x}}_0, t = 0_+) \xrightarrow{\dot{\mathbf{x}} = f(\mathbf{x})} (\hat{\mathbf{x}}, t = T_{f-}) \xrightarrow{\textit{continuity of velocity}} (\hat{\mathbf{x}}, t = T_{f+})$$

The map $\mathbf{f}_2$ can be constructed analytically while $\mathbf{f}_1$ should be constructed numerically. To construct $\mathbf{f}_2$, I use the assumption that the springy legged model generates a gait in a collisionless manner and the velocity vector is continuous. Figure 3-9 shows the continuity of the velocity at time $t = T_{f-}$. In Figure 3-9, $\mathbf{e}_i$s' are the unit vectors directing radial and transverse directions of the motion of the point mass with respect to the contact point of the corresponding stance leg while **i** and **j** are the unit vector of x and y direction respectively. Also, l_n and φ, which are not constants but variables, represent the length and angle of the stance leg of the new step respectively while l and θ represent the length and angle of the stance leg of the preceding step.

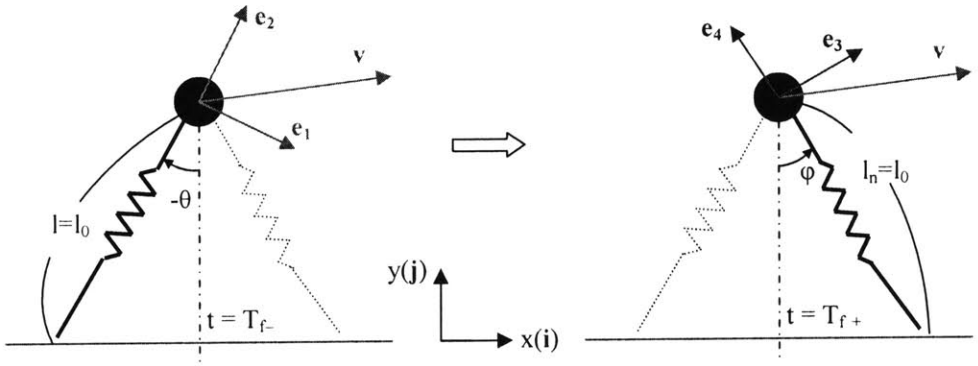

Figure 3-9: Continuity of velocity between the end of a step and the beginning of the next step.

As explained in 3.3.1, I need the length of stance leg be the unloaded leg length l_0 at both $t = T_{f-}$ and T_{f+}. Then, by geometry, the magnitude of $-\theta$ at $t = T_{f-}$ must be same as the magnitude of φ at $t = T_{f+}$. Let this magnitude of both angles be η. In other words, $\varphi(t = T_{f+}) = -\theta(t = T_{f-}) = \eta$. Using kinematics, I obtain $\mathbf{e}_1$, $\mathbf{e}_2$, $\mathbf{e}_3$ and $\mathbf{e}_4$ as

$$\begin{aligned}
\vec{e}_1 &= (\cos\eta)\mathbf{i} - (\sin\eta)\mathbf{j}, \\
\vec{e}_2 &= (\sin\eta)\mathbf{i} + (\cos\eta)\mathbf{j}, \\
\vec{e}_3 &= (\cos\eta)\mathbf{i} + (\sin\eta)\mathbf{j}, \text{and} \\
\vec{e}_4 &= (-\sin\eta)\mathbf{i} + (\cos\eta)\mathbf{j}.
\end{aligned} \qquad \text{Eq 3-6}$$

Also, by decomposing the velocity vectors at $t = T_{f-}$ and T_{f+} into the radial and transverse

directions,

$$\vec{v}\Big|_{t=Tf-} = \dot{l}\vec{e}_2 + (-l\dot{\theta})\vec{e}_1 \text{ and } \vec{v}\Big|_{t=Tf+} = \dot{l}_n\vec{e}_4 + (-l_n\dot{\varphi})\vec{e}_3 . \quad \text{Eq 3-7}$$

Using the continuity of the velocity, $\vec{v}\Big|_{t=Tf-} = \vec{v}\Big|_{t=Tf+}$. Comparing the **i** and **j** components after substituting Eq 3-6 into Eq 3-7,

$$\begin{aligned} \dot{l}(\sin\eta) - l\dot{\theta}(\cos\eta) &= -\dot{l}_n(\sin\eta) - l_n\dot{\varphi}(\cos\eta), \text{ and} \\ \dot{l}(\cos\eta) + l\dot{\theta}(\sin\eta) &= \dot{l}_n(\cos\eta) - l_n\dot{\varphi}(\sin\eta). \end{aligned} \quad \text{Eq 3-8}$$

In Eq 3-8, as discussed already, $l = l_n = l_0$ at $t = T_{f-}$ or T_{f+}, which is the time of concern. Additionally, I know all the state variables in the preceding step after I solve the ODE numerically and construct the map $\mathbf{f}_1$. Therefore, I know dl/dt at $t = T_{f-}$, η, which equals to $-\theta$ at $t = T_{f-}$, and $d\theta/dt$ at $t = T_{f-}$. As a result, I have two unknowns, which are dl_n/dt and $d\varphi/dt$ and two equations, which are given in Eq 3-8. Solving Eq 3-8, I obtain x_2 and x_4 at the beginning of the new step. Note that x_3 at the beginning of the new step is already obtained as η.

To summarize, with the Poincaré section selected in 3.3.1, the whole Poincaré map whose input and output are the reduced state vectors at $t= 0_+$ and $t = T_{f+}$ respectively is constructed as the following:

Step 1 Solve the evolution rule obtained in 3.2 with given initial condition, $\mathbf{x}(t=0) = \mathbf{x_0}$.

Step 2 Find the minimal positive time when x_1 becomes the unloaded length l_0, and define the time as T_f.

Step 4 Find the state vector (x_2, x_3, x_4) at T_{f-}, which is the time just before T_f.

Step 5 Find the state vector (x_2, x_3, x_4) at T_{f+}, which is the time right after T_f using the continuity of velocity vector. Results are

$$x_3\Big|_{t=Tf+} = \varphi\Big|_{t=Tf+} = \eta = \theta\Big|_{t=Tf-} = x_3\Big|_{t=Tf-}, \text{ and}$$

$$\left.\begin{pmatrix} x_2 \\ x_4 \end{pmatrix}\right|_{t=T_{f+}} = \begin{pmatrix} \dot{l}_n \\ \dot{\varphi} \end{pmatrix} = \begin{pmatrix} -\sin\eta & -l_0\cos\eta \\ \cos\eta & -l_0\sin\eta \end{pmatrix}^{-1} \left.\begin{pmatrix} \dot{l}(\sin\eta) - l_0\dot{\theta}(\cos\eta) \\ \dot{l}(\cos\eta) + l_0\dot{\theta}(\sin\eta) \end{pmatrix}\right|_{t=T_{f-}}.$$

Step 1 ~ 5 yield a map of $\mathbf{f} : (\hat{\mathbf{x}}_0, t = 0_+) \rightarrow (\hat{\mathbf{x}}, t = T_{f+})$.

3.4.2. Stability Analysis

As discussed in 3.3, with the selected initial position of $x_1(t=0) = l_0 \wedge x_3(t=0) = \alpha$, the horizontal initial velocity and the selected parameter values in Table 3-2, there is only one fixed point of the Poincaré map. I analyze the stability of the fixed point by investigating the eigenvalues of the derivative matrix of the Poincaré map.

Using numerical method, I obtain the eigenvalues of the derivative matrix of the Poincaré map that is constructed numerically and analytically in 3.4.1. Detailed source code is attached in Appendix B.2. The reduced state vector $\hat{\mathbf{x}}$ is a vector in a three-dimensional state space, and the derivative matrix $\mathbf{J} = \frac{\partial \mathbf{f}}{\partial \hat{\mathbf{x}}}$ has three eigenvalues, which are 7.6918, -0.6495 and 0.1999. The eigenvalue of 7.69 is located outside the unit circle. This guarantees the instability of the fixed point of the map.

To visualize the instability, I investigate the behavior of the small neighborhood of the fixed point. The deviation from the fixed point is caused by the deviation in x_2 (= dl/dt). In terms of $\mathbf{x}$, the obtained fixed point corresponds to $\mathbf{x}_0 = (1, -0.665, 0.3927, -1.6052)^T$. The value of x_2 of investigated neighborhood varies from -0.695 (m/s) to -0.635 (m/s). Instability is found locally in this small neighborhood as Figure 3-10 shows.

In Figure 3-10, ε is the difference between x_2 of the investigated point and x_2 of the fixed point, which is -0.665 (m/s). For example, ε = 0.03 corresponds to the case of initial value of

$x_2(t=0)$ = -0.635 (m/s). The green line with $\varepsilon = 0$ shows the behavior of the fixed point. The constant zero norm of ξ means that this point is truly a fixed point of the Poincaré map that does not change its state variables with increasing numbers of mapping. The norm of ξ with various initial values of x_2 in [-0.695, -0.635] (m/s) diverges from the zero norm of the fixed point as the numbers of mapping increases. This divergence results from the instability of the fixed point.

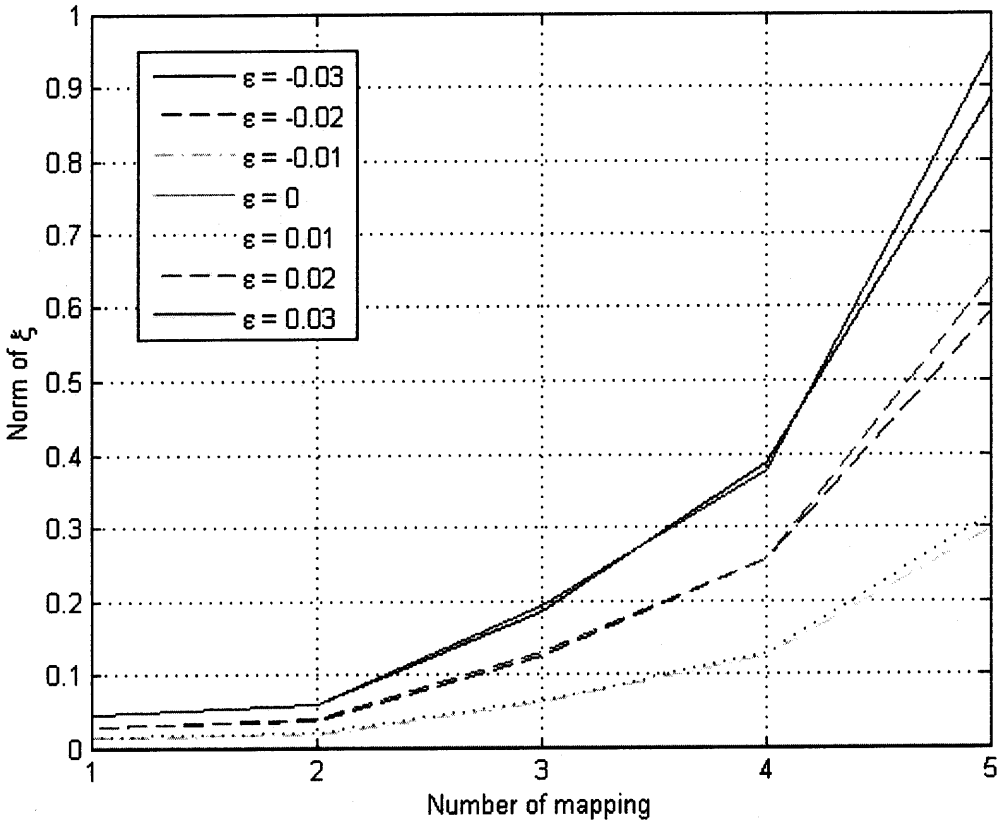

Figure 3-10: Instability of a period-one gait of the springy legged model without double stance

3.5. Summary and Discussion

Motivated by the result that the rimless wheel fails to make a period-one gait on a horizontal ground, I have analyzed a springy legged model without double stance. Theoretically,

by walking in a collisionless manner, the springy legged model can make a period-one gait without energy dissipation. However, the investigated period-one gait is turned out to be unstable, and the gait will lose periodicity with small perturbation.

Unstable fixed points of a dynamical system are almost impossible to be observed in the real world while normal gaits of humans survive under small perturbations. Therefore, if I want to provide some intuition to assist rehabilitation of bipedal gait, it is necessary to suggest a model that generates a stable periodic gait.

Although the springy legged model without double stance fails to have a stable period-one gait, another springy legged model with double stance is still worth investigating. I will analyze this springy legged model with double stance in the next chapter.

4. A Springy Legged Model with Double Stance

In the previous chapter, I analyze the motion of a springy legged model without double stance phase, which can make a period-one gait that is unstable. In this chapter, I extend my analysis to a springy legged model with double stance phase and investigate whether this model can make a stable period-one gait or not.

4.1. Assumptions and Definitions of Parameters

Assume that a point mass moves in a vertical plane under the influence of gravity, restrained by a springy massless leg. Double stance phase is allowed, but each leg is allowed only to be compressed or unloaded and can not be stretched. In other words, the springy legs can push the point mass, but they cannot pull it, which captures the behavior of ground reaction force of bipedal walking.

For definition of the parameters and coordinate, please see Figure 4-1 and Table 4-1. Contact point B is fixed during one step. Angle θ and l_2, which can be two of the state variables, determine the position of the point mass during the step. Stride length s, which is a given constant during the first step but may change its value at the next step, determines the initial value of l_1.

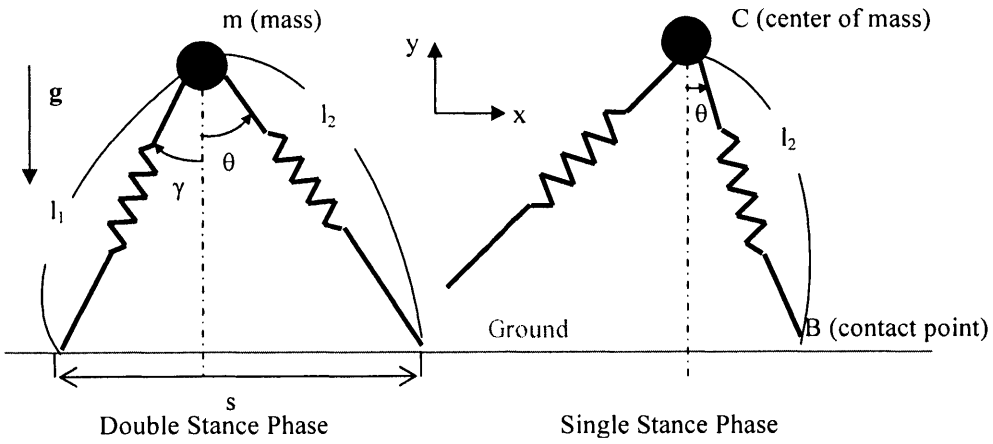

Figure 4-1: A springy legged model with double stance phase on a horizontal floor

Table 4-1: The meaning of parameters of a springy legged model with double stance phase

Parameter	Meaning
m	The mass of the inverted pendulum
k	The spring constant of a leg
l_1	The length of the trailing leg
l_2	The length of the leading leg
l_0	The unloaded length of a springy leg
s	The stride distance
θ	An angle during the single stance phase motion
α	The initial value of θ

4.2. Equations of Motion and Initial Conditions

With the assumption of fixed contact point B during one step, I derive equations of motion using a Lagrangian approach. The constraint is ideal, and all the active forces are conservative forces. As a result, all non-potential generalized forces are zero. I divide the motion into two parts: double stance phase and single stance phase.

4.2.1. Double Stance Phase

Please consult Figure 4-1. Let the generalized coordinates be (l_2, θ) and the Lagrangian be L.

$$L = T - V \text{, where}$$

$$T = \frac{1}{2}m\{\dot{l}_2^2 + (l_2\dot{\theta})^2\}\text{, and } V = \frac{1}{2}k(l_1 - l_0)^2 + \frac{1}{2}k(l_2 - l_0)^2 + mgl\cos\theta .$$

$$\Rightarrow L = \frac{1}{2}m\{\dot{l}_2^2 + (l_2\dot{\theta})^2\} - \frac{1}{2}k(l_1 - l_0)^2 - \frac{1}{2}k(l_2 - l_0)^2 - mgl\cos\theta .$$

Please note that as assumed, stride length is constant during one step, but it can change discretely step by step. Using kinematics,

$$l_1^2 = (s - l_2\sin\theta)^2 + (l_2\cos\theta)^2$$
$$\Rightarrow l_1 = \sqrt{(s - l_2\sin\theta)^2 + (l_2\cos\theta)^2}$$
$$\Rightarrow \frac{\partial l_1}{\partial l_2} = \frac{l_2 - s(\sin\theta)}{\sqrt{s^2 - 2sl_2\sin\theta + l_2^2}} \wedge \frac{\partial l_1}{\partial\theta} = \frac{-l_2 s(\cos\theta)}{\sqrt{s^2 - 2sl_2\sin\theta + l_2^2}}.$$

Using $\frac{d}{dt}\frac{\partial L}{\partial\dot{q}} - \frac{\partial L}{\partial q} = Q = 0 \wedge \frac{\partial L}{\partial l_2} = \frac{\partial L}{\partial l_1}\frac{\partial l_1}{\partial l_2} \wedge \frac{\partial L}{\partial\theta} = \frac{\partial L}{\partial l_1}\frac{\partial l_1}{\partial\theta}$, from $\frac{d}{dt}\frac{\partial L}{\partial\dot{l}_2} - \frac{\partial L}{\partial l_2} = 0$,

$$\ddot{l}_2 - \dot{\theta}^2 l_2 + \frac{k}{m}\{(l_2 - l_0) + (l_2 - s\sin\theta) - l_0\frac{l_2 - s(\sin\theta)}{\sqrt{s^2 - 2sl_2\sin\theta + l_2^2}}\} + g\cos\theta = 0, \text{and} \quad \text{Eq 4-1}$$

from $\frac{d}{dt}\frac{\partial L}{\partial\dot{\theta}} - \frac{\partial L}{\partial\theta} = 0$,

$$l_2\ddot{\theta} + 2\dot{l}_2\dot{\theta} + \frac{k}{m}s\cos\theta(\frac{l_0}{\sqrt{s^2 - 2sl_2\sin\theta + l_2^2}} - 1) - g\sin\theta = 0. \quad \text{Eq 4-2}$$

Let the state variables be l_2, dl_2/dt, θ and $d\theta/dt$, and let (l_2, dl_2/dt, θ, $d\theta/dt$) = (x_1, x_2, x_3, x_4) = $\mathbf{x}^T$. Then, Eq 4-1 and 4-2 can be expressed as

$$\frac{d}{dt}\begin{pmatrix} x_1 \\ x_2 \\ x_3 \\ x_4 \end{pmatrix} = \begin{pmatrix} x_2 \\ x_1 x_4^{\,2} - g\cos x_3 - \frac{k}{m}\{(x_1 - l_0) + (x_1 - s\sin x_3) - l_0 \frac{x_1 - s\sin x_3}{\sqrt{s^2 - 2s(x_1 \sin x_3) + x_1^{\,2}}}\} \\ x_4 \\ -\frac{2}{x_1}(x_2 x_4) + \frac{g}{x_1}\sin x_3 - \frac{k}{m} s\cos x_3 (\frac{l_0}{\sqrt{s^2 - 2s(x_1 \sin x_3) + x_1^{\,2}}} - 1) \end{pmatrix}. \quad \text{Eq 4-3}$$

Eq 4-3 or the combination of Eq 4-1 and 4-2, which are two coupled second-order differential equations, require four initial conditions to be solved; see Figure 4-2. The initial conditions can be divided into the initial conditions for position and the initial conditions for velocity. To initiate the motion from the exact moment when the leg begins to touch the ground, I define the initial position as $x_1=l_0$ and $x_2 = \alpha$ at $t = t_0 = 0$. The initial velocity is given by its magnitude of v_0 and the direction angle of β. To find the corresponding initial values of x_2 and x_4, I use the kinematics shown in Figure 4-3, which expresses the position vector with radial and transverse components. It can be easily shown that

$$\vec{v} = \frac{d}{dt}\vec{r} = \dot{r}\vec{e_r} + r\dot{\theta}\vec{e_\theta}.$$

By taking B as origin O in Figure 4-3 and comparing the component of radial and transverse directions, the initial value of x_2 (dl_2/dt) and x_4 ($d\theta/dt$) can be expressed in terms of v_0 and β. As a result, the initial conditions are obtained as

$$\begin{pmatrix} x_1 \\ x_2 \\ x_3 \\ x_4 \end{pmatrix}\Bigg|_{t=0} = \begin{pmatrix} l_0 \\ -v_0 \sin(\alpha - \beta) \\ \alpha \\ -\frac{v_0}{l_0}\cos(\alpha - \beta) \end{pmatrix}. \quad \text{Eq 4-4}$$

Eq 4-3 and Eq 4-4 provide the set of ODEs and initial conditions.

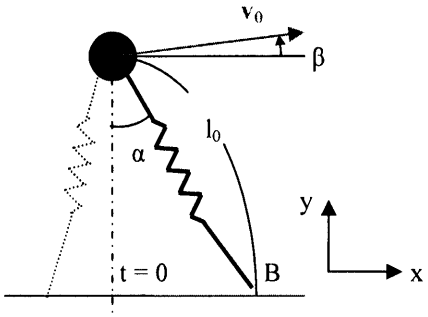

Figure 4-2: The initial position and velocity of the springy legged model with double stance

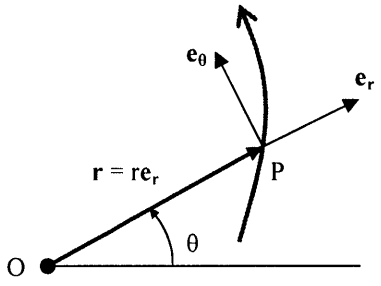

Figure 4-3: A position vector expressed in radial and transverse components

4.2.2. Single Stance Phase

During the single stance phase, the contribution of $\frac{1}{2}k(l_1 - l_0)^2$ vanishes. Let the generalized coordinates be (l_2, θ) and the Lagrangian be L.

$$L = T - V \text{, where}$$

$$T = \frac{1}{2}m\{\dot{l}_2^2 + (l_2\dot{\theta})^2\}, \text{ and } V = \frac{1}{2}k(l_2 - l_0)^2 + mgl\cos\theta .$$

$$\Rightarrow L = \frac{1}{2}m\{\dot{l}_2^2 + (l_2\dot{\theta})^2\} - \frac{1}{2}k(l_2 - l_0)^2 - mgl\cos\theta .$$

Using $\frac{d}{dt}\frac{\partial L}{\partial \dot{q}} - \frac{\partial L}{\partial q} = Q = 0$, from $\frac{d}{dt}\frac{\partial L}{\partial \dot{l}_2} - \frac{\partial L}{\partial l_2} = 0$,

$$\ddot{l}_2 - \dot{\theta}^2 l_2 + \frac{k}{m}(l_2 - l_0) + g\cos\theta = 0, \text{ and} \qquad \text{Eq 4-5}$$

from $\frac{d}{dt}\frac{\partial L}{\partial \dot{\theta}} - \frac{\partial L}{\partial \theta} = 0$,

$$l_2\ddot{\theta} + 2\dot{l}_2\dot{\theta} - g\sin\theta = 0. \qquad \text{Eq 4-6}$$

Let $(l_2, dl_2/dt, \theta, d\theta/dt) = (y_1, y_2, y_3, y_4) = \mathbf{y}^T$. Eq 4-5 and 4-6 can be expressed as

$$\frac{d}{dt}\begin{pmatrix} y_1 \\ y_2 \\ y_3 \\ y_4 \end{pmatrix} = \begin{pmatrix} y_2 \\ y_1 y_4^2 - g\cos y_3 - \frac{k}{m}(y_1 - l_0) \\ y_4 \\ -\frac{2}{y_1}(y_2 y_4) + \frac{g}{y_1}\sin y_3 \end{pmatrix}. \qquad \text{Eq 4-7}$$

I need four initial conditions to solve this ODE. The initial value of the state vector **y** of single stance motion is provided by the value of state vector **x** at the end of the double stance phase. To define the end of double stance as the moment when trailing leg begins to leave the floor, I define the end of the double stance phase as the first moment when l_1 becomes l_0 and define this moment as $t = T_{ds}$. The value of state variables of Eq 4-7 at $t = T_{ds}$ is given by

$$\begin{pmatrix} y_1 \\ y_2 \\ y_3 \\ y_4 \end{pmatrix}\Bigg|_{t = T_{ds}} = \begin{pmatrix} x_1 \\ x_2 \\ x_3 \\ x_4 \end{pmatrix}\Bigg|_{t = T_{ds}}. \qquad \text{Eq 4-8}$$

4.3. The Existence of a Period-One Gait

I define **x**, **y**, f and h as the following, where the definition of time T_{ds} is consistent with the definition in 4.2.2.

$$\mathbf{x}=\begin{pmatrix} x_1 \\ x_2 \\ x_3 \\ x_4 \end{pmatrix}=\begin{pmatrix} l_2 \\ \dot{l}_2 \\ \theta \\ \dot{\theta} \end{pmatrix}, \mathbf{x}_0=\begin{pmatrix} x_1 \\ x_2 \\ x_3 \\ x_4 \end{pmatrix}\Bigg|_{t=0}, f(\mathbf{x})=\begin{pmatrix} x_2 \\ x_1 x_4^2 - g\cos x_3 - \frac{k}{m}\{(x_1-l_0)+(x_1-s\sin x_3)-l_0\frac{x_1-s\sin x_3}{\sqrt{s^2-2s(x_1\sin x_3)+x_1^2}}\} \\ x_4 \\ -\frac{2}{x_1}(x_2x_4)+\frac{g}{x_1}\sin x_3-\frac{k}{m}s\cos x_3(\frac{l_0}{\sqrt{s^2-2s(x_1\sin x_3)+x_1^2}}-1) \end{pmatrix},$$

$$\mathbf{y}=\begin{pmatrix} l_2 \\ \dot{l}_2 \\ \theta \\ \dot{\theta} \end{pmatrix}=\begin{pmatrix} y_1 \\ y_2 \\ y_3 \\ y_4 \end{pmatrix}, \mathbf{y}\big|_{t=T_{ds}}=\mathbf{x}\big|_{t=T_{ds}} \text{ and } h(\mathbf{y})=\begin{pmatrix} y_2 \\ y_1 y_4^2 - g\cos y_3 - \frac{k}{m}(y_1-l_0) \\ y_4 \\ -\frac{2}{y_1}(y_2y_4)+\frac{g}{y_1}\sin y_3 \end{pmatrix}.$$

The dynamical system representing the motion of the springy legged model with double stance phase obeys the evolution rule, $\dot{\mathbf{x}}=f(\mathbf{x})$ and $\dot{\mathbf{y}}=h(\mathbf{y})$. In other words, the state vector evolves from x_0 as;

$$(\mathbf{x}_0,t=0)\xrightarrow{\dot{\mathbf{x}}=f(\mathbf{x})}(\mathbf{x},t=T_{ds})\wedge \mathbf{y}\big|_{t=T_{ds}}=\mathbf{x}\big|_{t=T_{ds}}\wedge(\mathbf{y},t=T_{ds})\xrightarrow{\dot{\mathbf{y}}=h(\mathbf{y})}(\mathbf{y},t).$$

Evolution of double stance phase

Evolution of single stance phase

Evolution of a whole one step

When I confine my interest to the case in which the model vaults over and makes the next

step, one of the crucial steps in finding a period-one gait is to find out the initial condition that recovers its value at the beginning of the following step. As mentioned before, to initiate the motion from the exact moment when the leg l_2 begins to touch the ground, I confine my analysis to the case of $x_1 = l_0$ at $t = 0$ and $x_3 = \alpha$ at $t = 0$. This set of initial condition captures the behavior of the ground reaction force that is zero before the touch down of the foot but becomes positive after touch down of the foot. Note that the initial conditions for position are replaced with parameter values, l_0 and α, and the only variables in initial conditions are x_2 and x_4, which are related only to initial velocity.

In terms of dynamical system, the period-one gait is equivalent to the fixed point of the Poincaré map. To find the fixed point of the Poincaré map, I need to select a proper Poincaré section and investigate the existence of fixed points. With some selected parameter values and initial speed with which the model does neither fail to vault over nor fly off, I find a fixed point of the Poincaré map.

4.3.1. The Poincaré Section

It is important to select a proper state variable acting as an anchor of the Poincaré section. By following similar arguments mentioned in 3.3.1, the proper Poincaré section can be anchored by the length of l_2. More concretely, the end of a step must be the moment when l_2 becomes the initial value of the l_1. In other words, the Poincaré map corresponding the stride function of this model is defined in the three dimensional Poincaré section Σ, which is

$\Sigma = \{(l_2, \dot{l}_2, \theta, \dot{\theta}) \mid l_2 = l_1|_{t=0} \wedge \dot{l} \in \mathbf{R} \wedge -\pi < \theta < \pi \wedge \dot{\theta} \in \mathbf{R}\}$, where "$\wedge$" means "AND."

4.3.2. Algorithm for Finding Fixed Points of the Poincaré Map

Please see Figure 4-2. Considering that the initial conditions for position are replaced with parameter values l_0 and α, the only variable initial conditions are v_0 and β, which are related to the initial velocity. Therefore, the fixed point can be expressed in terms of these two variables. With the Poincaré section that I selected in 4.3.1, I can evaluate the existence of the period-one gait by investigating whether the velocity vector and the angular displacement θ recover their initial values when y_1 or l_2 recovers the initial value of l_1. With the definitions of $\hat{\mathbf{y}} = \begin{pmatrix} y_2 \\ y_3 \\ y_4 \end{pmatrix} = \begin{pmatrix} \dot{l}_2 \\ \theta \\ \dot{\theta} \end{pmatrix}$, my algorithm for finding such an initial condition is the following:

Step 1 Assume an arbitrary initial velocity.

Step 2 Solve the evolution rule with that initial velocity.

Step 3 Find the minimal positive time when y_1 becomes the initial leg length $l_1(t=0)$, and define the time as T_{ss}.

Step 4 Find the desirable (y_2, y_3, y_4) at T_{ss} to make a period-one gait and define the transpose of this vector as $\hat{\mathbf{y}}_f = (y_{f2}, y_{f3}, y_{f4})^T$

Step 5 Let $\{(y_2(T_{ss})/ y_{f2} - 1), (y_3(T_{ss})/ y_{f3} - 1), (y_4(T_{ss})/ y_{f4} - 1)\}^T$ be the vector ξ. Note that I do not include $(y_1(T_{ss})/ l_1(t=0) - 1)$ so that ξ is in three-dimensional state space instead of four-dimensional state space because y_1 is the variable that acts as an anchor of the Poincaré section, and $(y_1(T_{ss})/ l_1(t=0) - 1)$ should be zero at every step.

Step 6 Minimize the cost function that is the norm of the normalized vector ξ with the initial conditions as variables. The minimum of the cost function should be zero

if any period-one gait exists.

Step 7 Check if this optimal initial condition actually yields a periodic gait that keeps the both springy legs from stretching; check the existence of a period-one gait.

In step 4, desirable state variables at $t = T_{ss}$ can be calculated by decomposing the velocity vector at that moment into radial and transverse components; please see Figure 4-4 . In terms of state variables, to achieve a period-one gait with the initial velocity whose magnitude and the angle are v_0 and β respectively, the system must satisfy

$$\left.\begin{pmatrix} y_1 \\ y_2 \\ y_3 \\ y_4 \end{pmatrix}\right|_{t=T_{ss}} = \left.\begin{pmatrix} l_1 \\ v_0 \sin(\gamma+\beta) \\ -\gamma \\ -\frac{v_0}{l_1}\cos(\gamma+\beta) \end{pmatrix}\right|_{t=0} = \mathbf{y}_f . \qquad \text{Eq 4-9}$$

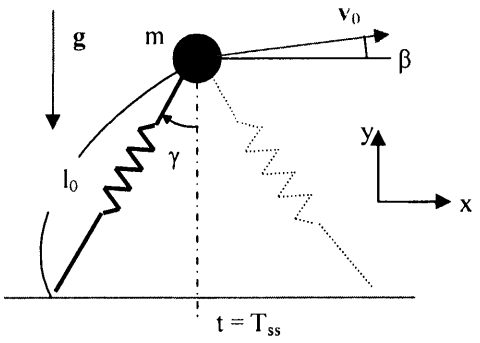

Figure 4-4: The state of the springy legged model at $t = T_{ss}$ for a period-one gait

To optimize the norm in step 6, I use the command "Fminsearch" in MATLAB. This command finds a local minimum of a scalar function of several variables, starting at an initial estimate. I can find an initial condition for a fixed point by changing the initial estimate over the

range where the model does neither fail to vault over nor fly off. The detailed source codes are attached in Appendix B.

4.3.3. The Fixed Point of the Poincaré Map

The parameter values and the initial values for s and θ of the model are shown in Table 4-2. The initial position of the model has unloaded leg l_2 and compressed leg l_1. The unloaded leg l_2 and α determine the relative position of the point mass with respect to the leading foot. Then, stride length s determines the initial compressed length of l_1.

Table 4-2: Parameter and initial state values of the springy legged model with double stance

Parameter	Value
m	10 kg
k	1000 N/m
g	9.81 m/s^2
l_0	1 m
s (at t=0)	0.75 m
α (θ at t=0)	0.4844 rad

With the parameter values in Table 4-2, one fixed point of the Poincaré map that makes the norm of ξ zero is obtained numerically as $\mathbf{x}_0^T$ = (1, -1.092, 0.484, -2.301) corresponding to the initial velocity of v_0 = 2.5465 (m/s) and β = 0.0412 (rad). The state variables with this initial condition are shown in Figure 4-5. I also checked the length of l_1 during the double stance phase, and plot the result in Figure 4-6. All the state variables remain in a physically reasonable domain, and, particularly, the both legs are kept compressed when in contact with the ground. Therefore, I can conclude the existence of a period-one gait.

One thing to clarify is that the uniqueness of the fixed point is not proved analytically.

As mentioned before, I search initial conditions for a fixed point using an algorithm that finds a local minimum of a scalar function, starting at an initial estimate. The used algorithm is a kind of unconstrained nonlinear optimization. Though I find an initial condition for a fixed point by changing the initial estimate over the range where the model can vault over, another fixed point might exist far away from the fixed point found by the local optimization algorithm.

However, if I confine my interest to the fixed point whose speed is comparable with the period-one gait of the springy legged model without double stance, I can focus on the fixed point found above. Hereafter, my analysis will be focused on this fixed point.

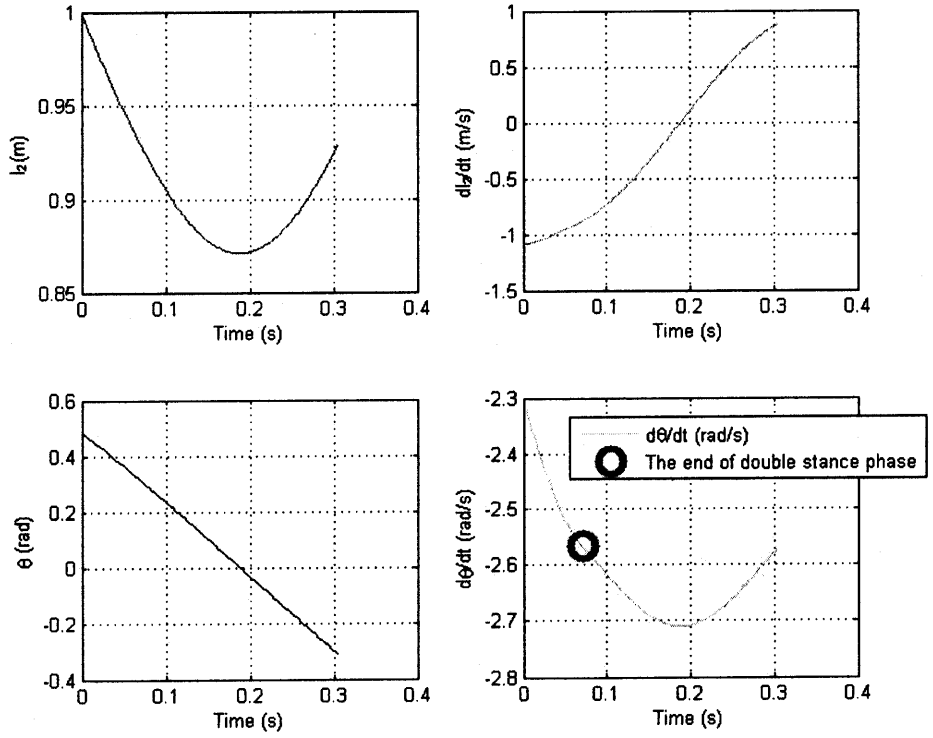

Figure 4-5: The state variables during one step with $v_0 = 2.5465$ (m/s) and $\beta = 0.0412$ (rad)

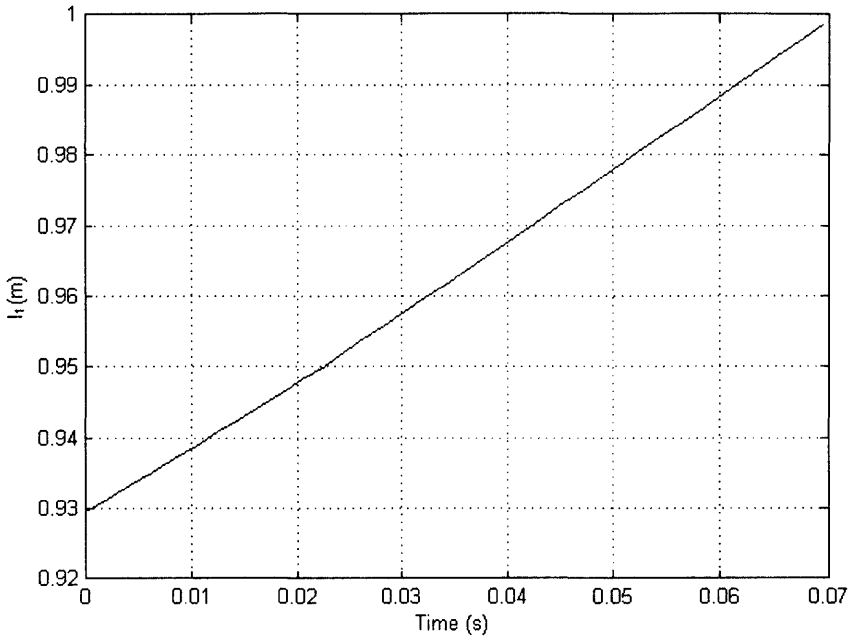

Figure 4-6: l_1 during one step with $v_0 = 2.5465$ (m/s) and $\beta = 0.0412$ (rad)

Please note that the state vector itself is not periodic. With the presence of double stance phase, to make a period-one gait, l_2, for example, must recover the initial value of l_1 rather than the initial value of l_2 itself at the end of one step. Therefore, as can be seen in Figure 4-5, it is natural that l_2 does not recover its starting length to make a period-one gait.

Periodicity of motion of the model at the fixed point can be checked by visualizing the motion of the point mass in the Cartesian coordinate. Converting the state variables to the x and y coordinates, I visualize the trajectory of the point mass with $v_0 = 2.5465$ (m/s) and $\beta = 0.0412$ (rad) in Figure 4-7. Also, the trajectory that is amplified in y direction is shown in Figure 4-8.

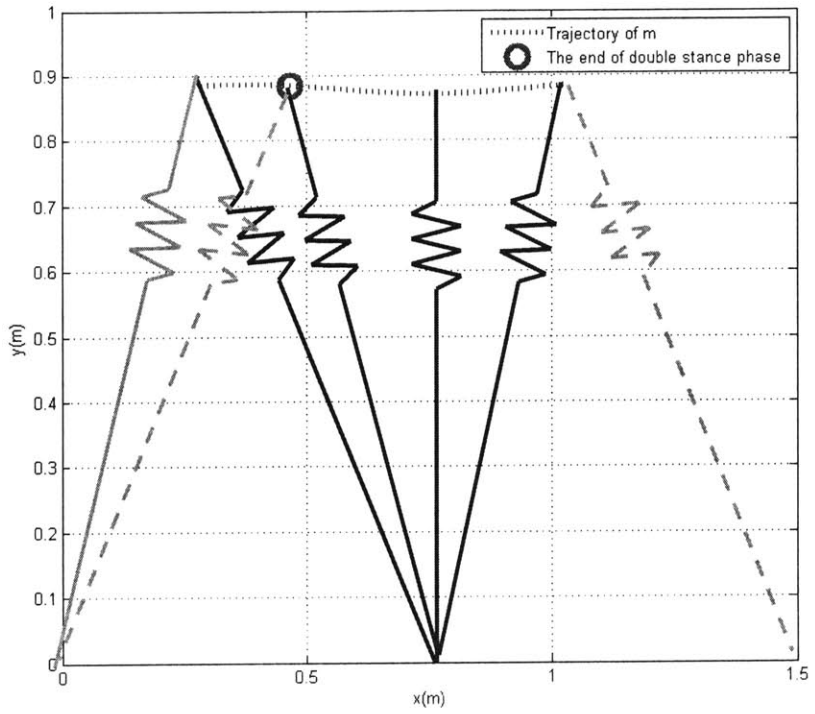

Figure 4-7: The trajectory of the point mass with $v_0 = 2.5465$ (m/s) and $\beta = 0.0412$ (rad)

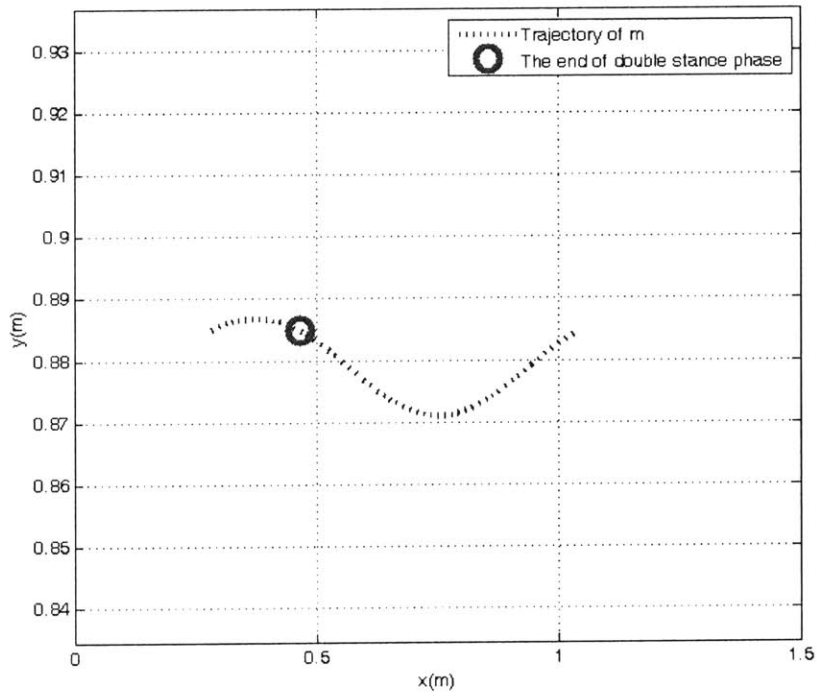

Figure 4-8: The trajectory shown in Figure 4-7, which is amplified in y direction

4.4. Stability of the Fixed Point of Period-One Gait

As mentioned in 1.4, I treat the stride function of each step as a Poincaré map and analyze the stability of the fixed point of the map. To construct the Poincaré map, I need to combine (A) the map whose input and output are the reduced state vectors at the beginning of a step and the end of a step respectively with (B) the map whose input and output are the reduced state vectors of the end of one step and the beginning of the following step respectively. After constructing Poincaré map, I perform stability analysis by following three steps: (1) I find a fixed point of the Poincaré map that generates period-one gait, which was already done in 4.3; (2) I assess the stability by investigating the eigenvalues of the derivative matrix of the Poincaré map at the fixed point; and, (3) I visualize the stability or instability by showing the behavior of the small neighborhood of the fixed point. Definitions of state vector $\mathbf{x}$ and $\mathbf{y}$, reduced state vector $\hat{\mathbf{y}}$, state variable x_i and y_i, vector ξ and evolution rule f and h, which were established in 4.3, are still valid throughout this section. Additionally, I define the reduced state vector $\hat{\mathbf{x}}$ as

$$\hat{\mathbf{x}} = \begin{pmatrix} x_2 \\ x_3 \\ x_4 \end{pmatrix} = \begin{pmatrix} \dot{l}_2 \\ \theta \\ \dot{\theta} \end{pmatrix} \text{ during the double stance phase.}$$

4.4.1. Constructing the Poincaré Map

As mentioned in 4.3.1, I select the length of a springy leg as an indicator of the completion of a step and define the Poincaré section accordingly. I reuse the definition of T_{ds} and T_{ss} introduced in 4.2.2 and 4.3.2; T_{ds} is the minimal time when l_1 becomes l_0, and T_{ss} is the minimal time for the stance leg during the single stance phase, which is y_1, to become the initial leg length of

$l_1(t=0)$, which I define as l^*, hereafter. I also define T_{ss-} and T_{ss+} as the time just before and right after the time T_{ss} respectively.

If I solve the ODE established in 4.2.1, I can obtain a state vector at any time including T_{ds}. Therefore, I can construct a map whose input and output are the reduced state vectors at $t = 0_+$ and $t = T_{ds}$ respectively. Let this map be $\mathbf{f_d}$.

$$\mathbf{f_d} : (\hat{\mathbf{x}}_0, t = 0_+) \xrightarrow{\dot{\mathbf{x}} = f(\mathbf{x})} (\hat{\mathbf{x}}, t = T_{ds}).$$

If I solve the ODE established in 4.2.2, with the initial condition of $\mathbf{y}|_{t=T_{ds}} = \mathbf{x}|_{t=T_{ds}}$, I can obtain a state vector at any time including T_{ss-}. Therefore, I can construct a map whose input and output are the reduced state vectors at $t = T_{ds}$ and $t = T_{ss-}$ respectively. Let this map be $\mathbf{f_s}$.

$$\mathbf{f_s} : (\hat{\mathbf{y}}, t = T_{ds}) \xrightarrow{\dot{\mathbf{y}} = h(\mathbf{y})} (\hat{\mathbf{y}}, t = T_{ss-}).$$

I combine $\mathbf{f_d}$ and $\mathbf{f_s}$ to construct a map whose input and output are the reduced state vectors at $t = 0_+$ and $t = T_{ss-}$. Let this map be $\mathbf{f_1}$.

$$\mathbf{f_1} : (\hat{\mathbf{x}}_0, t = 0) \xrightarrow{\dot{\mathbf{x}} = f(\mathbf{x})} (\hat{\mathbf{x}}, t = T_{ds}) \wedge \hat{\mathbf{y}}|_{t=T_{ds}} = \hat{\mathbf{x}}|_{t=T_{ds}} \wedge (\hat{\mathbf{y}}, t = T_{ds}) \xrightarrow{\dot{\mathbf{y}} = h(\mathbf{y})} (\hat{\mathbf{y}}, t = T_{ss-}).$$

I need to complete the whole map by adding the map whose input and output are the reduced state vectors at $t = T_{ss-}$ and $t = T_{ss+}$ respectively. Let this map be $\mathbf{f_2}$. Because this model does not involve any collision or impulsive force, the acceleration is finite all the time, which means the velocity vector is continuous. The map $\mathbf{f_2}$ can be considered as the transition of a state vector describing the state of the point mass in terms of the corresponding stance leg and can be obtained using the continuity of velocity.

$$\mathbf{f_2} : (\hat{\mathbf{y}}, t = T_{ss-}) \xrightarrow{\textit{continuity of velocity}} (\hat{\mathbf{x}}, t = T_{ss+}).$$

The combination of $\mathbf{f_1}$ and $\mathbf{f_2}$ makes the whole map corresponding to the Poincaré map whose input and output are the reduced state vectors at $t = 0_+$ and $t = T_{ss+}$ respectively. Let the

whole map be **f**.

$$\mathbf{f} = \mathbf{f}_2 \circ \mathbf{f}_1 : (\hat{\mathbf{x}}_0, t = 0_+) \rightarrow (\hat{\mathbf{y}}, t = T_{ss-}) \xrightarrow{\text{continuity of velocity}} (\hat{\mathbf{x}}, t = T_{ss+})$$

The map $\mathbf{f}_2$ can be constructed analytically while $\mathbf{f}_1$ should be constructed numerically. To construct map $\mathbf{f}_1$ with the Poincaré section selected in 4.3.1, I must consider the variation in the stride distance, s. Please note that if the gait is not a period-one gait, the stride distance s can vary step by step. Figure 4-9 shows an example. The leading leg length l_2 is shortened and then grows to reach the length of l*, which is the beginning length of the trailing leg, if I assume that the leg length l_2 reach the length of l* with positive derivative at time $t = T_{ss}$. In the example shown in Figure 4-9, the magnitude of θ at $t = T_{ss}$ is greater than γ_0 and therefore, the step stride, s becomes larger than the stride of the preceding step; $s_1 > s_0$.

Generally, in the case of the springy legged model with double stance phase, I must take care of the modification of the stride length at each mapping because the equation of motion contains the stride length. I achieve this by setting the stride length as a state variable whose derivative is zero during a step. The source code of this algorithm is attached in Appendix B.3.

To construct $\mathbf{f}_2$, I use the assumption that the springy legged model generates a gait in a collisionless manner and the velocity vector is continuous. Figure 4-10 shows the continuity of the velocity at time $t = T_{ss}$. In Figure 4-10, $\mathbf{e}_i$s' are the unit vectors directing radial and transverse directions of the motion of the point mass with respect to the contact point of the corresponding stance leg while **i** and **j** are the unit vector of x and y direction respectively. Also, l_n and φ, which are not constants but variables, represent the length and angle of the stance leg of the new step respectively while l_2 and θ represent the length and angle of the stance leg of the preceding step.

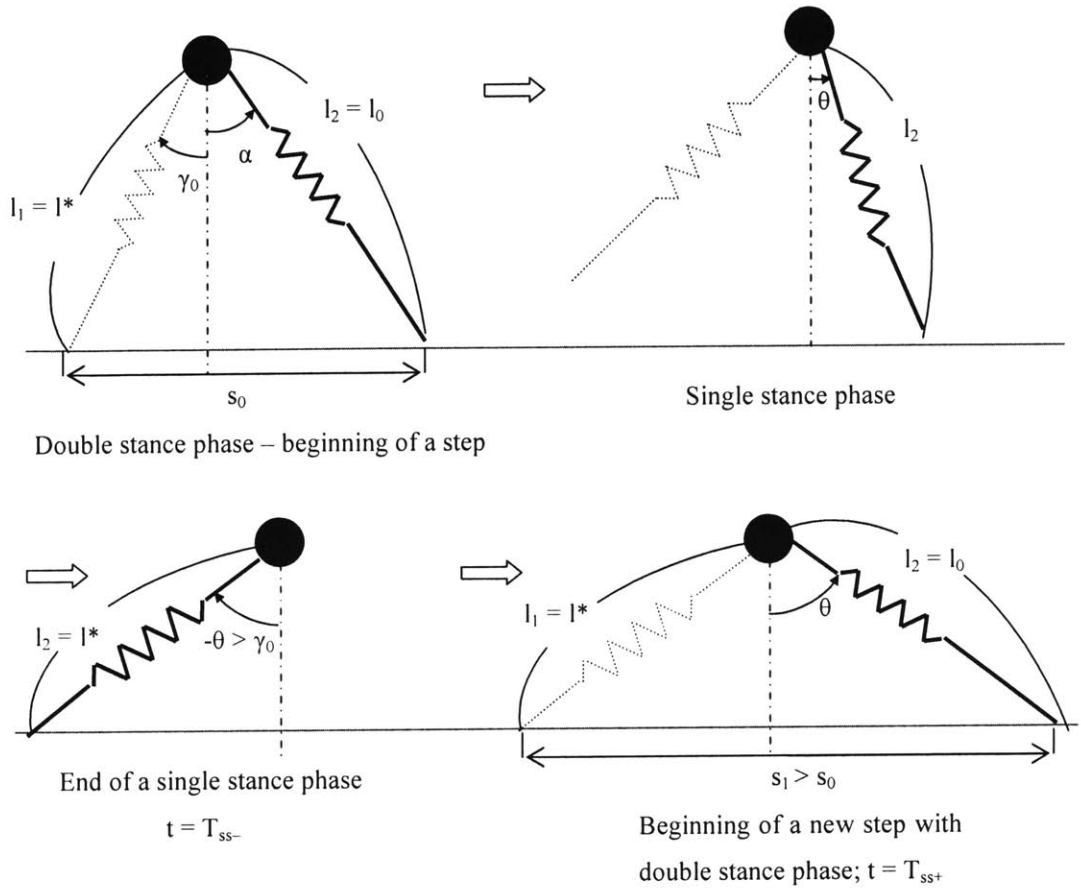

Figure 4-9: An example of a gait of the springy legged model with double stance phase

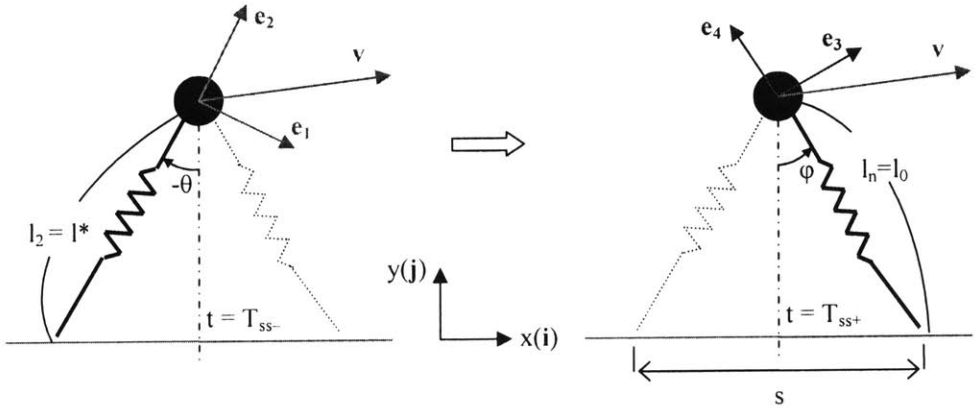

Figure 4-10: Continuity of velocity between the end of a step and the beginning of the next step.

Let η be the value of $-\theta$ at $t = T_{ss}$. As explained in 4.3.1, I need the length of the new stance leg l_n be the unloaded leg length l_0 at $t = T_{ss+}$. Then, φ at $t = T_{ss}$, which I define as β hereafter, and the new stride distance s are determined by geometry because I know the values of l_2 at $t = T_{ss}$, which is l^*, and $-\theta$ at $t = T_{ss}$, which is η, in the preceding step. Please recall that s is also a state variable that is a constant during a step but must be updated at each step. To summarize, at $t = T_{ss}$, $-\theta = \eta$, $\varphi = \beta$, $l_2 = l^*$ and $l_n = l_0$. Using kinematics, I obtain $\mathbf{e_1}$, $\mathbf{e_2}$, $\mathbf{e_3}$ and $\mathbf{e_4}$ as

$$\begin{aligned}
\vec{e}_1 &= (\cos\eta)\mathbf{i} - (\sin\eta)\mathbf{j}, \\
\vec{e}_2 &= (\sin\eta)\mathbf{i} + (\cos\eta)\mathbf{j}, \\
\vec{e}_3 &= (\cos\beta)\mathbf{i} + (\sin\beta)\mathbf{j}, \text{and} \\
\vec{e}_4 &= (-\sin\beta)\mathbf{i} + (\cos\beta)\mathbf{j}.
\end{aligned} \qquad \text{Eq 4-10}$$

Also, by decomposing the velocity vectors at $t = T_{ss-}$ and T_{ss+} into the radial and transverse directions,

$$\vec{v}\Big|_{t=T_{ss-}} = \dot{l}_2\vec{e}_2 + (-l_2\dot{\theta})\vec{e}_1 \text{ and } \vec{v}\Big|_{t=T_{ss+}} = \dot{l}_n\vec{e}_4 + (-l_n\dot{\varphi})\vec{e}_3. \qquad \text{Eq 4-11}$$

Using the continuity of the velocity, $\vec{v}\Big|_{t=T_{ss-}} = \vec{v}\Big|_{t=T_{ss+}}$. Comparing the **i** and **j** components after substituting Eq 4-10 into Eq 4-11,

$$\begin{aligned}
\dot{l}_2(\sin\eta) - l_2\dot{\theta}(\cos\eta) &= -\dot{l}_n(\sin\beta) - l_n\dot{\varphi}(\cos\beta), \text{and} \\
\dot{l}_2(\cos\eta) + l_2\dot{\theta}(\sin\eta) &= \dot{l}_n(\cos\beta) - l_n\dot{\varphi}(\sin\beta)
\end{aligned} \qquad \text{Eq 4-12}$$

In Eq 4-12, as discussed already, $l_2 = l^*$ and $l_n = l_0$ at $t = T_{ss-}$ or T_{ss+}, which is the time of concern. Additionally, I know all the state variables in the preceding step after I solve the ODE numerically and construct the map $\mathbf{f_1}$. Therefore, I know dl_2/dt at $t = T_{ss-}$, η, which equals to $-\theta$ at $t = T_{ss-}$, and $d\theta/dt$ at $t = T_{ss-}$. As a result, I have two unknowns, which are dl_n/dt and $d\varphi/dt$ and two equations, which are given in Eq 4-12. Solving Eq 4-12, I obtain x_2 and x_4 at the beginning of the new step. Note that x_3 at the beginning of the new step is already obtained as β.

To summarize, with the Poincaré section selected in 4.3.1, the whole Poincaré map whose input and output are the reduced state vectors at t= 0_+ and t = T_{ss+} respectively is constructed as the following:

Step 1 Solve the evolution rule obtained in 4.2 with given initial condition, $\mathbf{x}(t=0) = \mathbf{x}_0$.

Step 2 Find the minimal positive time when y_1 becomes the initial value of l_1, which I define as l*, and define the time as T_{ss}.

Step 4 Find the state vector (y_2, y_3, y_4) at T_{ss-}, which is the time just before T_{ss}.

Step 5 Find the state vector (x_2, x_3, x_4) at T_{ss+}, which is the time right after T_{ss} using the continuity of velocity vector. Results are

$$x_3\big|_{t=T_{ss+}} = \varphi\big|_{t=T_{ss+}} = \beta = \cos^{-1}\left(\frac{l^*}{l_0}\cos\eta\right)$$
$$= \cos^{-1}\left(\frac{l^*}{l_0}\cos(-\theta\big|_{t=T_{ss-}})\right) = \cos^{-1}\left(\frac{l^*}{l_0}(-y_3\big|_{t=T_{ss-}})\right) \quad \text{, and}$$

$$\begin{pmatrix} x_2 \\ x_4 \end{pmatrix}\Big|_{t=T_{f+}} = \begin{pmatrix} \dot{l}_n \\ \dot{\varphi} \end{pmatrix} = \begin{pmatrix} -\sin\beta & -l_0\cos\beta \\ \cos\beta & -l_0\sin\beta \end{pmatrix}^{-1} \begin{pmatrix} \dot{l}_2(\sin\eta) - l^*\dot{\theta}(\cos\eta) \\ \dot{l}_2(\cos\eta) + l^*\dot{\theta}(\sin\eta) \end{pmatrix}\Big|_{t=T_{ss-}}.$$

Step 1 ~ 5 yield a map of $\mathbf{f}:(\hat{\mathbf{x}}_0, t=0_+) \rightarrow (\hat{\mathbf{x}}, t=T_{ss+})$.

4.4.2. Stability Analysis

As discussed in 4.3, with the selected initial position of $x_1(t=0) = l_0 \ \wedge \ x_3(t=0) = \alpha$, and the selected parameter values in Table 4-2, there exists a fixed point of the Poincaré map. For the obtained fixed point of $\mathbf{x}_0^T$ = (1, -1.092, 0.484, -2.301), I analyze stability by investigating the eigenvalues of the derivative matrix of the Poincaré map.

Using a numerical method, I obtain the eigenvalues of the derivative matrix of the Poincaré map that is constructed in 4.4.1. The reduced state vector $\hat{\mathbf{x}}$, is a vector in a three-

dimensional state space, and the derivative matrix $\mathbf{J} = \frac{\partial \mathbf{f}}{\partial \hat{\mathbf{x}}}$ has three eigenvalues, which are 5.2587, -0.2447 and 0.4857. The eigenvalue of 5.2587 is located outside the unit circle. This guarantees the instability of the fixed point of the Poincaré map.

To visualize the instability, I investigate the behavior of the small neighborhood of the fixed point. The deviation from the fixed point is caused by the deviation in x_2 ($=dl_2/dt$) so that the value of x_2 of investigated neighborhood varies from -1.122 (m/s) to -1.062 (m/s). Instability is found in this small neighborhood as Figure 4-11 shows.

In Figure 4-11, ε is the difference between x_2 of the investigated point and x_2 of the fixed point, which is -1.092 (m/s). For example, ε = 0.03 corresponds to the case of initial value of $x_2(t=0)$ = -1.062 (m/s). To visualize the behavior of the fixed point, I needed to cut off some residual error due to numerical simulation. I cut off the residual errors less than the minimal error norm of the fixed point, which is 0.001 to zero. The norm of ξ with initial x_2 in [-1.122, 1.062] (m/s) diverges from zero norm of the fixed point as the numbers of mapping increases. This divergence results from the instability of the fixed point.

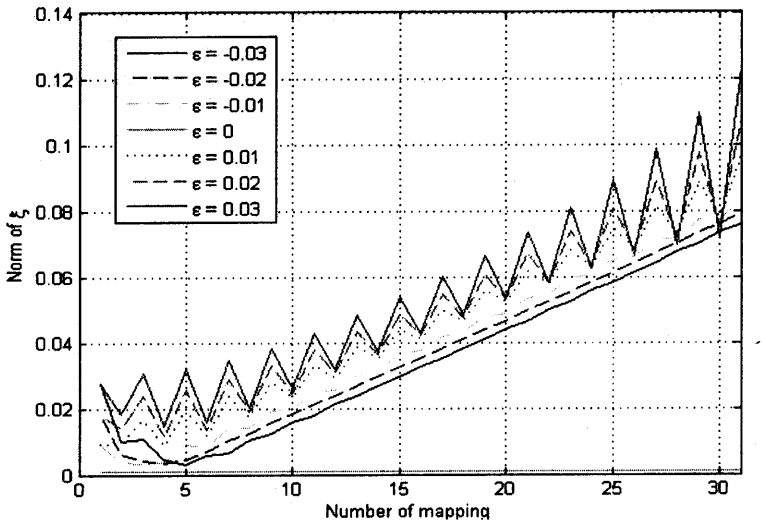

Figure 4-11: Instability of a period-one gait of the springy legged model with double stance

4.5. Analysis of the Contribution of Double Stance to Stability

Considering stability analysis using linearization, let $\hat{\mathbf{x}} = \hat{\mathbf{x}}_{eq} + \xi$, where $\hat{\mathbf{x}}_{eq}$ is a fixed point of a map **f**, and ξ be a vector indicating a very small error. Then,

$$\mathbf{f}(\hat{\mathbf{x}}) = \mathbf{f}(\hat{\mathbf{x}}_{eq} + \xi) = \mathbf{f}(\hat{\mathbf{x}}_{eq}) + \frac{\partial \mathbf{f}}{\partial \hat{\mathbf{x}}}\xi + O(\xi^2)$$

$$\Rightarrow \mathbf{f}(\hat{\mathbf{x}}) - \mathbf{f}(\hat{\mathbf{x}}_{eq}) \cong \frac{\partial \mathbf{f}}{\partial \hat{\mathbf{x}}}\xi.$$

Hence, the maximum magnitude of the eigenvalues of $\mathbf{J} = \frac{\partial \mathbf{f}}{\partial \hat{\mathbf{x}}}$, if it is greater than one, determines the exponent of growth of error magnitude $|\xi|$ when the state vector is aligned with the corresponding eigenvector. Accordingly, a larger value of the maximum eigenvalue magnitude implies stronger instability.

As discussed in 3.4.2, the eigenvalue of the derivative matrix of the Poincaré map outside the unit circle was obtained as 7.6918 in case of the springy legged model without double stance phase. With almost the same parameter values, including the stride length, the maximum magnitude of the eigenvalue decreased from 7.6918 to 5.2587 with the presence of the double stance phase. This result is worthy of further investigation because it suggests the possibility that the double stance phase contributes to the stability of gait. With this motivation, I investigate the eigenvalues of the derivative matrix of the Poincaré map by varying portion of the stride spent in the double stance phase.

Please see Figure 4-12. Let σ be the half of the angle between the two legs with the length of l_0 when the stride distance is given as s. The difference $\delta = \alpha - \sigma$ indicates the extent of the double stance phase. In other words, a large value of $\delta = \alpha - \sin^{-1}(\frac{s}{2l_0})$ means a large double stance phase. In particular, if $\alpha = \sigma$ at the initial position with some progressive velocity,

there is no double stance phase. I investigate cases of δ = 0.06, 0.08 and 0.10 (rad). Table 4-3 shows the results.

The results in Table 4-3 show that increasing the double stance phase does not necessarily decrease the maximal eigenvalue magnitude or the growth rate of the error vector ξ norm. In other words, for a passive walker with springy legs, stability is not expected to appear by simply increasing the portion of the double stance phase.

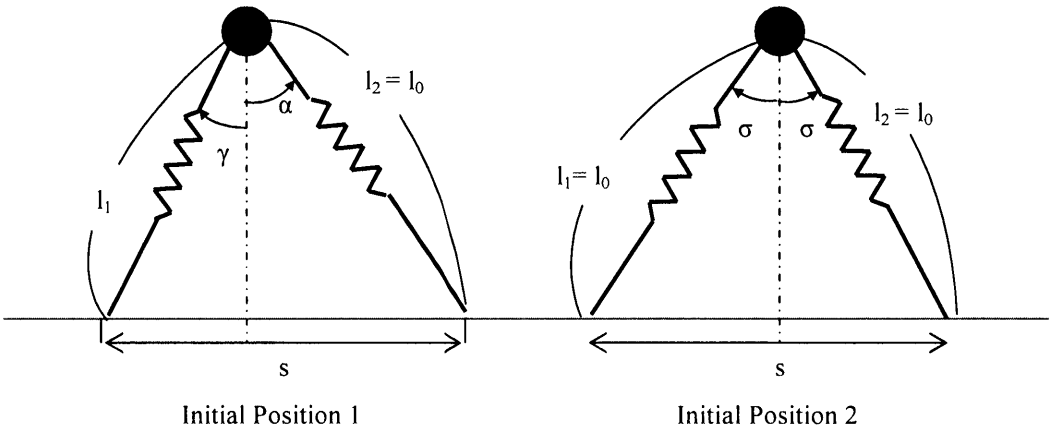

Figure 4-12: Two initial positions of a springy legged model with double stance phase

Table 4-3: Eigenvalues of the derivative matrix of Poincaré map with varying δ

δ	Eigenvalues of the derivative matrix of Poincaré map
0.06	3.5221 and 0.0695 ± j0.476
0.08	2.8618, -0.3554 and -0.2705
0.10	5.2587, -0.2447 and 0.4857

4.6. Summary and Discussion

When I confine my interest to the fixed point whose speed is comparable with the period-one gait of the springy legged model without double stance, the springy legged model with double stance also fails to have a stable period-one gait, just as the springy legged model without double stance does. One thing to note is that in each case of the springy legged model, one of the eigenvalues of the derivative matrix of the Poincaré map representing the stride function is outside the unit circle. Considering the studied systems do not involve any energy dissipation or energy supply, this result is worthy of further investigation. A continuous dynamical system with constant energy conserves the phase space volume and the maximal magnitude of the eigenvalues of the derivative matrix of the map should be unity. In contrast, the derivative matrices of the maps of the studied models have eigenvalues outside the unit circle at fixed points regardless of the constant energy they conserve. One possible reason why the springy legged models have hyperbolic unstable fixed point is that the constraints of the systems are not holonomic. It is known that a conservative system with non holonomic constraints or piecewise holonomic constraints can have a hyperbolic fixed point [14, 15].

One more thing to clarify is that the studied model with double stance phase is not totally passive. To initiate a new double stance phase when the stance leg length becomes the length of the other leg at the beginning of the previous double stance phase, the model must memorize the leg length. However, this active behavior does not involve any kind of energy supply or dissipation. On the contrary, this active behavior is necessary if I want to define the beginning of a step in a manner such that the potential energy of springy legs is constant at every beginning of a step.

In conclusion, the instability of the period-one gaits of the springy legged models motivates introduction of actuation to make a model that achieves a stable periodic gait. With this motivation, the analysis of a simple ankle actuated model will be presented in the next chapter.

5. An Ankle Actuated Model in a Vertical Plane

As discussed in the preceding chapters, a rimless wheel on a slight slope can make a stable period-one gait while a springy legged model cannot have a stable fixed point that generates a period-one gait. The springy legged model walks in a collisionless manner so that the total energy is constant all the time. It suffers no dissipation of energy and no supply of energy. On the other hand, the rimless wheel suffers some loss and compensation of the energy during one step.

In the qualitative analysis of the stability of the rimless wheel in 2.2.4, I mentioned that the stability is based on two facts: (A) constant amount of the work done by gravity, which compensates for the loss of kinetic energy and (B) the constant factor of the reduction of the kinetic energy by collisions.

Therefore, I can reasonably suggest that an active walker with a constant amount of energy supply per step will make a stable gait with loss of kinetic energy due to the collision at each step. I establish an ankle actuated model that is governed by a simple command of ankle torque. This model has a stable fixed point that generates a period-one gait with some proper parameter values.

5.1. Assumptions and Definitions of Parameters

A point mass moves in a vertical plane under the influence of gravity, restrained by rigid massless legs. The swing leg can be instantaneously moved in front of the mass. Please see Figure 5-1 and Table 5-1. Each the leg has two joints—a hip and an ankle.

During a step, the hip joint is assumed as a hinge joint, which cannot apply any torque. However, I assume that the angle between the legs is always reset as 2α at the beginning of a step.

I can achieve this resetting by assuming a feedforward command of fixed angle of attack. Due to the assumption of massless legs, resetting the angle between the legs does not require any energy.

The model has double stance phase. The ankle of the leading leg acts as a hinged joint during the double stance phase and the following single stance phase. On the other hand, the ankle of the other leg, which is the trailing leg, is actuated during the double stance phase.

There are some prior works suggesting models of ankle torque [16, 17]. In this model, I assume that the amount of actuating ankle torque is given by a simple equation that is exactly same as the equation of a linear torsional spring as

$$T = k(\pi - \psi). \qquad \text{Eq 5-1}$$

The torque becomes zero when ψ reaches π, or the double stance ends. Please see Figure 5-1 for the definition of ψ. By virtue of the zero mass of the trailing foot, segment AD can move instantaneously as long as the actuation torque is nonzero. Therefore, I can assume that double stance ends at the very moment when ψ reaches π.

For the sequence of motions of the model please consult Figure 5-1. During the double stance phase, the model acts like four linked bars: imaginary bar AB, bar BC, bar CD and bar DA. At the moment when ψ reaches π, the double stance ends, and the single stance begins. During the single stance, there is no actuation torque, and the dynamics of the swing leg is out of concern because it has no mass; the model acts like an inverted pendulum hinged at point B.

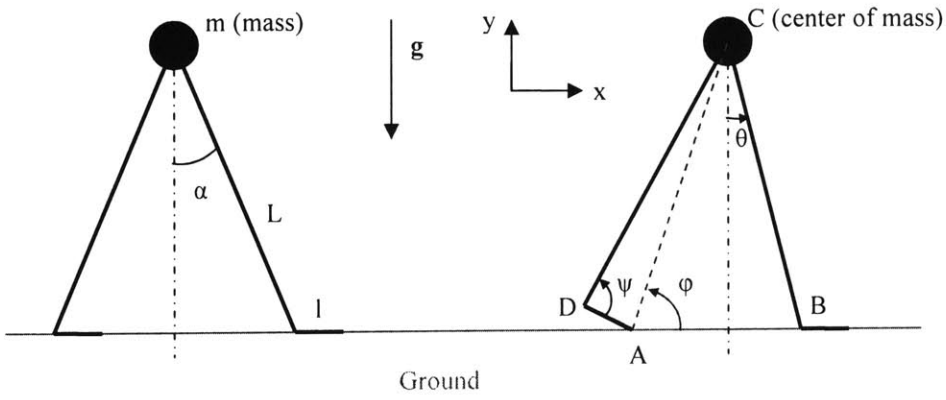

Figure 5-1: An ankle actuated walking model; definitions of parameters

Table 5-1: The meaning of parameters of the ankle actuated model described in Figure 5-1

Parameter	Meaning
m	The mass of the inverted pendulum
k	The torsional spring constant of an ankle
L	The length of a rigid leg
l	The length of a foot.
θ	An angle during the inverted pendulum motion
α	The initial value of θ, or a half of the angle between two legs at the beginning of a step
A	The position of the toe of the leg that is going to be a swing leg; fixed during double stance
B	The hinged ankle of the stance leg; fixed during a double stance phase
C	The Center of mass
D	The actuated ankle of the leg; that is going to be a swing leg

5.2. Equations of Motion

I derive the equation of motion using a Newtonian approach rather than a Lagrangian approach because I want to know the direction and amount of the acting force more explicitly. The degree of freedom of this system is one. Therefore, I choose variable θ and its derivatives to

describe the dynamics of this system. I divide the motion into two parts: double stance phase and single stance phase.

5.2.1. Double Stance Phase

The net force and torque applied to any segment of each leg must be zero because the leg is massless. Please consult Figure 5-1. The actuating torque **T** is applied at point A. Considering the Free Body Diagram (FBD) of the massless bar DA (Figure 5-2), a ground reaction force (GRF) must be applied at point A to compensate for the torque. Then, to make the net force zero, another reaction force with same magnitude and opposite direction must be applied to point D from the bar CD. Similar argument applies to bar CD (Figure 5-3).

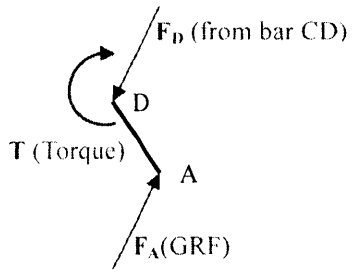

Figure 5-2: The free body diagram of bar DA in Figure 5-1

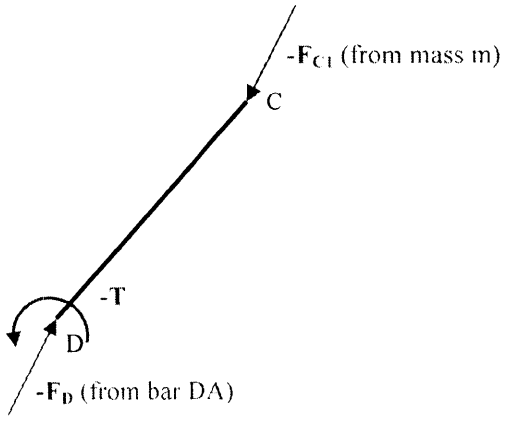

Figure 5-3: The free body diagram of bar CD in Figure 5-1

Note that force $\mathbf{F}_{C1}$ and $-\mathbf{F}_D$ have the same magnitude and opposite direction. Also, as mentioned, the applied torque must balance the torque due to $\mathbf{F}_{C1}$. As a result,

$$\vec{T} = -\vec{r}_{DA} \times \overrightarrow{F_A} = \vec{r}_{DC} \times \overrightarrow{F_{C1}}, \text{ and} \qquad \text{Eq 5-2}$$

$$\overrightarrow{F_A} = -\overrightarrow{F_D} = -\overrightarrow{F_{C1}}. \qquad \text{Eq 5-3}$$

Now, I consider the FBD of the other leg. From the assumption that the leg is massless and the joint is hinged so that it cannot apply torque, only forces that are parallel with the leg are permitted; see Figure 5-4. Again, from the force balance that is necessary due to the assumption of a massless leg,

$$\overrightarrow{F_B} = -\overrightarrow{F_{C2}} \qquad \text{Eq 5-4}$$

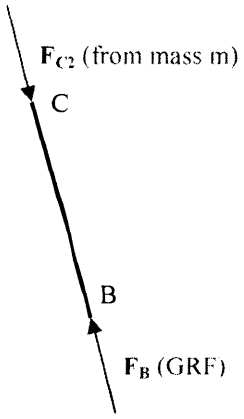

Figure 5-4: The free body diagram of bar BC in Figure 5-1

Finally, I can deduce the forces applied at the mass. The FBD of mass m is shown in Figure 5-5. Please note that from Eq 5-3 and 5-4, the contact forces acting on mass m, which are $\mathbf{F}_{C1}$ and $\mathbf{F}_{C2}$, can be expressed as $\mathbf{F}_A$ and $\mathbf{F}_B$, which are the ground reaction forces. As mentioned above, the direction of $\mathbf{F}_B$ must be parallel with the bar BC. Therefore, the direction of $\mathbf{F}_B$ is explicitly obtained from θ. Also, the direction of $\mathbf{F}_A$ is obtained from Eq 5-2, which shows that $\mathbf{F}_A$ must be aligned with line AC. Therefore, the direction of $\mathbf{F}_A$ is obtained from ψ, which is a function of θ.

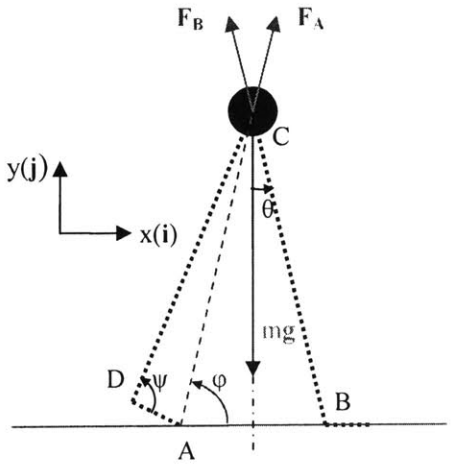

Figure 5-5: The free body diagram of point mass m in Figure 5-1

To derive the equation of motion, let B be the origin.

$$\vec{r}_{BC} = -L\sin\theta\mathbf{i} + L\cos\theta\mathbf{j},$$

$$\vec{v}_{BC} = \frac{d}{dt}\vec{r}_{BC} = -L\dot{\theta}\cos\theta\mathbf{i} - L\dot{\theta}\sin\theta\mathbf{j}, \text{ and}$$

$$\vec{a}_{BC} = \frac{d}{dt}\vec{v}_{CM} = (-L\ddot{\theta}\cos\theta + L\dot{\theta}^2\sin\theta)\mathbf{i} + (-L\ddot{\theta}\sin\theta - L\dot{\theta}^2\cos\theta)\mathbf{j}. \qquad \text{Eq 5-5}$$

Using the linear momentum principle in the x direction,

$$F_A\cos\varphi - F_B\sin\theta = m(-L\ddot{\theta}\cos\theta + L\dot{\theta}^2\sin\theta). \qquad \text{Eq 5-6}$$

Using the linear momentum principle in the y direction,

$$F_A\sin\varphi + F_B\cos\theta - mg = m(-L\ddot{\theta}\sin\theta - L\dot{\theta}^2\cos\theta). \qquad \text{Eq 5-7}$$

Adding Eq 5-6 multiplied by cosθ to Eq 5-7 multiplied by sinθ,

$$mL\ddot{\theta} = mg\sin\theta - F_A(\sin\theta\sin\varphi + \cos\theta\cos\varphi). \qquad \text{Eq 5-8}$$

Let $\angle DAC = \gamma$. From Eq 5-1, 5-2 and 5-3,

$$T = k(\pi - \psi) = F_A l\sin\gamma. \qquad \text{Eq 5-9}$$

From Eq 5-8 and 5-9,

$$mL\ddot{\theta} = mg\sin\theta - \frac{k(\pi-\psi)}{l\sin(\gamma)}(\sin\theta\sin\varphi + \cos\theta\cos\varphi). \qquad \text{Eq 5-10}$$

Now, I can get the equation of motion if I express ψ, γ and φ in terms of θ. This can be achieved by considering the geometry of the model. Let the stride length be s, which equals to 2Lsinα. Then, the length of AB equals to s – l. See Figure 5-6. Using the second cosine rule,

$$L^2 + l^2 - 2Ll\cos\psi = \left|\overline{AC}\right|^2 = L^2 + (s-l)^2 - 2L(s-l)\cos(\frac{\pi}{2}-\theta).$$

Therefore,

$$\cos\psi = \frac{-s^2 + 2sl + 2L(s-l)\cos(\frac{\pi}{2}-\theta)}{2Ll}.$$

Using s = 2Lsinα,

$$\psi = \cos^{-1}\left(\frac{-4L^2\sin^2\alpha + 4Ll\sin\alpha + 2L(2L\sin\alpha - l)\cos(\frac{\pi}{2}-\theta)}{2Ll}\right). \qquad \text{Eq 5-11}$$

Again, using the second cosine rule,

$$L^2 = \left|\overline{AC}\right|^2 + l^2 - 2l\left|\overline{AC}\right|\cos\gamma \text{, where } \left|\overline{AC}\right| = \sqrt{L^2 + (s-l)^2 - 2L(s-l)\cos(\frac{\pi}{2}-\theta)}.$$

Using s = 2Lsinα,

$$\gamma = \cos^{-1}\left(\frac{(2L\sin\alpha - l)^2 + l^2 - 2L(2L\sin\alpha - l)\cos(\frac{\pi}{2}-\theta)}{2l\sqrt{L^2 + (2L\sin\alpha - l)^2 - 2L(2L\sin\alpha - l)\cos(\frac{\pi}{2}-\theta)}}\right). \qquad \text{Eq 5-12}$$

Finally, using the geometry,

$$\tan\varphi = \frac{L\cos\theta}{s - l - L\sin\theta} = \frac{L\cos\theta}{2L\sin\alpha - l - L\sin\theta} \quad , \text{or}$$

$$\varphi = \tan^{-1}\left(\frac{L\cos\theta}{2L\sin\alpha - l - L\sin\theta}\right). \qquad \text{Eq 5-13}$$

From Eq 5-11, 5-12 and 5-13, I get the expressions of ψ, γ and φ in terms of θ. Eq 5-10, combined with Eq 5-11, 5-12 and 5-13, yields the equation of motion.

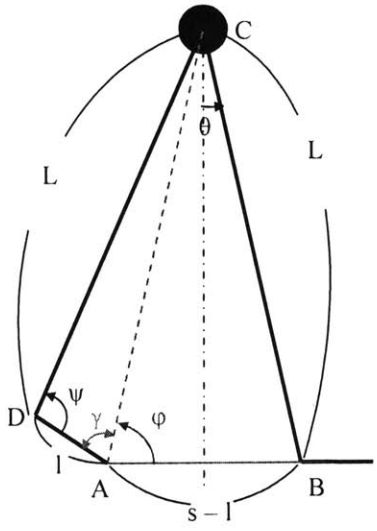

Figure 5-6: The geometry of the ankle actuated model during double stance phase

5.2.2. Single Stance Phase

During the single stance phase, the model obeys a motion of a simple inverted pendulum, which is already studied in 2.2.4, and the equation of motion becomes

$$\ddot{\theta} = \frac{g}{L}\sin\theta. \qquad \text{Eq 5-14}$$

5.3. Ground Reaction Forces

Zero or negative ground reaction forces imply that the foot is detached from the ground. Therefore, it is of great importance to investigate whether the ground reaction forces become zero or negative. I divide analysis into two parts: double stance phase and single stance phase.

5.3.1. Ground Reaction Forces during Double Stance Phase

Assuming that $\mathbf{F}_A$ points towards the +x and +y direction and $\mathbf{F}_B$ points towards the -x and +y direction during the double stance phase. I can satisfy these constraints by setting proper value of α, L and l. Then, F_A and F_B, which are the magnitude of $\mathbf{F}_A$ and $\mathbf{F}_B$ respectively, must satisfy Eq 5-6 and 5-7 with positive values. If F_A or F_B obtained from Eq 5-6 and 5-7 becomes zero or negative at some moment during the double stance phase, at least one foot of the model will leave the floor during the double stance phase, which is unreasonable. My goal is to maintain F_A and F_B positive throughout the double stance phase.

Ground Reaction Force at A: $\mathbf{F_A}$

F_A is positive as long as the torque **T** is applied the in assumed direction. Therefore, I don't have to worry about F_A.

Ground Reaction Force at B: $\mathbf{F_B}$

F_B can be negative if (1) F_A is so excessive that the mass m is lifted regardless of gravity, or (2) the velocity is so excessive that the mass m is lifted due to centrifugal force. Therefore, I need to investigate the explicit form of F_B.

Substituting Eq 5-7 multiplied by cosθ from Eq 5-6 multiplied by sinθ,

$$(F_A\cos\varphi - F_B\sin\theta)\sin\theta - F_A\sin\varphi\cos\theta - F_B\cos^2\theta + mg\cos\theta = mL\dot{\theta}^2, \text{ or}$$

$$F_B = F_A(\cos\varphi\sin\theta - \sin\varphi\cos\theta) + mg\cos\theta - mL\dot{\theta}^2$$

From Eq 9, $F_A = \dfrac{k(\pi - \psi)}{l\sin\gamma}$, and

$$F_B = \frac{k(\pi - \psi(\theta))}{l\sin\gamma(\theta)}(\cos\varphi(\theta)\sin\theta - \sin\varphi(\theta)\cos\theta) + mg\cos\theta - mL\dot{\theta}^2. \quad \text{Eq 5-15}$$

From Eq 5-11, 5-12 and 5-13, ψ, γ and φ can be expressed in terms of θ. Therefore, I can obtain the ground reaction force $F_B(t)$ after I solve the equation of motion (Eq 5-10) expressed in terms of θ and $d^2\theta/dt^2$.

Let me assume that $\theta < \pi/4 < \varphi$ during the double stance phase. Actually, this assumption is reasonable considering the geometry of a model that resembles the geometry of humans. Under this assumption, $(\cos\varphi\sin\theta - \sin\varphi\cos\theta)$ becomes negative. Then, it can be easily seen that large F_A due to large k or large speed due to large dθ/dt jeopardize F_B to be negative. This result agrees with my intuition mentioned above.

5.3.2. Ground Reaction Forces during Single Stance Phase

The single stance phase is simply a motion of an inverted pendulum, and the condition that keeps the model from flying off is same as the condition investigated in 2.1.2. To summarize, I need to keep $mg\cos\theta - m\frac{v^2}{l} = f(\theta)$ above zero to keep the model from flying off. The function $f(\theta)$, which equals to the magnitude of the ground reaction force $\mathbf{F}_B$, has the minimum at the end of the single phase because cosθ has the minimum at $\theta = -\alpha$, and v^2 has the maximum at the

same moment of $\theta = -\alpha$. Therefore, the sign of $f(-\alpha)$ indicates whether the model flies off or not.

5.4. Existence of a Period-One Gait

The actuation torque is a function of θ. The work done by the torque is written $W = \int_{\theta_0}^{\theta_f} T(\theta) d\theta$, where θ_f indicates the value of θ at the end of the double stance phase. From Eq 5-1, actuation torque T is a function of ψ, which is determined by the state variable θ. Work done by T is not path-dependent, and the initial and final values of ψ in each step are constant by my assumption. Therefore, the energy supplied by actuation torque via ankle is constant per step as long as the model has a proper speed so that (1) it can vault over to make the next step, (2) both feet do not leave the floor during the double stance phase, and (3) the model does not fly off during the single stance phase.

On the other hand, as studied in the passive rimless wheel in 2.1.2, the kinetic energy is reduced by the factor of $\cos^2 2\alpha$ per each collision. Considering the stable period-one gait of the rimless wheel on a slope is due to a constant amount of work done by gravity and a constant reduction ratio of the kinetic energy, it can reasonably be inferred that this ankle actuated model has a stable period-one gait.

As can be seen from Eq 5-10 and 5-14, the equations of motion of this system are second-order differential equations. I choose θ and $d\theta/dt$ as a set of state variables. By the assumption of the fixed angle of attack α, the end of a step is defined by the variable θ. In other words, the Poincaré section is anchored at the state where $\theta = -\alpha$. Then, the periodicity can be examined by investigating whether $d\theta/dt$ recovers its value at the end of one step. Figure 5-7 shows the sequence of the whole step.

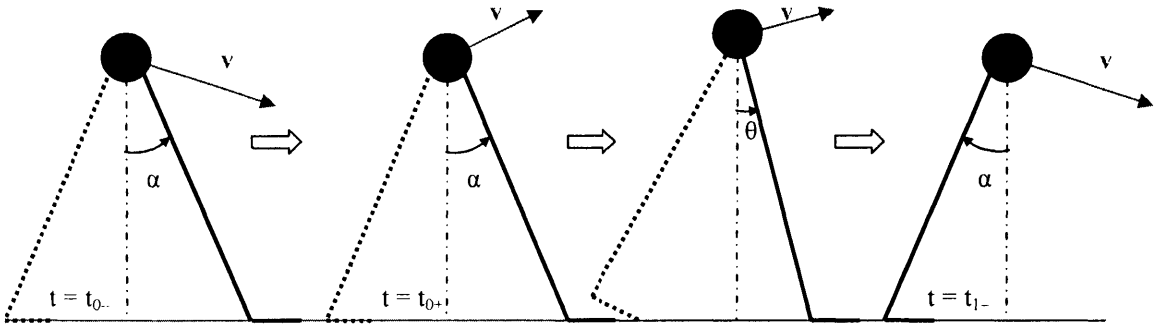

Figure 5-7: The sequence of a step of the ankle actuated model; collisions occur at $t=t_0$ and $t=t_1$

Let collisions occur at $t = t_0$ and $t = t_1$. To make a period-one gait,

$$\vec{v}(t = t_{0-}) = \vec{v}(t = t_{1-}) \equiv \vec{v}_C \text{, or } \dot{\theta}(t = t_{0-}) = \dot{\theta}(t = t_{1-}) \equiv \dot{\theta}_C$$

In terms of energy, the loss of kinetic energy due to the collision must be exactly compensated for by the work done by the ankle torque. Therefore, to make a period-one gait,

$$W = \int_{\theta_0}^{\theta_f} T(\theta)d\theta = \int_{\psi_0}^{\psi_f} k(\pi - \psi)d\psi = \int_{\frac{\pi}{2}-\alpha}^{\pi} k(\pi - \psi)d\psi = \frac{1}{2}mv_C^2(1 - \cos^2 2\alpha), \text{ or}$$

$$\frac{1}{2}k(\frac{\pi}{2} + \alpha)^2 = \frac{1}{2}mv_C^2(1 - \cos^2 2\alpha) = \frac{1}{2}mL^2\dot{\theta}_C^2(1 - \cos^2 2\alpha).$$

Among the roots of the above equation, considering I am interested in the case of progressing model, only positive v_C or negative $\dot{\theta}_C$ is valid. Therefore, a unique value of v_C or $\dot{\theta}_C$ for a period-one gait, if any, is obtained as

$$v_C = \sqrt{\frac{k(\frac{\pi}{2} + \alpha)^2}{m(1 - \cos^2 2\alpha)}}, \text{ or } \dot{\theta}_C = -\frac{1}{L}\sqrt{\frac{k(\frac{\pi}{2} + \alpha)^2}{m(1 - \cos^2 2\alpha)}}. \qquad \text{Eq 5-16}$$

Analytically, this value of $\dot{\theta}_C$ must be the unique value of a fixed point of the Poincaré map (1) if the model can vault over and make the next step with this speed, (2) if this speed keeps the model from lifting the front foot during the double phase stance, and (3) if this speed keeps the model from flying off during the single phase stance. After checking the ground reaction forces

using Eq 5-15 and the argument in 5.3.2, it turns out that the tuned value of v_C does not always satisfy all three conditions of (1), (2) and (3) above.

For example, please see the parameter values of Table 5-2 except the value of k. With the spring stiffness of k = 10 (N-m/rad), F_B, which is obtained from Eq 5-15, shows that the value of v_C, which is tuned by Eq 5-16, cannot keep the GRF F_B positive during the double stance phase, which means that the front foot is lifted by large amount of F_A due to the large torque. The beginning of a step, which suffers the largest active torque, might have the highest possibility to generate negative GRF F_B. This result is shown in Figure 5-8. On the other hand, Figure 5-9 shows the case of k = 8 (N-m/rad), when the tuned value of v_C succeed to keep the front foot on the ground.

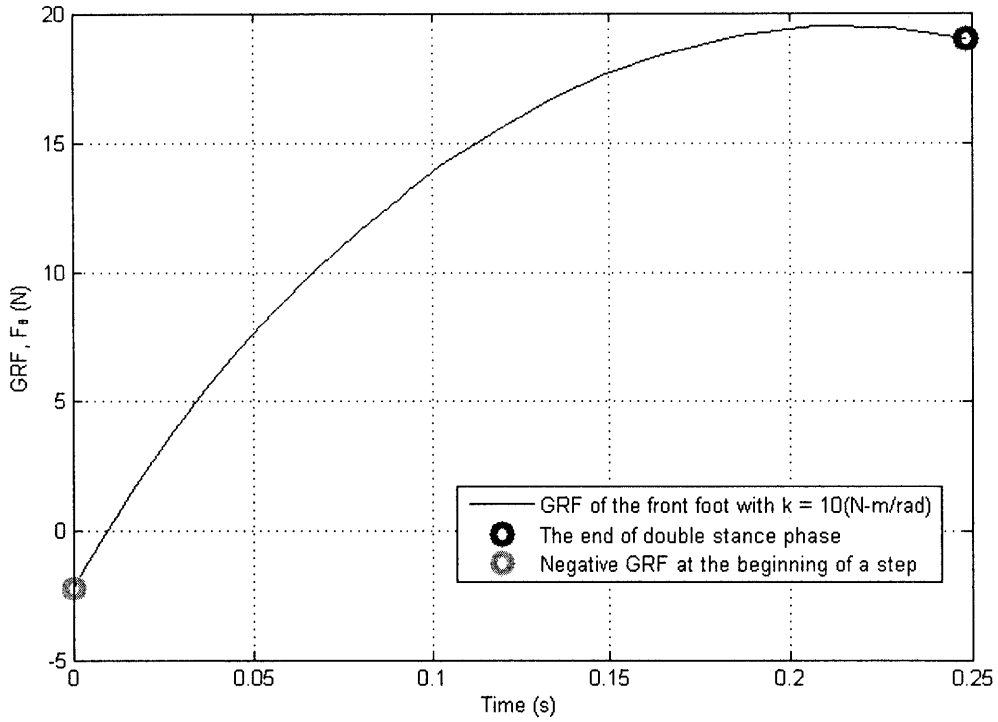

Figure 5-8: Ground reaction force F_B of the ankle actuated model with k = 10 (N-m/rad)

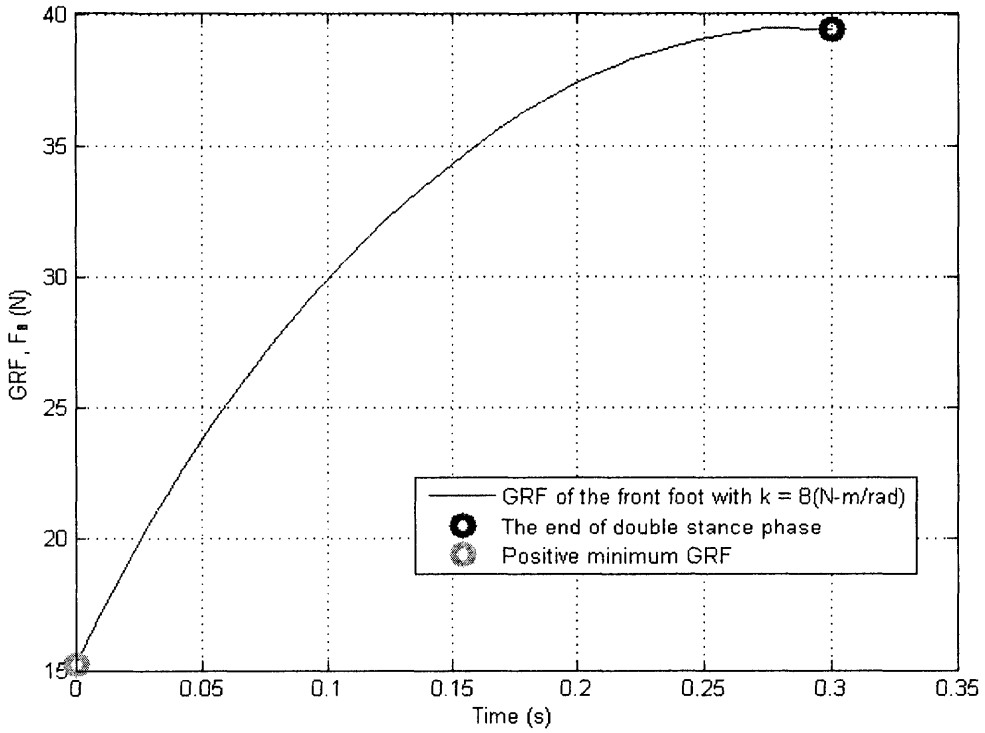

Figure 5-9: Ground reaction force F_B of the ankle actuated model with k = 8 (N-m/rad)

Some excessively low value of k, which generates excessively low torque, cannot supply enough energy to make the model vault over. For example, with k = 4 (N-m/rad) and other parameter values shown in Table 5-2, the tuned value of v_C cannot make the model vault over. In this case there is no fixed point of the Poincaré map.

The lower limit of the stiffness that marginally makes the model vault over can be obtained analytically. Let the marginal stiffness be k_C. The speed of the fixed point obtained from Eq 5-16 comes from the energy balance

$$\frac{1}{2}k_C(\frac{\pi}{2}+\alpha)^2 = \frac{1}{2}mv_C{}^2(1-\cos^2 2\alpha). \qquad \text{Eq 5-17}$$

In the case in which the model vaults over marginally, the kinetic energy of the model becomes zero at the apex of $\theta = 0$. Therefore,

$$\frac{1}{2}mv_C^2\cos^2 2\alpha + \frac{1}{2}k_C(\frac{\pi}{2}+\alpha)^2 + Lmg\cos\alpha = Lmg + 0. \qquad \text{Eq 5-18}$$

From Eq 5-17 and 18,

$$k_C(\frac{\pi}{2}+\alpha)^2 = \frac{2Lmg(1-\cos\alpha)}{(1-\cos^2 2\alpha)} \quad \text{or} \quad k_C = \frac{2Lmg(1-\cos\alpha)}{(1-\cos^2 2\alpha)(\frac{\pi}{2}+\alpha)^2}. \qquad \text{Eq 5-19}$$

For the parameter values shown in Table 5-2, k_C is 4.49 (N-m/rad). Therefore, the stiffness of 4 (N-m/rad) cannot make the model vault over with the speed of the fixed point, as mentioned above.

In conclusion, with parameter values of Table 5-2, the tuned value of v_C satisfies all the three conditions of (1), (2) and (3) and makes the fixed point of the stride function. In particular, the minimum GRF at B is about 15N during the double stance phase and 38 N during the single stance phase. Both values are positive. The state variables of θ and dθ/dt with the parameter values in Table 5-2 and the value of v_C, which is tuned by Eq 5-16, are plotted in Figure 5-10.

Table 5-2: Selected parameter values for the period-one gait of the ankle actuated model

Parameter	Value
m	10 kg
k	8 N-m/rad
L	1 m
l	0.2 m
g	9.81 m/s^2
α	π/6

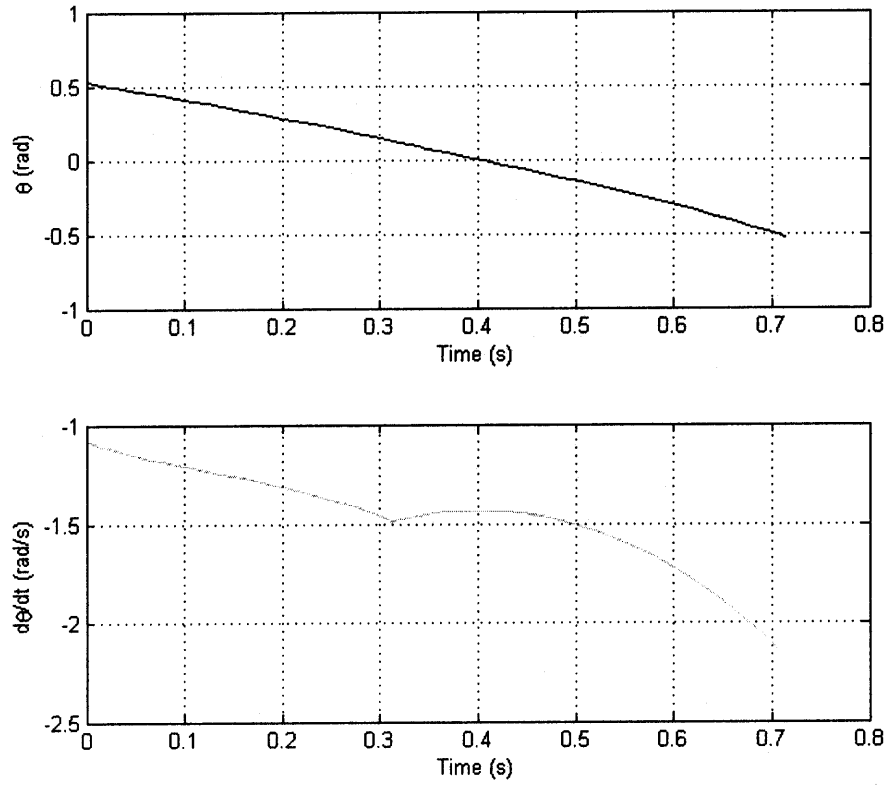

Figure 5-10: θ and $\dot{\theta}$ with the selected parameter values and initial speed for the period-one gait

5.5. Poincaré Map and Stability Analysis

As mentioned in 1.4, I treat the stride function of each step as a Poincaré map and analyze the stability of the fixed point of the map. To construct the Poincaré map, I need to combine (A) the map whose input and output are the reduced state vectors at the beginning of a step and the end of a step respectively with (B) the map whose input and output are the reduced state vectors of the end of one step and the beginning of the following step respectively. Alternatively, I can construct the Poincaré map analytically, using work-energy principle.

After constructing Poincaré map in either way, I perform stability analysis by following

three steps: (1) I find the fixed point of the Poincaré map that generates the period-one gait, which was already done in 5.4; (2) I assess stability by investigating the eigenvalues of the derivative matrix of the Poincaré map at the fixed point; and, (3) I visualize the stability or instability by showing the behavior of the small neighborhood of the fixed point.

5.5.1. Constructing the Poincaré Map

The equations of motion, which determine the evolution rule of the dynamical system were obtained in 5.2. For the double stance phase, I define $\mathbf{x} = \begin{pmatrix} \theta \\ \dot{\theta} \end{pmatrix} = \begin{pmatrix} x_1 \\ x_2 \end{pmatrix}$ and $U(\mathbf{x})$ as

$$\frac{d}{dt}\begin{pmatrix} x_1 \\ x_2 \end{pmatrix} = \begin{pmatrix} x_2 \\ \frac{1}{mL}[mg\sin x_1 - \frac{k(\pi - \psi(x_1))}{l\sin(\gamma(x_1))}\{\sin x_1 \sin\varphi(x_1) + \cos x_1 \cos\varphi(x_1)\}] \end{pmatrix} = U(\mathbf{x}), \text{ Eq 5-20}$$

where ψ, γ and φ can be expressed in terms of $x_1 (= \theta)$ from Eq 5-11, 5-12 and 5-13. The initial condition of Eq 5-20 is given by $\mathbf{x}_0 = \begin{pmatrix} \alpha \\ \dot{\theta}_0 \end{pmatrix}$.

For the single stance phase, I define $\mathbf{y} = \begin{pmatrix} \theta \\ \dot{\theta} \end{pmatrix} = \begin{pmatrix} y_1 \\ y_2 \end{pmatrix}$ and the evolution rule $V(\mathbf{y})$ as

$$\frac{d}{dt}\begin{pmatrix} y_1 \\ y_2 \end{pmatrix} = \begin{pmatrix} y_2 \\ \frac{g}{L}\sin y_1 \end{pmatrix} = V(\mathbf{y}). \qquad \text{Eq 5-21}$$

The initial condition of Eq 5-21 is obtained by continuity of the state vector at the transition from the double stance phase to the single stance phase. At the end of the double stance, there is no impulsive force acting of the system, and therefore, the state variables, which are the angular displacement and angular velocity, are continuous. Let T_{ds} be the time when ψ becomes π. In other words, at $t = T_{ds}$, the double stance phase ends and the single stance phase begins. By continuity of the state vector,

$$\left.\begin{pmatrix} y_1 \\ y_2 \end{pmatrix}\right|_{t=T_{ds}} = \left.\begin{pmatrix} x_1 \\ x_2 \end{pmatrix}\right|_{t=T_{ds}} . \qquad \text{Eq 5-22}$$

Eq 5-22 serves as the initial condition of Eq 5-21.

As mentioned in 5.4, I select the angle θ as an indicator of the completion of a step and define the Poincaré section Σ as

$$\Sigma = \{(\theta,\dot{\theta}) \,|\, \theta = \pm\alpha \wedge \dot{\theta} \in \mathbf{R}\} .$$

To define Poincaré map in this selected Poincaré section, I define the reduced state vectors as the following: $\hat{\mathbf{x}} = (\dot{\theta}) = (x_2)$ during double stance phase and $\hat{\mathbf{y}} = (\dot{\theta}) = (y_2)$ during single stance phase. Also, I define T_{ss} as the time when x_2 (= θ) becomes $-\alpha$ and collision occurs. Accordingly, time T_{ss-} and T_{ss+} are defined as the time just before and right after the time T_{ss} respectively.

If I solve Eq 5-20 with any given initial condition, I can obtain a state vector at any time including T_{ds}. Therefore, I can construct a map whose input and output are the reduced state vectors at $t = 0_+$ and $t = T_{ds}$ respectively. Let this map be $\mathbf{f_d}$.

$$\mathbf{f_d} : (\hat{\mathbf{x}}_0, t = 0_+) \xrightarrow{\dot{\mathbf{x}}=U(\mathbf{x})} (\hat{\mathbf{x}}, t = T_{ds}) .$$

If I solve Eq 5-21, with the initial condition of Eq 5-22 or $\mathbf{y}|_{t=T_{ds}} = \mathbf{x}|_{t=T_{ds}}$, I can obtain a state vector at any time including T_{ss-}. Therefore, I can construct a map whose input and output are the reduced state vectors at $t = T_{ds}$ and $t = T_{ss-}$ respectively. Let this map be $\mathbf{f_s}$.

$$\mathbf{f_s} : (\hat{\mathbf{y}}, t = T_{ds}) \xrightarrow{\dot{\mathbf{y}}=V(\mathbf{y})} (\hat{\mathbf{y}}, t = T_{ss-}) .$$

I combine $\mathbf{f_d}$ and $\mathbf{f_s}$ to construct a map whose input and output are the reduced state vectors at $t = 0_+$ and $t = T_{ss-}$. Let this map be $\mathbf{f_1}$.

$$\mathbf{f_1} : (\hat{\mathbf{x}}_0, t = 0) \xrightarrow{\dot{\mathbf{x}}=U(\mathbf{x})} (\hat{\mathbf{x}}, t = T_{ds}) \wedge \hat{\mathbf{y}}|_{t=T_{ds}} = \hat{\mathbf{x}}|_{t=T_{ds}} \wedge (\hat{\mathbf{y}}, t = T_{ds}) \xrightarrow{\dot{\mathbf{y}}=V(\mathbf{y})} (\hat{\mathbf{y}}, t = T_{ss-}) .$$

I need to complete the whole map by adding the map whose input and output are the reduced state vectors at t = T_{ss-} and t = T_{ss+} respectively. Let this map be $\mathbf{f}_2$. Map $\mathbf{f}_2$ can be otained by analyzing the collision, which is done in 2.1.2.

$$\mathbf{f}_2 : (\hat{\mathbf{y}}, t = T_{ss-}) \xrightarrow{Collision} (\hat{\mathbf{x}}, t = T_{ss+}) .$$

The combination of $\mathbf{f}_1$ and $\mathbf{f}_2$ makes the whole map corresponding to the Poincaré map whose input and output are the reduced state vectors at t = 0_+ and t = T_{ss+} respectively. Let the whole map be **f**.

$$\mathbf{f} = \mathbf{f}_2 \circ \mathbf{f}_1 : (\hat{\mathbf{x}}_0, t = 0_+) \rightarrow (\hat{\mathbf{y}}, t = T_{ss-}) \xrightarrow{Collision} (\hat{\mathbf{x}}, t = T_{ss+})$$

The map $\mathbf{f}_2$ can be constructed analytically while $\mathbf{f}_1$ should be constructed numerically. To construct $\mathbf{f}_2$, I use the result of the analysis in 2.1.2 and obtain

$$\hat{\mathbf{x}}\Big|_{t=T_{ss+}} = \begin{pmatrix} \theta \\ \dot{\theta} \end{pmatrix}\Bigg|_{t=T_{ss+}} = \begin{pmatrix} -\theta \\ (\cos 2\alpha)\dot{\theta} \end{pmatrix}\Bigg|_{t=T_{ss-}} = \begin{pmatrix} \alpha \\ (\cos 2\alpha)\dot{\theta} \end{pmatrix}\Bigg|_{t=T_{ss-}} .$$

To summarize, with the selected Poincaré section of $\Sigma = \{(\theta, \dot{\theta}) \,|\, \theta = \pm\alpha \wedge \dot{\theta} \in \mathbf{R}\}$, the whole Poincaré map whose input and output are the reduced state vectors at t= 0_+ and t = T_{ss+} respectively is constructed numerically as the following:

Step 1 Solve the evolution rule of Eq 5-20 and 5-21 with initial condition, $\mathbf{x}(t=0) = \mathbf{x}_0$.

Step 2 Find the minimal positive time when y_1 becomes $-\alpha$, and define the time as T_{ss}.

Step 4 Find the state vector (y_2, y_3, y_4) at T_{ss-}, which is the time just before T_{ss}.

Step 5 Find the state vector (x_2, x_3, x_4) at T_{ss+}, which is the time right after T_{ss} using the analysis of the collision.

On the other hand, I can also construct the Poincaré map analytically using work energy principle. Following the argument in Appendix A.1, the Poincaré map becomes

$$\dot{\theta}(t = T_{ss+}) = -\frac{\cos 2\alpha}{L}\sqrt{L^2\dot{\theta}_{0+}{}^2 + \frac{k}{m}(\frac{\pi}{2}+\alpha)^2} = \mathbf{f}(\dot{\theta}_{0+}), \text{ where } \dot{\theta}_{0+} = \dot{\theta}(t = 0_+). \text{ Eq 5-23}$$

5.5.2. Stability Analysis

Stability Analysis Using the Derivative Matrix of the Poincaré Map

As discussed in 5.4, with the selected parameter values in Table 5-2, there exists a fixed point of the Poincaré that keeps the both feet from flying off. Eq 5-16 provides the analytical solution of the fixed point. Considering Eq 5-16 determines the speed just before the collision when the system is at the fixed point, $\dot{\theta}(t = 0_+)$ at the fixed point becomes

$$\dot{\theta}(t = 0_+)_{\text{fixed}} = -\frac{\cos 2\alpha}{L}\sqrt{\frac{k(\frac{\pi}{2}+\alpha)^2}{m(1-\cos^2 2\alpha)}}. \qquad \text{Eq 5-24}$$

From Eq 5-23, the derivative matrix of the map becomes

$$\frac{\partial \mathbf{f}(\hat{\mathbf{x}}_0)}{\partial \hat{\mathbf{x}}_0} = -\cos 2\alpha \frac{\dot{\theta}_{0+}}{\sqrt{\dot{\theta}_{0+}{}^2 + \frac{k(\frac{\pi}{2}+\alpha)^2}{mL^2}}}, \text{ where } \dot{\theta}_{0+} = \dot{\theta}(t = 0_+).$$

Therefore, the derivative matrix of the Poincaré map at the fixed point becomes

$$\left.\frac{\partial \mathbf{f}(\hat{\mathbf{x}}_0)}{\partial \hat{\mathbf{x}}_0}\right|_{\text{fixed}} = \left.-\cos 2\alpha \frac{\dot{\theta}_{0+}}{\sqrt{\dot{\theta}_{0+}{}^2 + \frac{k(\frac{\pi}{2}+\alpha)^2}{mL^2}}}\right|_{\dot{\theta}_{0+} = -\frac{\cos 2\alpha}{L}\sqrt{\frac{k(\frac{\pi}{2}+\alpha)^2}{m(1-\cos^2 2\alpha)}}} = \cos^2 2\alpha.$$

With parameter value of $\alpha = \pi/6$ rad, the eigenvalue of the derivative matrix of the

Poincaré map at the fixed point is obtained analytically as 0.25, which is located inside the unit circle. This guarantees the asymptotic stability of the fixed point of the map. Furthermore, if I confine the range of α to $(0, \pi/4)$, which is also reasonable for human bipedal walking, that the eigenvalue of the derivative matrix of the Poincaré map at the fixed point is $\cos^2 2\alpha$ implies that increasing step size increases α and further increases stability.

On the other hand, using numerical method, I also obtain the eigenvalues of the derivative matrix of the Poincaré map. With the selected parameter values in Table 5-2, the eigenvalue of the derivative matrix of the Poincaré map at the fixed point that is obtained numerically is 0.25, which is same as the result from analytic work.

Visualization of Asymptotic Stability

I check if the analytically obtained fixed point behaves like a fixed point of the Poincaré map that is numerically constructed. Then, I investigate the behavior of the small neighborhood of this fixed point. From Eq 5-16 and the selected parameter values, the angular speed just before a collision is 2.1631 (rad/s) when the system is at its fixed point. The angular speed in the investigated neighborhood varies from 1.8631 (rad/s) to 2.4631 (rad/s). Asymptotic stability is found in this small neighborhood as Figure 5-11 shows.

In Figure 5-11, $(d\theta/dt)_0$ is $d\theta/dt$ just before a collision when the system is at the fixed point, and ε is the difference between the investigated angular speed just before a collision and $(d\theta/dt)_0$. For example, $\varepsilon = 0.3$ corresponds to the angular speed of 2.4631 (rad/s). The green line with $\varepsilon = 0$, which indicates the angular speed of 2.1631 (rad/s), shows the behavior of the fixed point obtained analytically. The constant zero deviation means that the analytically obtained fixed point is truly a fixed point of the Poincaré map that does not change its state variables with increasing numbers of mapping. The various angular speeds in [1.8631, 2.4631] (rad/s), converge to $(d\theta/dt)_0$ of the fixed

point as the numbers of mapping increases. This convergence indicates that the fixed point is asymptotically stable.

However, the asymptotic stability can be observed only when this system is guaranteed to vault over and not to fly off the floor at every step. In other words, the velocity of the point mass must satisfy (1), (2) and (3) in 5.4. For example, if the initial speed is so small that the system fails to vault over, it cannot show a stable fixed point. Therefore, obviously, the convergence on the state of the fixed point is not a global but a local behavior that is guaranteed only when the model vaults over and does not fly off the ground. However, the local behavior of convergence implies that the period-one gait of the ankle actuated model is stable even in the presence of small perturbations.

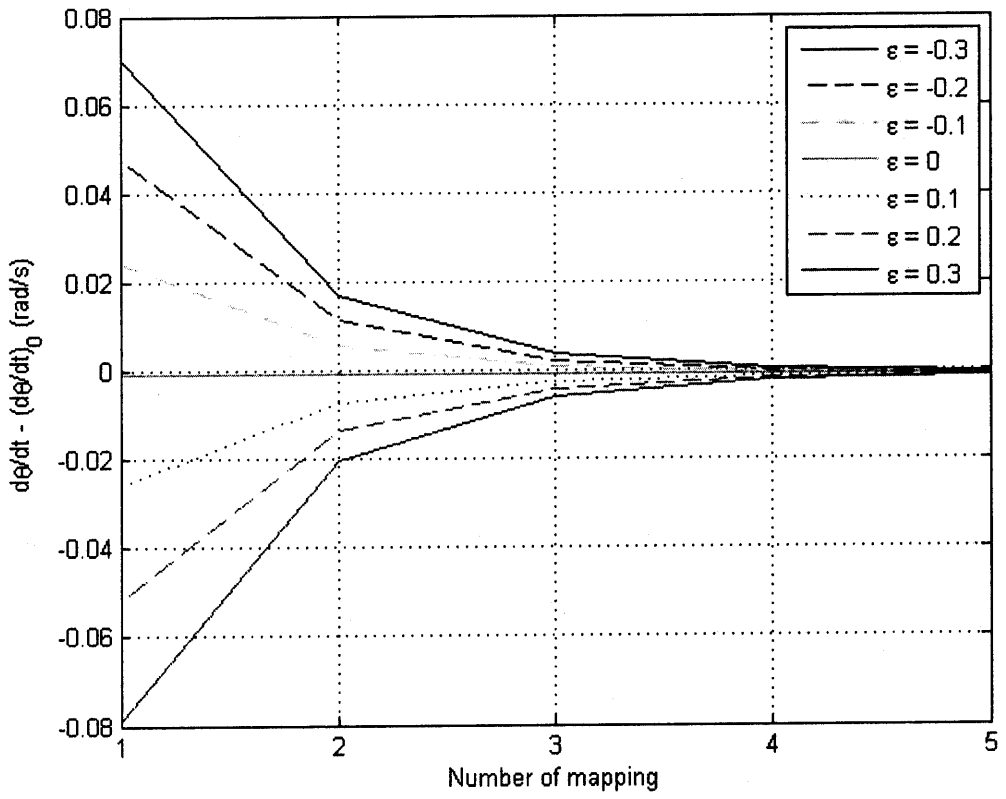

Figure 5-11: Asymptotic stability of the period-one gait of the ankle actuated model

5.6. Discussion and Future Work

5.6.1. Discussion

The ankle actuated model succeeds in making a stable period-one gait on horizontal ground. This success is analogous to the stable period-one gait of the rimless wheel on a slight slope, which was studied in 2.2. As with the rimless wheel on a slight slope, this ankle actutated model obtains constant energy by external force at every step while the kinetic energy is lost by a constant reduction ratio due to collisions. Consequently, the analysis of the ankle actuated model and the rimless wheel on a slope gives the fundamental intuition how the stability of period-one gait can be achieved.

Particularly, related to the rehabilitation strategy, one possible way to assist a patient to make a stable period-one gait on a horizontal ground is to supply constant energy through an ankle robot assuming that collision in every step dissipates the kinetic energy with a constant or almost constant ratio. This result suggests that an ankle robot with a simple actuation or control algorithm that supplies constant energy per step may be effective for rehabilitation of locomotion.

5.6.2. Future Work

This study can provide a theoretical foundation to support the usage of a therapy robot module for the ankle for rehabilitation of locomotion. I aim to make future work so that the analysis can support practical design of an ankle robot controller.

In the model studied, the applied torque is a linear function of ankle angle. However, ankle torque actuation using time rather than angle as the dependent variable may be more convenient for practical application of the ankle robot. I need to investigate whether the actuation

algorithm whose reference variable is time can yield a stable gait of a simple bipedal model. Extended from this investigation, I can further test different ankle torque profiles and investigate how the dynamics of the model varies with different ankle torques.

Another thing to clarify is that the constant work done per step depends on the assumption of massless feet that can instantaneously move with some finite ankle torque. The actuation always supplies kinetic energy because the trailing toe is attached to the ground as long as ankle torque is non zero, for the foot is massless. However, in the application of a practical ankle robot, each segment has mass that is not negligible. Therefore, in the application of a real ankle robot, I need to check whether the actuation always supplies kinetic energy to the body.

6. Balancing Using Ankle Torque in a Frontal Plane

An analysis of the contribution of ankle torque to balancing on one foot in a frontal plane is a starting point for analysis of the role of frontal plane ankle torque during locomotion. In fact, the analysis of balancing in standing is more than a starting point. In terms of input effort, balancing with one foot in a frontal plane requires less effort in walking than in standing. This argument is based on two observations: (1) balancing with nonzero progressive speed needs smaller torque in a frontal plane than balancing with zero speed; and, (2) balancing in walking only requires the body does not to fall before the swing foot becomes the next stance foot. Although it is not obvious whether (1) is valid for human gait and balancing, I will show (1) is valid at least for an inverted pendulum in a later part of this chapter. Consequently, if I succeed to make a model that stands stably using ankle torque control in a frontal plane, it also implies that a similar model can walk stably using smaller ankle torque in a frontal plane.

Another motivation of the analysis of balancing with ankle torque is the development of a therapy robot module for the ankle. An ankle robot developed by Newman Laboratory at MIT provides simultaneous control of inversion/eversion motion as well as plantar/dorsiflexion motion. Inversion/eversion torque control studied in this chapter may be used to assist or rehabilitate frontal-plane balance using the therapy robot module for the ankle.

With these motivations, I analyze the effect of inversion/eversion torque from an ankle joint on balanced standing in the presence of small perturbations. I describe a model representing the human balancing with one foot and analyze the dynamics of the system in state space representation. Considering the maximum ankle torque a human can apply, I design a controller to minimize input effort, which is ankle torque, and deviation from the fixed point via optimal control. Then, I confirm results using simulation

6.1. Assumptions and Definitions of Parameters

I treat balancing with one foot in a frontal plane as controlling a double inverted pendulum with torque input at one joint. The free body diagram of the model and the meaning of parameters are shown in Figure 6-1 and Table 6-1.

In Figure 6-1, point A and B represent an ankle and the middle point of two hips respectively. Controlled torque is applied at point A while point B is a hinge connected with passive elements—a torsional spring and a damper. As a result, hip torque of this model is not voluntarily modified though the passive elements supplies necessary torque to hold the upper body when the spring is sufficiently stiff to provide static stability for the upper body in upright pose. I analyze the dynamics of a double inverted pendulum with a general geometry that can illustrate human bodies.

Considering the model represents a human standing with one foot, C_1, which is the center of mass of lower body, is deviated from the line AB. Therefore, I have to take the angles α and γ into account as parameter values. For example, suppose a human lift the right foot slightly and want to balance with the left foot. Point A represents the ankle and ground contact point of the left foot while point B represents the middle point of the left and right hips. In frontal plane, the center of mass of the lower body must be aligned with the line from B to the middle point of both feet. Therefore, C_1 should be deviated from line AB

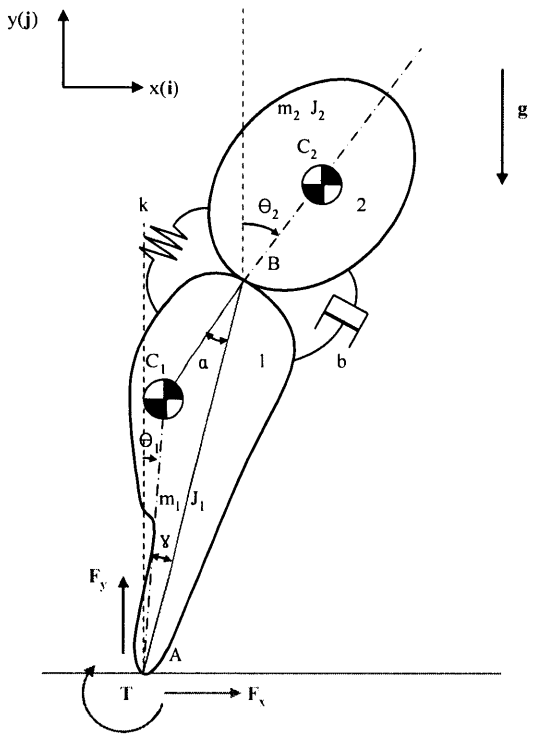

Figure 6-1: The free body diagram of the ankle controlled model in a frontal plane

Table 6-1: The meaning of parameters of the ankle controlled model in a frontal plane

Parameter	Meaning
Body 1	The lower body
Body 2	The upper body
m_1, m_2	The mass of each body
J_1, J_2	The moment of inertia of each body
θ_1, θ_2	The angular displacement of each body during the inverted pendulum motion
C_1, C_2	The center of mass of each body
A	The ankle joint
B	The middle point of two hip joints
α	Angle of $\angle ABC_1$
γ	Angle of $\angle BAC_1$
k	The stiffness of the torsional spring
b	The damping coefficient of the torsional damper

6.2. Equations of Motion

I derive the equations of motion using a Newtonian approach and confirm the result using a Lagrangian approach. I need to know the ground reaction forces in the x and y directions to assess whether the necessary friction coefficient is reasonable. The free body diagram is shown in Figure 6-1.

Body 1

The angular momentum principle about point B gives,

$$\frac{d}{dt}\overrightarrow{H_B} + \overrightarrow{v_B} \times \overrightarrow{P} = \overrightarrow{M_B} .$$

Since $\mathbf{v}_B$ // $\mathbf{P}$,

$$\frac{d}{dt}\overrightarrow{H_B} = \overrightarrow{M_B} . \qquad \text{Eq 6-1}$$

Here,

$$\overrightarrow{H_B} = \overrightarrow{H_{C1}} + \vec{P} \times \vec{r}_{C1B} = J_1\dot{\theta}_1(-\mathbf{k}) + \vec{P} \times r_{C1B}\{\sin(\alpha+\gamma+\theta_1)\mathbf{i} + \cos(\alpha+\gamma+\theta_1)\mathbf{j}\}, \text{ and}$$

$$\vec{P} = m_1\dot{\theta}_1 r_{AC1}(\cos\theta_1\mathbf{i} - \sin\theta_1\mathbf{j}) .$$

Therefore,

$$\overrightarrow{H_B} = J_1\dot{\theta}_1(-\mathbf{k}) + m_1\dot{\theta}_1 r_{AC1} r_{C1B}\{\cos\theta_1\cos(\alpha+\gamma+\theta_1) + \sin\theta_1\sin(\alpha+\gamma+\theta_1)\}\mathbf{k} .$$

Using $\cos\theta_1\cos(\alpha+\gamma+\theta_1) + \sin\theta_1\sin(\alpha+\gamma+\theta_1) = \cos(\alpha+\gamma)$,

$$\overrightarrow{H_B} = [J_1\dot{\theta}_1 - m_1\dot{\theta}_1 r_{AC1} r_{C1B}\cos(\alpha+\gamma)](-\mathbf{k}), \text{ and}$$

$$\frac{d}{dt}\overrightarrow{H_B} = [J_1 - m_1 r_{AC1} r_{C1B}\cos(\alpha+\gamma)]\ddot{\theta}_1(-\mathbf{k}) . \qquad \text{Eq 6-2}$$

Now, $\mathbf{M}_B$ is calculated

$$\overrightarrow{M_B} = T(-\mathbf{k}) + \vec{r}_{BC1} \times m_1\vec{g} + \vec{r}_{BA} \times \vec{F} + k(\theta_2 - \theta_1 - \theta_0)(-\mathbf{k}) + b(\dot{\theta}_2 - \dot{\theta}_1)(-\mathbf{k}),$$

where $\vec{F} = F_x\mathbf{i} + F_y\mathbf{j}$, and θ_0 is the unloaded angular displacement of the torsional spring. Therefore,

$$\overrightarrow{M_B} = T(-\mathbf{k}) + r_{C_1B}m_1 g\sin(\alpha+\gamma+\theta_1)(\mathbf{k}) + r_{BA}\{-\sin(\gamma+\theta_1)\mathbf{i} - \cos(\gamma+\theta_1)\mathbf{j}\}\times\{F_x\mathbf{i}+F_y\mathbf{j}\} + k(\theta_2-\theta_1-\theta_0)(-\mathbf{k}) + b(\dot{\theta}_2-\dot{\theta}_1)(-\mathbf{k}), \text{ or}$$

$$\overrightarrow{M_B} = [T - r_{C_1B}m_1 g\sin(\alpha+\gamma+\theta_1) + r_{BA}\{F_y\sin(\gamma+\theta_1) - F_x\cos(\gamma+\theta_1)\} + k(\theta_2-\theta_1-\theta_0) + b(\dot{\theta}_2-\dot{\theta}_1)](-\mathbf{k}) \quad \text{Eq 6-3}$$

From Eq 6-1, Eq 6-2 and Eq 6-3,

$$[J_1 - m_1 r_{AC_1} r_{C_1B}\cos(\alpha+\gamma)]\ddot{\theta}_1 = T - r_{C_1B}m_1 g\sin(\alpha+\gamma+\theta_1) + k(\theta_2-\theta_1-\theta_0) + b(\dot{\theta}_2-\dot{\theta}_1) + r_{BA}\{F_y\sin(\gamma+\theta_1) - F_x\cos(\gamma+\theta_1)\}. \quad \text{Eq 6-4}$$

Body 2:

The angular momentum principle about point B gives,

$$\frac{d}{dt}\overrightarrow{H_B} + \overrightarrow{v_B}\times\overrightarrow{P} = \overrightarrow{M_B}. \quad \text{Eq 6-5}$$

Here,

$$\overrightarrow{H_B} = \overrightarrow{H_{C_2}} + \vec{P}\times\vec{r}_{C_2B} = J_2\dot{\theta}_2(-\mathbf{k}) + m_2(\vec{v}_B + \vec{v}_{BC_2})\times\vec{r}_{C_2B}, \text{ where}$$

$$\vec{v}_B = \dot{\theta}_1 r_{AB}\{\cos(\theta_1+\gamma)\mathbf{i} - \sin(\theta_1+\gamma)\mathbf{j}\},$$

$$\vec{r}_{C_2B} = r_{BC_2}\{-\sin\theta_2\mathbf{i} - \cos\theta_2\mathbf{j}\} \text{ and}$$

$$\vec{v}_{BC_2} = \dot{\theta}_2 r_{BC_2}\{\cos\theta_2\mathbf{i} - \sin\theta_2\mathbf{j}\}.$$

Therefore,

$$\overrightarrow{H_B} = J_2\dot{\theta}_2(-\mathbf{k}) + m_2\dot{\theta}_1 r_{AB} r_{BC_2}\{-\cos(\theta_1+\gamma)\cos\theta_2 - \sin(\theta_1+\gamma)\sin\theta_2\}\mathbf{k} + m_2\dot{\theta}_2(r_{BC_2})^2\{-\cos\theta_2\cos\theta_2 - \sin\theta_2\sin\theta_2\}\mathbf{k}.$$

Using $\cos\theta_2\cos(\theta_1+\gamma)+\sin\theta_2\sin(\theta_1+\gamma)=\cos(\theta_1+\gamma-\theta_2)$,

$$\overrightarrow{H_B}=[J_2\dot{\theta}_2+m_2\dot{\theta}_1 r_{AB}r_{BC2}\cos(\theta_1+\gamma-\theta_2)+m_2\dot{\theta}_2(r_{BC2})^2](-\mathbf{k}), \text{ and}$$

$$\frac{d}{dt}\overrightarrow{H_B}=[\{J_2+m_2(r_{BC2})^2\}\ddot{\theta}_2+m_2 r_{AB}r_{BC2}\{\cos(\theta_1+\gamma-\theta_2)\ddot{\theta}_1-\dot{\theta}_1(\dot{\theta}_1-\dot{\theta}_2)\sin(\theta_1+\gamma-\theta_2)\}](-\mathbf{k}). \quad \text{Eq 6-6}$$

Now, $\mathbf{M}_B$ is calculated

$$\overrightarrow{M_B}=\vec{r}_{BC2}\times m_2\vec{g}+k(\theta_2-\theta_1-\theta_0)(\mathbf{k})+b(\dot{\theta}_2-\dot{\theta}_1)(\mathbf{k}), \text{ or}$$

$$\overrightarrow{M_B}=\{r_{BC2}m_2 g\sin\theta_2-k(\theta_2-\theta_1-\theta_0)-b(\dot{\theta}_2-\dot{\theta}_1)\}(-\mathbf{k}). \quad \text{Eq 6-7}$$

On the other hand,

$$\overrightarrow{v_B}\times\overrightarrow{P}=\vec{v}_B\times m_2(\vec{v}_B+\vec{v}_{BC2})=m_2(\vec{v}_B\times\vec{v}_{BC2}), \text{ where}$$

$$\vec{v}_B=\dot{\theta}_1 r_{AB}\{\cos(\theta_1+\gamma)\mathbf{i}-\sin(\theta_1+\gamma)\mathbf{j}\} \text{ and}$$

$$\vec{v}_{BC2}=\dot{\theta}_2 r_{BC2}\{\cos\theta_2\mathbf{i}-\sin\theta_2\mathbf{j}\}.$$

Therefore,

$$\overrightarrow{v_B}\times\overrightarrow{P}=m_2\dot{\theta}_1\dot{\theta}_2 r_{AB}r_{BC2}\{-\cos(\theta_1+\gamma)\sin\theta_2+\sin(\theta_1+\gamma)\cos\theta_2\}\mathbf{k}.$$

Using $-\cos(\theta_1+\gamma)\sin\theta_2+\sin(\theta_1+\gamma)\cos\theta_2=\sin(\theta_1+\gamma-\theta_2)$,

$$\overrightarrow{v_B}\times\overrightarrow{P}=-m_2\dot{\theta}_1\dot{\theta}_2 r_{AB}r_{BC2}\sin(\theta_1+\gamma-\theta_2)(-\mathbf{k}). \quad \text{Eq 6-8}$$

From Eq 6-5, Eq 6-6, Eq 6-7 and Eq 6-8,

$$\begin{aligned}&\{J_2+m_2(r_{BC2})^2\}\ddot{\theta}_2+m_2 r_{AB}r_{BC2}\{\cos(\theta_1+\gamma-\theta_2)\ddot{\theta}_1-\dot{\theta}_1(\dot{\theta}_1-\dot{\theta}_2)\sin(\theta_1+\gamma-\theta_2)\}\\&-m_2\dot{\theta}_1\dot{\theta}_2 r_{AB}r_{BC2}\sin(\theta_1+\gamma-\theta_2)=\{r_{BC2}m_2 g\sin\theta_2-k(\theta_2-\theta_1-\theta_0)-b(\dot{\theta}_2-\dot{\theta}_1)\}.\end{aligned} \quad \text{Eq 6-9}$$

Now, I use the linear momentum principle to find expressions for F_x and F_y. Let CM be the center of mass of the whole double inverted pendulum system. From the linear momentum principle,

$$(m_1+m_2)\vec{a}_{CM}=(m_1+m_2)\frac{d^2}{dt^2}\vec{r}_{CM}=\sum\vec{F}=F_x\mathbf{i}+\{F_y-(m_1+m_2)g\}\mathbf{j}. \qquad \text{Eq 6-10}$$

The left hand side of Eq 6-10 is obtained as follows:

$$\vec{r}_{CM}=\frac{1}{m_1+m_2}(m_1\vec{r}_{AC_1}+m_2\vec{r}_{AC_2})=\frac{1}{m_1+m_2}\{m_1\vec{r}_{AC_1}+m_2(\vec{r}_{AB}+\vec{r}_{BC_2})\}$$
$$=\frac{1}{m_1+m_2}[m_1r_{AC_1}(\sin\theta_1\mathbf{i}+\cos\theta_1\mathbf{j})+m_2r_{AB}\{\sin(\theta_1+\gamma)\mathbf{i}+\cos(\theta_1+\gamma)\mathbf{j}\}+m_2r_{BC_2}(\sin\theta_2\mathbf{i}+\cos\theta_2\mathbf{j})]$$
$$=\frac{1}{m_1+m_2}[\{m_1r_{AC_1}\sin\theta_1+m_2r_{AB}\sin(\theta_1+\gamma)+m_2r_{BC_2}\sin\theta_2\}\mathbf{i}+\{m_1r_{AC_1}\cos\theta_1+m_2r_{AB}\cos(\theta_1+\gamma)+m_2r_{BC_2}\cos\theta_2\}\mathbf{j}],$$

$$\vec{v}_{CM}=\frac{d}{dt}\vec{r}_{CM}$$
$$=\frac{1}{m_1+m_2}[\dot{\theta}_1\{m_1r_{AC_1}\cos\theta_1+m_2r_{AB}\cos(\theta_1+\gamma)\}+\dot{\theta}_2m_2r_{BC_2}\cos\theta_2]\mathbf{i}$$
$$-\frac{1}{m_1+m_2}[\dot{\theta}_1\{m_1r_{AC_1}\sin\theta_1+m_2r_{AB}\sin(\theta_1+\gamma)\}+\dot{\theta}_2m_2r_{BC_2}\sin\theta_2]\mathbf{j} \qquad \text{and}$$

$$(m_1+m_2)\vec{a}_{CM}=(m_1+m_2)\frac{d}{dt}\vec{v}_{CM}$$
$$=[\ddot{\theta}_1\{m_1r_{AC_1}\cos\theta_1+m_2r_{AB}\cos(\theta_1+\gamma)\}-\dot{\theta}_1^2\{m_1r_{AC_1}\sin\theta_1+m_2r_{AB}\sin(\theta_1+\gamma)\}$$
$$+\ddot{\theta}_2m_2r_{BC_2}\cos\theta_2-\dot{\theta}_2^2m_2r_{BC_2}\sin\theta_2]\mathbf{i}$$
$$-[\ddot{\theta}_1\{m_1r_{AC_1}\sin\theta_1+m_2r_{AB}\sin(\theta_1+\gamma)\}+\dot{\theta}_1^2\{m_1r_{AC_1}\cos\theta_1+m_2r_{AB}\cos(\theta_1+\gamma)\}$$
$$+\ddot{\theta}_2m_2r_{BC_2}\sin\theta_2+\dot{\theta}_2^2m_2r_{BC_2}\cos\theta_2]\mathbf{j}.$$

Eq 6-11

From Eq 6-10 and Eq 6-11,

$$F_x=[\ddot{\theta}_1\{m_1r_{AC_1}\cos\theta_1+m_2r_{AB}\cos(\theta_1+\gamma)\}-\dot{\theta}_1^2\{m_1r_{AC_1}\sin\theta_1+m_2r_{AB}\sin(\theta_1+\gamma)\}$$
$$+\ddot{\theta}_2m_2r_{BC_2}\cos\theta_2-\dot{\theta}_2^2m_2r_{BC_2}\sin\theta_2], \text{ and} \qquad \text{Eq 6-12}$$

$$F_y=[-\ddot{\theta}_1\{m_1r_{AC_1}\sin\theta_1+m_2r_{AB}\sin(\theta_1+\gamma)\}-\dot{\theta}_1^2\{m_1r_{AC_1}\cos\theta_1+m_2r_{AB}\cos(\theta_1+\gamma)\}$$
$$-\ddot{\theta}_2m_2r_{BC_2}\sin\theta_2-\dot{\theta}_2^2m_2r_{BC_2}\cos\theta_2+(m_1+m_2)g]. \qquad \text{Eq 6-13}$$

Substituting expressions in Eq 6-12 and Eq 6-13 into Eq 6-4,

$$[J_1 - m_1 r_{AC_1} r_{C_1B}\cos(\alpha+\gamma) + m_1 r_{AB} r_{AC_1}\cos\gamma + m_2 (r_{AB})^2]\ddot{\theta}_1 + [m_2 r_{AB} r_{BC_2}\cos(\theta_1+\gamma-\theta_2)]\ddot{\theta}_2$$
$$= T - m_1 g r_{C_1B}\sin(\theta_1+\alpha+\gamma) + (m_1+m_2) g r_{AB}\sin(\theta_1+\gamma) + k(\theta_2-\theta_1-\theta_0) + b(\dot{\theta}_2-\dot{\theta}_1)$$
$$+ (m_1 r_{AB} r_{AC_1}\sin\gamma)\dot{\theta}_1^2 - \{m_2 r_{AB} r_{BC_2}\sin(\theta_1+\gamma-\theta_2)\}\dot{\theta}_2^2.$$

Eq 6-14

Also, from Eq 6-9,

$$[J_2 + m_2 (r_{BC_2})^2]\ddot{\theta}_2 + [m_2 r_{AB} r_{BC_2}\cos(\theta_1+\gamma-\theta_2)]\ddot{\theta}_1$$
$$= m_2 r_{AB} r_{BC_2}\sin(\theta_1+\gamma-\theta_2)\dot{\theta}_1^2 + r_{BC_2} m_2 g\sin\theta_2 - k(\theta_2-\theta_1-\theta_0) - b(\dot{\theta}_2-\dot{\theta}_1).$$

Eq 6-15

Eq 6-14 and 6-15 provide two equations of motion.

I have double checked the equations of motion. The equations of motion that are derived from a Lagrangian approach are same as Eq 6-14 and Eq 6-15.

6.3. Linearization

The obtained equations of motion are nonlinear. To design a controller using methods for linear time invariant systems, I need to linearize the nonlinear evolution rule.

6.3.1. Selection of the Point about Which Linearization is Performed

To linearize the evolution rule, I need to select the point about which the linearization is performed. I assess the validity of two candidates. One is an operating point with nonzero input torque, which yields a straight posture, and the other is a fixed point with zero input torque

(A) The Operating Point Yielding a Straight Posture

Humans tend to maintain a straight posture in normal standing rather than tilt their body. Motivated by this tendency, I first try an operating point of straight standing as the point about which I linearize the evolution rule. Please see Figure 6-2.

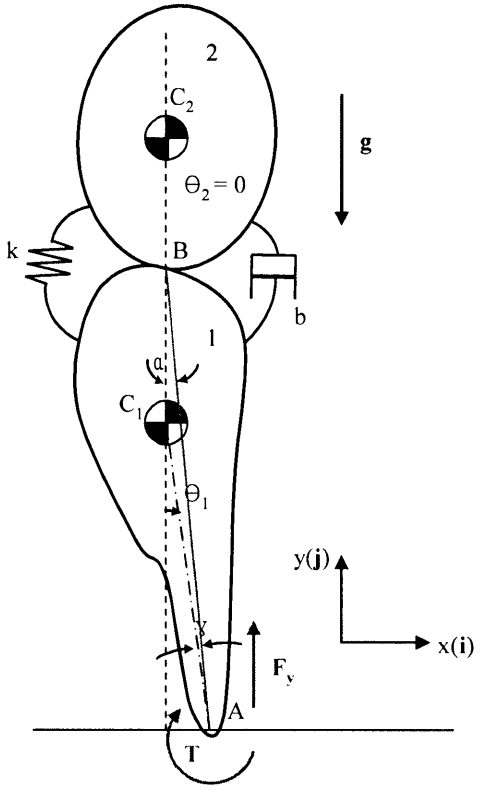

Figure 6-2: The operating point yielding a straight posture of the ankle-controlled model

The operating point in Figure 6-2 requires nonzero constant torque. The torque due to gravity force must balance with the constant torque T, which is applied at A, in order to maintain static equilibrium. To achieve straight standing, θ_2 should be zero, and θ_1 should be $-(\alpha + \gamma)$. At the operating point, all the time derivatives go to zero. Therefore, Eq 6-14 and Eq 6-15 become,

$$T = m_1 g\, r_{C1B} \sin(\theta_1 + \alpha + \gamma) - (m_1 + m_2) g\, r_{AB} \sin(\theta_1 + \gamma) - k(\theta_2 - \theta_1 - \theta_0), \text{ and}$$

$$r_{BC2} m_2 g \sin\theta_2 = k(\theta_2 - \theta_1 - \theta_0).$$

Using $\theta_2 = 0$ and $\theta_1 = -(\alpha + \gamma)$,

$$T = (m_1 + m_2)\, g\, r_{AB} \sin\alpha\,.$$

I select parameter values of the model to be similar to the values of an adult. With the parameter values shown in Table 6-2, the constant torque turns out to be 164 (N-m). However, the maximum ankle torque of inversion and eversion is less than 10 (N-m) for healthy adults [18]. Therefore, considering the capability of human muscular skeletal system, the operating point of straight posture turns out to be unreasonable.

This result tells that humans cannot stand with one foot without tilting their body. In other words, the failure of the operating point of exactly vertical legs and upper body implies that most humans need to move hips to balance with one foot

Table 6-2: Parameter values of the ankle controlled model in a frontal plane

Parameter	Value	Parameter	Value
m_1	44 kg	r_{AC1}	0.4966 m
J_1	6.107 kg-m^2	r_{C1B}	0.54545 m
m_2	40 kg	r_{AB}	1.0198 m
J_2	3.744 kg-m^2	r_{BC2}	0.4 m
α	0.1974 rad	g	9.81 m/s^2
γ	0.21711 rad	k[19]	86.556 N-m/rad
b[19]	1 N-m-s/rad		

The parameter values in Table 6-2 are biologically realistic. J_1 and J_2 are moment of inertia about the center of mass of each body. I selected plausible values of J_1 and J_2 considering the mass and shape of an adult. By deviating J_1 and J_2 from the moment of inertia of a sphere, I looked for

reasonable geometry using the MATLAB toolbox, SimMechanics. The spring constant and damping coefficient were found in the literature [19], and all the lengths of the model were obtained based on reasonable geometry of an adult.

(B) The Fixed Point with Zero Input Torque

Since the operating point that is suggested in the above section is not reasonable to use considering the order of maximal inversion/everion torque and the order of parameter values of a normal adult, a fixed point of the dynamical system, if any, can be an alternative point for linearization. At fixed point, all the time derivatives go to zero. Therefore, Eq 6-14 and Eq 6-15 become,

$$T = m_1 g\, r_{C1B} \sin(\theta_1 + \alpha + \gamma) - (m_1 + m_2) g\, r_{AB} \sin(\theta_1 + \gamma) - k(\theta_2 - \theta_1 - \theta_0), \text{ and} \quad \text{Eq 6-16}$$

$$r_{BC2} m_2 g \sin\theta_2 = k(\theta_2 - \theta_1 - \theta_0). \quad \text{Eq 6-17}$$

Without further analysis, it is not so obvious whether the Eq 6-16 and 6-17 yield a unique fixed point. However, it can be deduced that fixed points can be a function of parameter k and θ_0. One way to decide a reasonable fixed point is the following:

Step 1 Set a reasonable geometry of a desired fixed point and θ_0.

Step 2 Tune the value of k to make the preset geometry resulting from the fixed point.

Step 3 Investigate if the fixed point satisfies Eq 6-16 and 6-17.

Step 4 Investigate if the tuned k remains in a reasonable range; check if the value of tuned k is similar to the stiffness of human muscle and tendon.

I assume that the torsional spring is unloaded at normal standing of straight lower body and straight upper body, which is reasonable if a normal standing of humans is assumed to be symmetric. Consequently, θ_0 is set to be $\alpha + \gamma$.

Additionally, I confine my interest to the fixed point of $\theta_1 = 0$. Please consult Figure 6-3. This posture of the fixed point can be obtained by alignment of the A, C_1 and C_2. The torque of the spring compensates for the torque due to gravity acting on the upper rigid body. With the value of θ_0 that is $\alpha + \gamma$ and θ_1 that is zero,

$$m_1 g r_{C_1 B} \sin(\alpha + \gamma) = (m_1 + m_2) g r_{AB} \sin(\gamma) + k(\theta_2 - \theta_0), \text{ and} \qquad \text{Eq 6-18}$$

$$r_{BC_2} m_2 g \sin\theta_2 = k(\theta_2 - \theta_0). \qquad \text{Eq 6-19}$$

On the other hand, from the geometry of Fig 3, $r_{C_1 B} \sin(\alpha + \gamma) = r_{BC_2} \sin(-\theta_2)$, which makes $\theta_2 = -\sin^{-1}\{\frac{r_{C_1 B}}{r_{BC_2}} \sin(\alpha + \gamma)\}$. Let this be θ_{20}. Plugging this value in Eq 6-19 yields

$$k = \frac{r_{BC_2} m_2 g \sin(\theta_{20})}{(\theta_{20} - \alpha - \gamma)}.$$

Now, because I used geometry constraint first, I need to check if these values of k and θ_{20} also satisfy Eq 6-18. Substituting the obtained k and θ_{20} in Eq 6-18 yields

$$m_1 g r_{C_1 B} \sin(\alpha + \gamma) = (m_1 + m_2) g r_{AB} \sin(\gamma) - m_2 g r_{C_1 B} \sin(\alpha + \gamma), \text{ or}$$

$$r_{C_1 B} \sin(\alpha + \gamma) = r_{AB} \sin(\gamma),$$

which is true from the geometry.

Finally, with the parameter values in Table 6-2, the tuned value of k becomes 87 (N-m/rad). On the other hand, the angular stiffness of the muscles near hip joints can be estimated as being in the order of magnitude of 100 (N-m/rad) considering the stiffness of the muscles of mammals [19]. Therefore, the tuned value of k = 87 (N-m/rad) is considered reasonable. The results are summarized as follows:

(1) The fixed point of my interest is $\theta_{10} = 0$ and $\theta_{20} = -\sin^{-1}\{\frac{r_{C_1 B}}{r_{BC_2}} \sin(\alpha + \gamma)\}$.

(2) The stiffness and unloaded angle are $k = \frac{r_{BC_2} m_2 g \sin(\theta_{20})}{(\theta_{20} - \alpha - \gamma)}$ and $\theta_0 = \alpha + \gamma$ respectively.

(3) The stiffness is reasonable compared to mammalian muscle.

Arguments in this section show that a human cannot stand straight with one foot, considering the maximum torque an ankle can generate. Particularly, this model, with the assumption of no active torque at point B in Figure 6-3, must tilt its body to balance. In conclusion, I select the fixed point obtained as the point about which I linearize the evolution rule of the dynamical system.

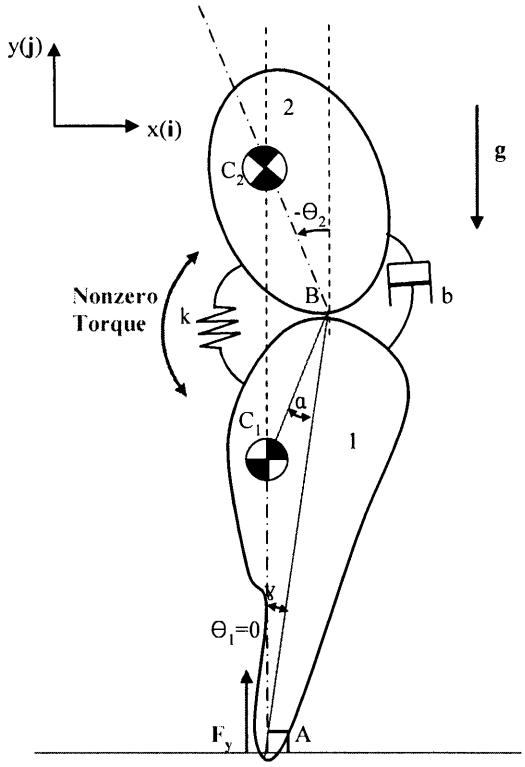

Figure 6-3: The fixed point of the ankle controlled model that yields zero torque

6.3.2. Linearization about the Fixed Point

I linearize Eq 6-14 and Eq 6-15 to obtain the state space representation of the corresponding LTI system. I have two second-order differential equations, so I need four state variables. Let $\mathbf{x}^T = [\theta_1\ \omega_1\ \theta_2\ \omega_2]$, where $\omega = d\theta/dt$, and $\mathbf{u} = T$. Evolution rules can be rewritten

$$\frac{d\mathbf{x}}{dt} = F(\mathbf{x},\mathbf{u}) = \begin{bmatrix} f_1(\mathbf{x},\mathbf{u}) \\ f_2(\mathbf{x},\mathbf{u}) \\ f_3(\mathbf{x},\mathbf{u}) \\ f_4(\mathbf{x},\mathbf{u}) \end{bmatrix}, \text{ and}$$

the model that is linearized about the fixed point $\mathbf{x}_0$, $\mathbf{u}_0$ ($\mathbf{u}_0 = 0$) is given by

$$\frac{d}{dt}\delta\mathbf{x} = D_{\mathbf{x}}F(\mathbf{x}_0,\mathbf{u}_0)\delta\mathbf{x} + D_{\mathbf{u}}F(\mathbf{x}_0,\mathbf{u}_0)\delta\mathbf{u} + O(\varepsilon^2), \qquad \text{Eq 6-20}$$

where $\delta\theta_1$ and $\delta\theta_2$ mean the (small) deviations from the value of θ_1 and θ_2 at the fixed point of the dynamical system, and

$$\delta\mathbf{x} = \begin{bmatrix} \delta\theta_1 \\ \omega_1 \\ \delta\theta_2 \\ \omega_2 \end{bmatrix}.$$

I obtain the following linearized model:

$$\frac{d}{dt}\delta\mathbf{x} = \underbrace{\begin{bmatrix} \partial f_1/\partial\theta_1 & \partial f_1/\partial\omega_1 & \partial f_1/\partial\theta_2 & \partial f_1/\partial\omega_2 \\ \partial f_2/\partial\theta_1 & \partial f_2/\partial\omega_1 & \partial f_2/\partial\theta_2 & \partial f_2/\partial\omega_2 \\ \partial f_3/\partial\theta & \partial f_3/\partial\omega_1 & \partial f_3/\partial\theta_2 & \partial f_3/\partial\omega_2 \\ \partial f_4/\partial\theta_1 & \partial f_4/\partial\omega_1 & \partial f_4/\partial\theta_2 & \partial f_4/\partial\omega_2 \end{bmatrix}_{(\mathbf{x}_0,\mathbf{u}_0)}}_{\mathbf{A}} \delta\mathbf{x} + \underbrace{\begin{bmatrix} \partial f_1/\partial u \\ \partial f_2/\partial u \\ \partial f_3/\partial u \\ \partial f_4/\partial u \end{bmatrix}_{(\mathbf{x}_0,\mathbf{u}_0)}}_{\mathbf{B}} \delta\mathbf{u}, \quad \text{or}$$

$$\frac{d}{dt}\delta\mathbf{x} = \mathbf{A}\delta\mathbf{x} + \mathbf{B}\delta\mathbf{u}.$$

The expressions for **A** and **B** are computed using MATLAB's Symbolic Math Toolbox, and then checked by paper work. The general expressions of matrix **A** and **B** are complicated, so I just attach the source code finding the general expressions of **A** and **B** in Appendix B.5. After substitution of all parameter values in Table 6-2, I obtain:

$$\mathbf{A} = \begin{bmatrix} 0 & 1 & 0 & 0 \\ 9.2676 & -0.0472 & 0.7404 & 0.0472 \\ 0 & 0 & 0 & 1 \\ -2.0263 & 0.1524 & 3.6751 & -0.1524 \end{bmatrix}, \text{ and } \mathbf{B} = \begin{bmatrix} 0 \\ 0.022 \\ 0 \\ -0.0252 \end{bmatrix}. \qquad \text{Eq 6-21}$$

Transfer functions that are expressed in Laplace transforms are written

$$\frac{\delta\Theta_1(s)}{T(s)} = \frac{0.02205s^2 + 0.002174s - 0.09965}{s^4 + 0.1996s^3 - 12.94s^2 - 1.603s + 35.56}, \text{ and} \qquad \text{Eq 6-22}$$

$$\frac{\delta\Theta_2(s)}{T(s)} = \frac{-0.02515s^2 + 0.002174s + 0.1884}{s^4 + 0.1996s^3 - 12.94s^2 - 1.603s + 35.56}. \qquad \text{Eq 6-23}$$

6.4. Controller Design

One important goal of the analysis of the ankle controlled model in a frontal plane is to investigate whether this double inverted pendulum can be controlled and stabilized with input torque at the ankle alone. More specifically, the center of pressure under the foot must remain within the base of support. Furthermore, I restrict the angular velocity of the upper and lower bodies based on the frequency of normal postural sway of humans with a specific perturbation.

In addition, I must consider some constraints; (1) the amount of input torque is limited by the capacity of human muscular skeletal system, and (2) the horizontal ground reaction force must

stay in a reasonable range so that excessive friction is not required. In this section, I investigate the controllability of this system and design a controller satisfying all the defined requirements.

6.4.1. Block Diagram

The block diagram of the closed loop system is shown in Figure 6-4. The input to the system is the ankle torque, **u**. The outputs are the deviations of θ_1 and θ_2 from the fixed point and their derivatives, which are expressed as vector **y**. The disturbance d(t) is a perturbation added to the state variable $\delta\mathbf{x}(t)$ in the way that it can affect the controlled input.

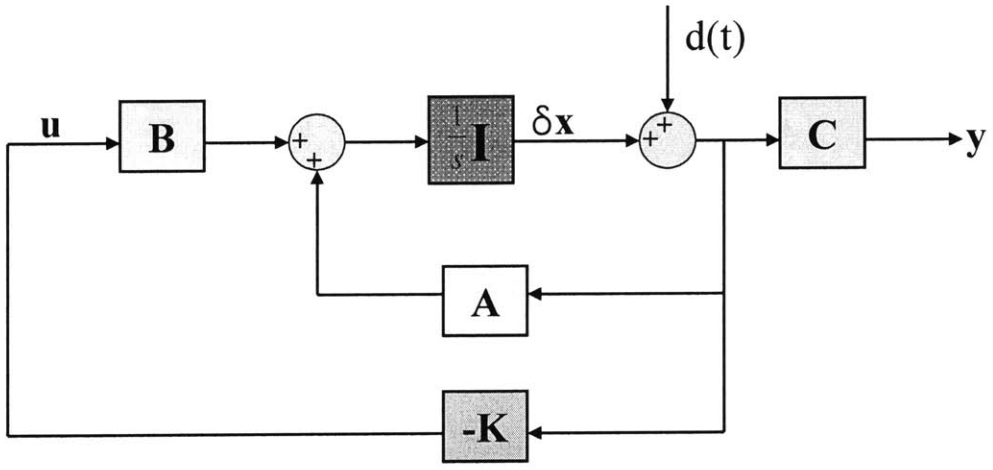

Figure 6-4: The block diagram of the closed loop system of the ankle controlled model

6.4.2. Assumptions Regarding the Sensor and Actuator

The Sensor and Actuator of the Modeled System

All angular deviations and angular velocities can be detected by various human sensory organs. Sensing vision through the eyes, sensing posture through tactile organs in foot, hip, etc and sensing equilibrium through the inner ears can be combined to detect the current posture and

the angular velocity of the upper and lower bodies. Therefore, I model the combination of the sensory organs as a proper sensor that indicates the current state variables to a central nervous system (CNS).

The muscular skeletal system involving ankle torque is modeled as the actuator. The controller, which is a generic model of the CNS, commands the muscles attached to an ankle joint to generate the proper force to make the proper torque for balancing.

Practical Implications

Considering that the plant is the human body, there is a limitation of input torque that an ankle joint can apply. A recent study shows that a normal healthy young woman can apply inversion/eversion ankle torque up to approximately 8.6 (N-m) [18]. I take account of this limitation by saturating the input signal. Any torque input whose absolute value is greater than 10 (N-m) is transmitted as torque whose magnitude is 10 (N-m) with the same direction as the original torque.

Considering another practical implication, there is some biological time delay when a human senses the deviation in angle or nonzero angular velocity and takes a proper action. However, I assume that the speed of response of the sensor and actuator is high enough, and the time delay is negligible. I neglect the time delay in this study, and assign consideration of the sensor and actuator dynamics to future work.

Moreover, I assumed no noise. Consideration of the biological noise in sensory organs can also be assigned to future work.

6.4.3. Controller Design

Stability of the Uncompensated System

The pole - zero plot demonstrates the instability of the uncompensated system. The transfer function of each output versus input is obtained in Eq 6-22 and 6-23. The poles of these transfer functions are shown in Figure 6-5. The uncompensated system is unstable because with the selected parameter values whose orders of magnitude are comparable to those of humans, there are two poles in the right half plane.

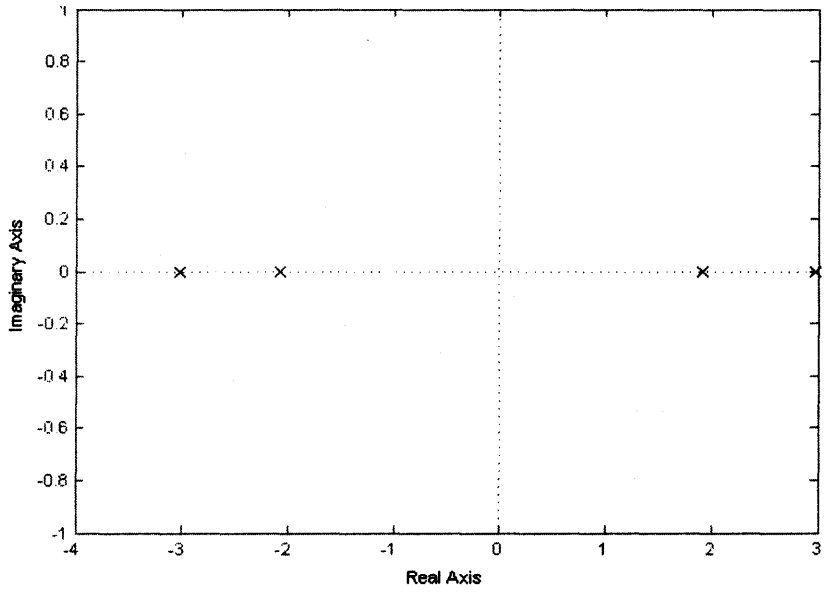

Figure 6-5: Poles of the uncompensated system of the balancing model in a frontal plane

Required System Performance

Rather than considering system performance in terms of steady state error, response time or overshoot, I confine my interest to reasonable balancing of human body with reasonable ankle torque and ground reaction forces. As a result, I require the system to satisfy the following:

(1) One possible definition of balancing is keeping the center of pressure within the base

of support. I aim to satisfy this requirement by confining the deviation of θ_1 and θ_2 to a certain range. More specifically, the deviation of θ_1 and θ_2 from the fixed point should remain in the range of [-15, 15] (deg). This range is selected from some relevant work on postural sway of humans [20].

(2) Requirements (1) must be satisfied with some small perturbation in impulsive form. The specific amount of the "small" perturbation might not be decisive, but I choose a perturbation of 300 (N) $\times$ 0.0087 (sec) impulsive pulse with the period of 3 (sec), which is applied at point B.

(3) The angular velocity of the upper body and the lower body must remain in the range of [-5, 5] (deg/sec). This range was calculated from the dominant frequency of postural sway and the displacement of each segment. The frequency of sway was related to the frequency of the perturbation described in (2), and the displacement is described in (1). The relation between the frequency of perturbation and postural sway, which I consulted is discussed in [20].

(4) Requirements (1) & (3) must be satisfied with the ankle torque in [-10, 10] (N-m), which is approximately the maximal inversion/eversion torque an adult can apply [18].

(5) Requirements (1) & (3) must be satisfied with some reasonable value of the friction coefficient of the floor. I choose the maximum value of the friction coefficient as 0.5.

Design Method

The outputs of the system are the deviations of θ_1 and θ_2 from the fixed point while the input is the ankle torque. Therefore, the system is a single input and multi output (SIMO) system, and I have two transfer functions. If I try to design a compensator by design method in frequency domain, it would be difficult to meet the requirements in both transfer functions simultaneously.

Also, I have strong constraint in the amount of the input and state variables. Therefore, it is reasonable to design a controller as a Linear Quadratic Regulator (LQR), which is one of the optimal control methods.

Controllability

Before jumping into the controller design, I check if this system has controllability. Controllability is determined by the rank of the controllability matrix, $\Gamma = [\mathbf{B} \quad \mathbf{AB} \quad \mathbf{A^2B} \quad \mathbf{A^3B}]$. Substituting **A** and **B** from Eq 6-21, the rank of Γ is obtained as four, and this system is controllable. In other words, I can place closed loop poles wherever I want to with the control law of $\mathbf{u} = -\mathbf{K}\delta\mathbf{x}$.

Controller Design Using LQR

I describe the quadratic cost function as

$$J(\mathbf{u}) = \int_0^\infty (\delta\mathbf{x}^{\mathrm{T}}\mathbf{Q}\,\delta\mathbf{x} + \mathbf{u}^{\mathrm{T}}\mathbf{R}\mathbf{u})\,dt \,.$$

The LQR method finds the optimal value of the **K** matrix that minimizes the cost function J with the feedback control of $\mathbf{u} = -\mathbf{K}\delta\mathbf{x}$. By trial and error, I select proper values of **Q** and **R** that yield feedback control satisfying the requirements (1) ~ (4). Then, I check whether the requirement (5) is satisfied with the obtained closed loop system. Using saturation in input signal, I can preclude the violation of requirement (4).

Note that the evolution rule has been constructed for the state $\delta\mathbf{x}$ in the unit of [rad] and [rad/s]. However, I want to illustrate the result in [deg] and [deg/s] rather than [rad] and [rad/s]. Therefore, I need to take the conversion of unit into account in construction of the gain matrix **K**.

As a result, I find the optimal gain matrix **K** satisfying the requirements (1) ~ (5).

$$\mathbf{Q} = \begin{pmatrix} 1 & 0 & 0 & 0 \\ 0 & 0.1 & 0 & 0 \\ 0 & 0 & 1 & 0 \\ 0 & 0 & 0 & 0.1 \end{pmatrix}, \mathbf{R} = 0.001 \text{ and}$$

$$\mathbf{K} = [\, 4993.36 \quad 1816.10 \quad 2632.90 \quad 1196.20]$$

makes the closed loop system with $\mathbf{u} = -\mathbf{K}\delta\mathbf{x}$ satisfy all the requirements.

I assessed the reasonableness of this gain matrix by investigating the necessary control effort by assuming reasonable value of the deviation of each state variable from the fixed point satisfying the requirement (1) & (3) and multiplying it by the obtained gain matrix. Because I required the system to balance even with an impulsive perturbation, the order of magnitude of the norm of the gain matrix is excessive, compared to the actuator capability. However, saturation in input signal can preclude excessive input torque that is beyond the actuator capability. Detailed results follow.

6.5. Results from Simulation

6.5.1. Time Response of State Variables

The impulsive perturbation acting on B is shown in Figure 6-6. With this perturbation, I plot the time response of state variables in Figure 6-7, Figure 6-8, Figure 6-9 and Figure 6-10.

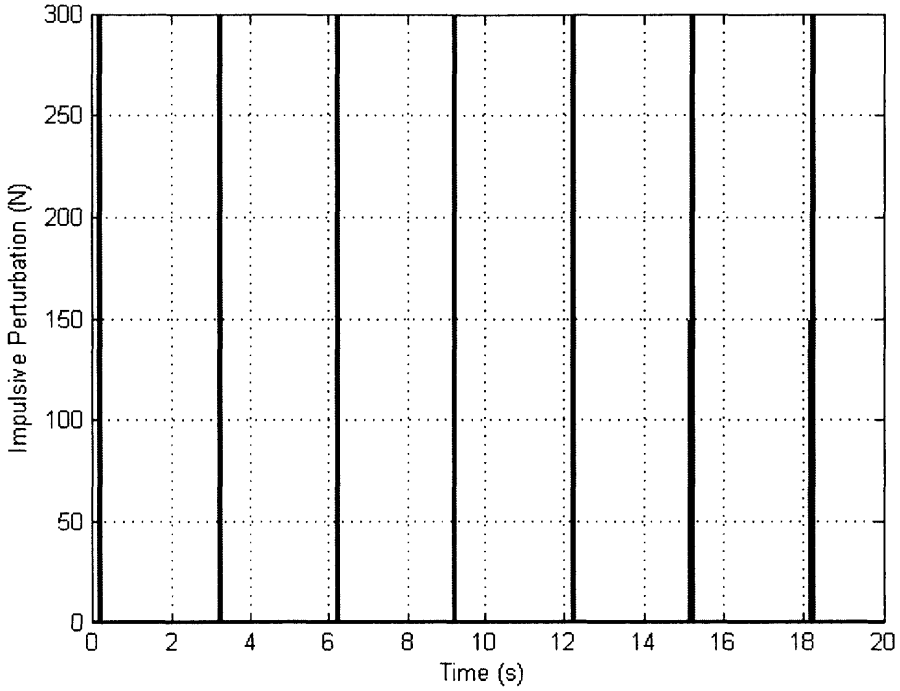

Figure 6-6: Impulsive perturbation acting on B of the ankle controlled model in a frontal plane

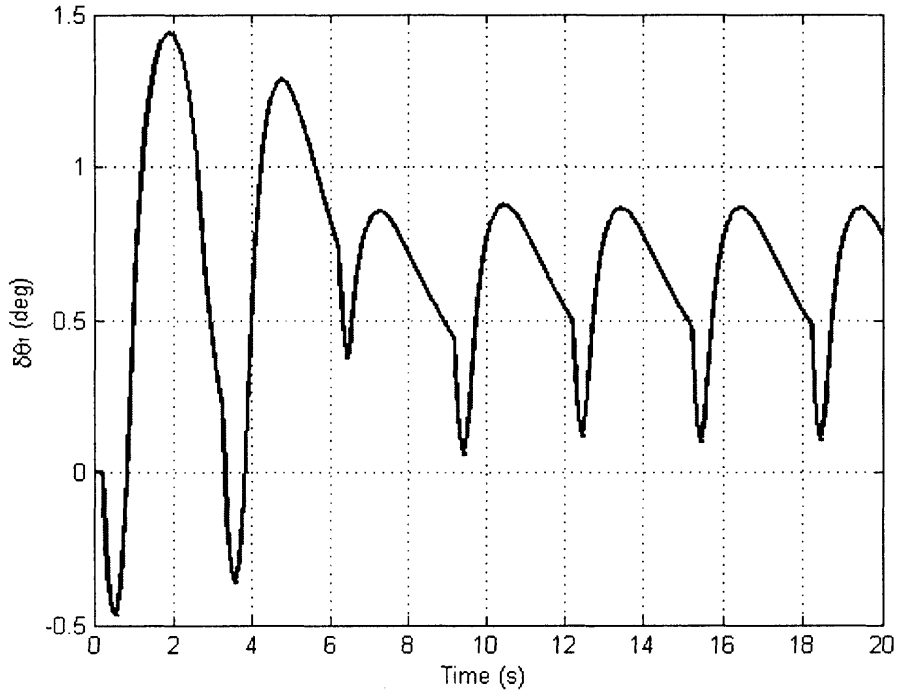

Figure 6-7: Time response of $\delta\theta_1$ of the model with the input torque in [-10, 10] (N-m)

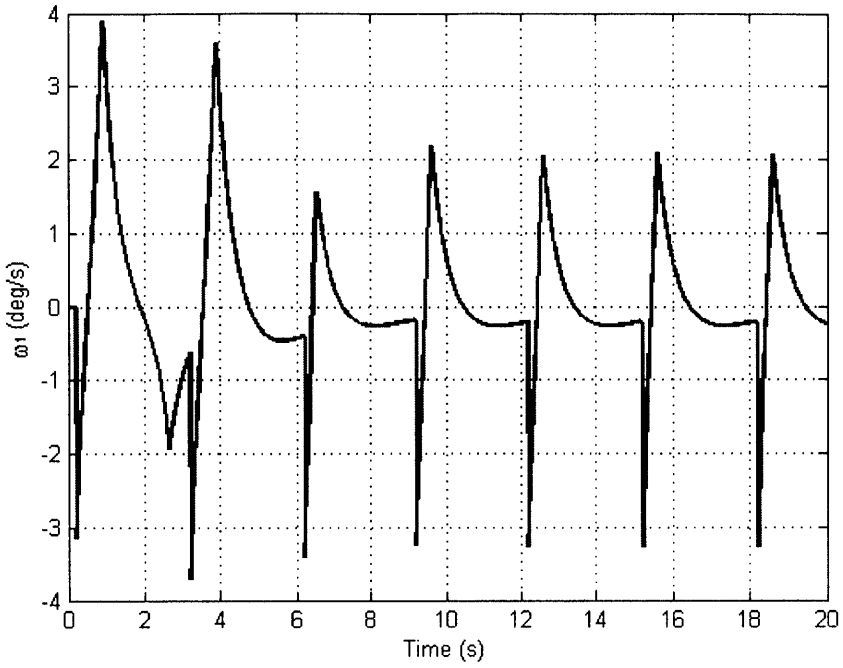

Figure 6-8: Time response of ω_1 of the model with the input torque in [-10, 10] (N-m)

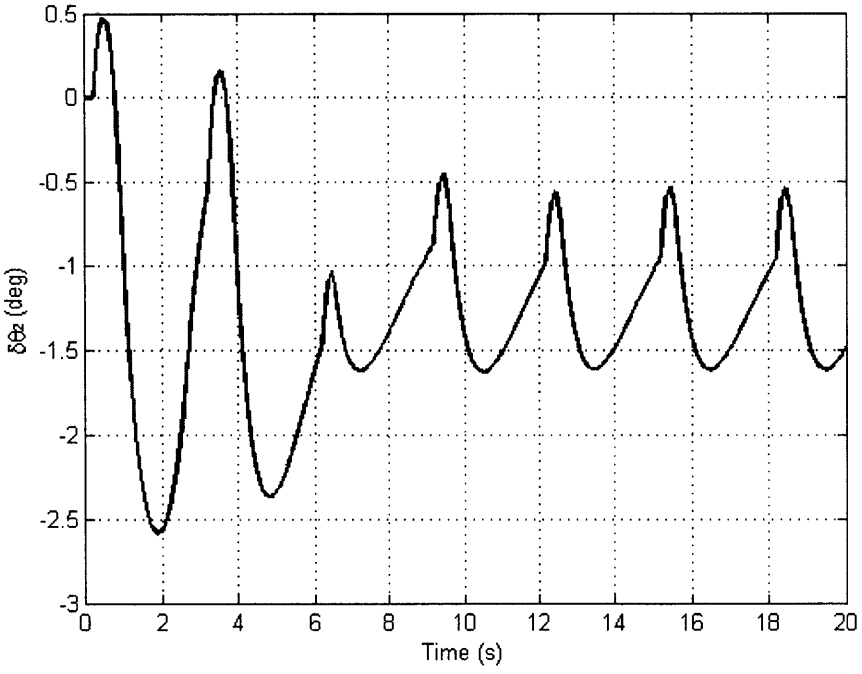

Figure 6-9: Time response of $\delta\theta_2$ of the model with the input torque in [-10, 10] (N-m)

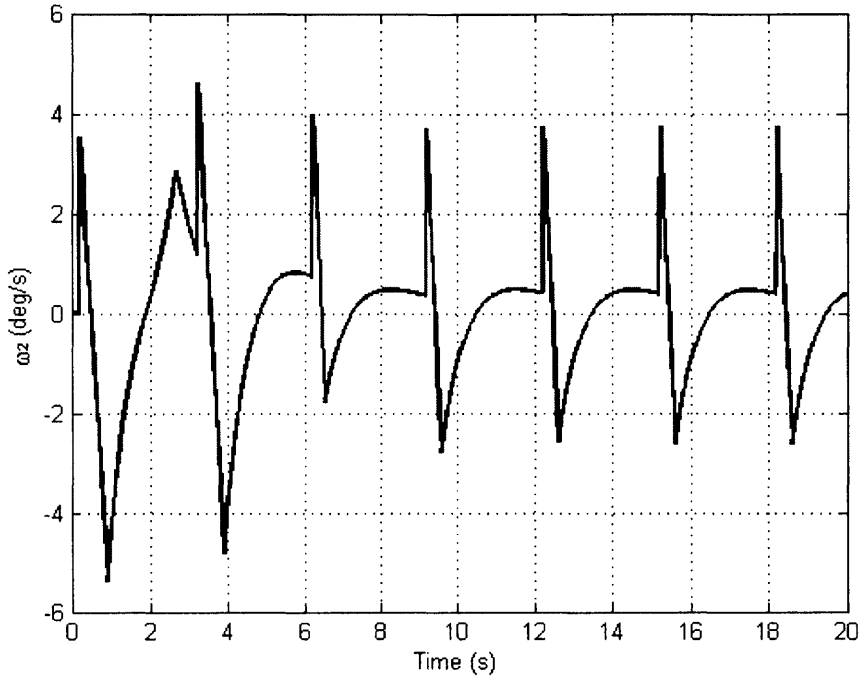

Figure 6-10: Time response of ω_1 of the model with the input torque in [-10, 10] (N-m)

6.5.2. Time Response of the Ankle Torque and Ground Reaction Forces

With the impulsive perturbation shown in Figure 6-6, I plot the time response of the controlled input torque and ground reaction forces in Figure 6-11, Figure 6-12 and Figure 6-13.

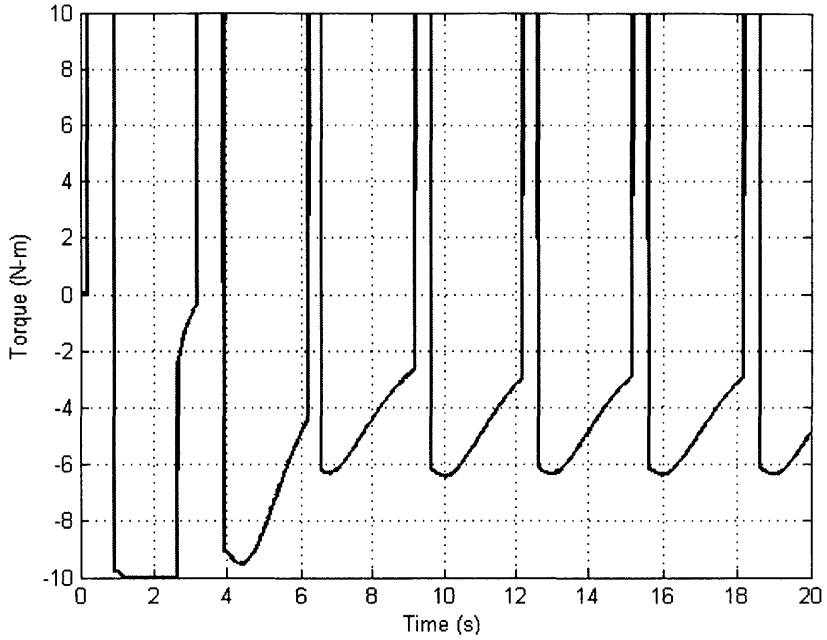

Figure 6-11: The controlled ankle torque of the ankle controlled model in a frontal plane

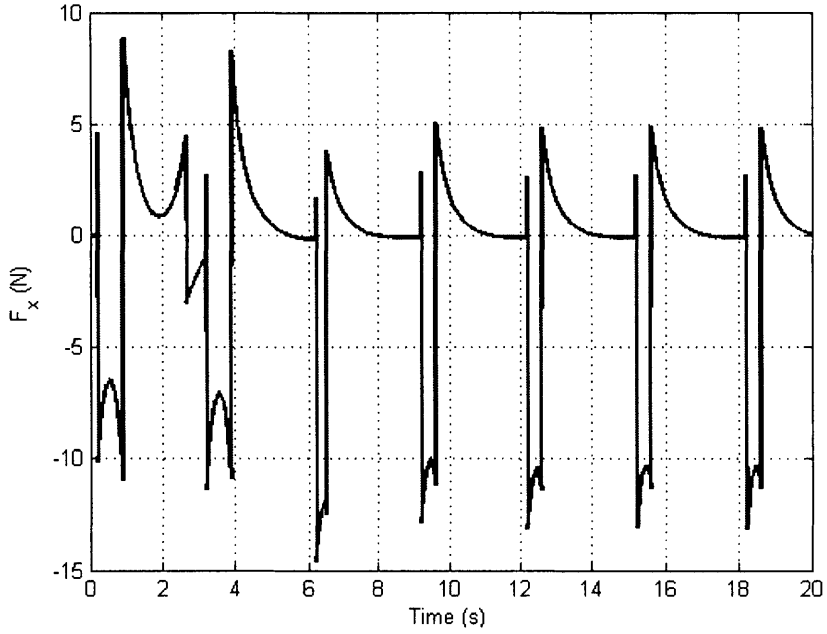

Figure 6-12: The ground reaction force in the x direction of the ankle controlled model

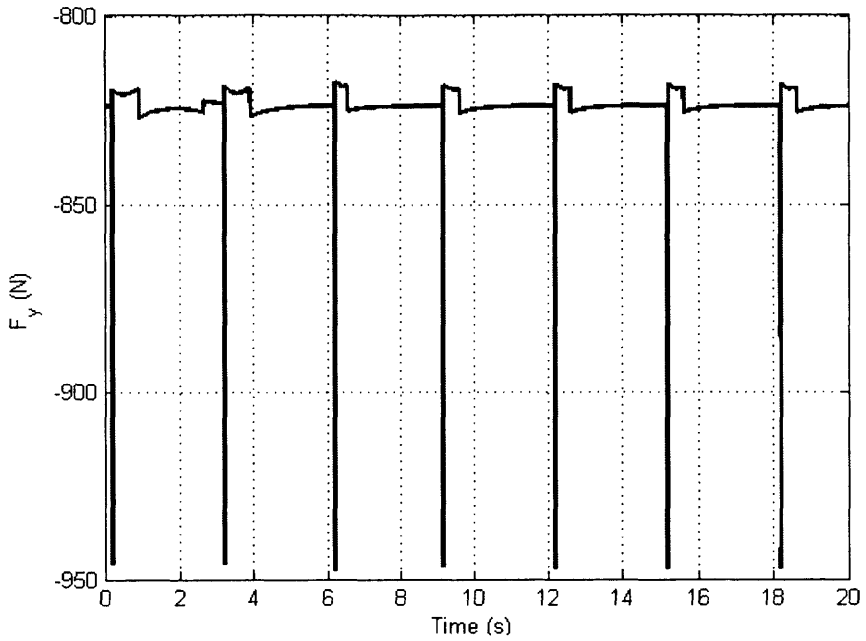

Figure 6-13: The ground reaction force in the y direction of the ankle controlled model

6.5.3. Friction Coefficient

I can obtain the friction coefficient by investigating the ground reaction forces in x direction and y direction. From Figure 6-12 and Figure 6-13, the maximal magnitude of the horizontal ground reaction force is approximately 15 (N) while the minimal magnitude of the vertical ground reaction force is approximately 820 (N). Therefore, I need the friction coefficient of which the magnitude is, at least, 15/820 = 0.0183. This friction coefficient is lower than 0.5 and satisfies the requirement (5) in 6.4.3.

6.5.4. Further Analysis

Angular Displacement with Varying Amplitude of Perturbation

I investigate the time responses with smaller and larger perturbations. Figure 6-14 and

Figure 6-15 show the time response of $\delta\theta_1$ and $\delta\theta_2$ with the perturbation of pulse with the amplitude of 100, 150, 200 and 250 (N), the duration 0.0087 (sec) and the period of 3 (sec). It is indicated that the deviation angle fluctuates less with smaller perturbations. Figure 6-16 and Figure 6-17 show the time responses of $\delta\theta_1$ and $\delta\theta_2$ with the perturbation of pulse with amplitude of 310 (N), same duration and same period. The simulation ends before the preset simulation time because the body falls before the preset time. Please note that the time responses of $\delta\theta_1$ and $\delta\theta_2$ never converge stably with perturbation with amplitude over 310 (N).

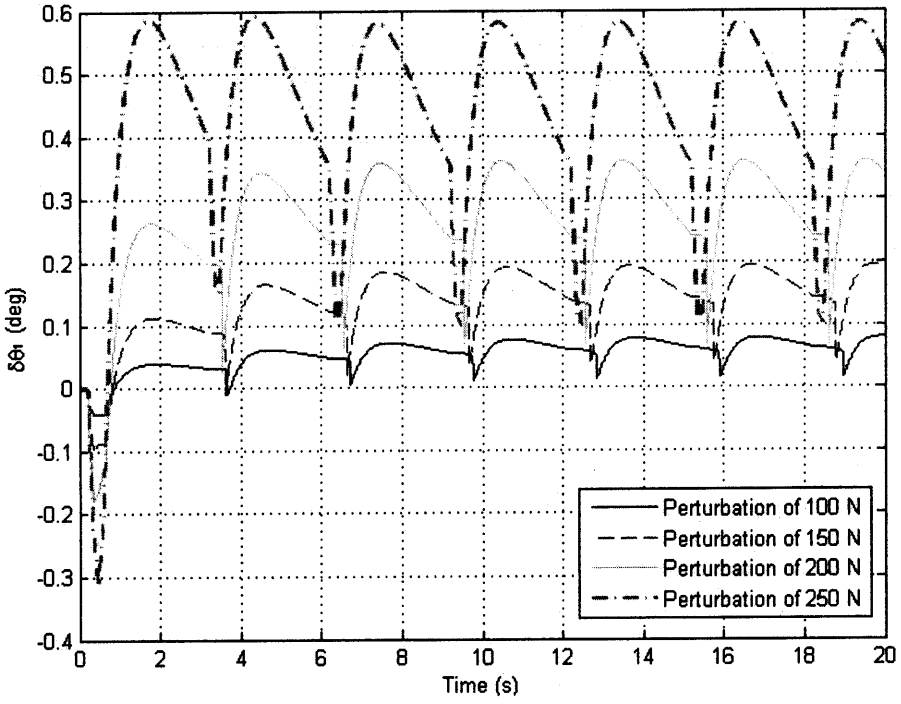

Figure 6-14: $\delta\theta_1$ with the perturbation with amplitude of 100, 150, 200 and 250 (N)

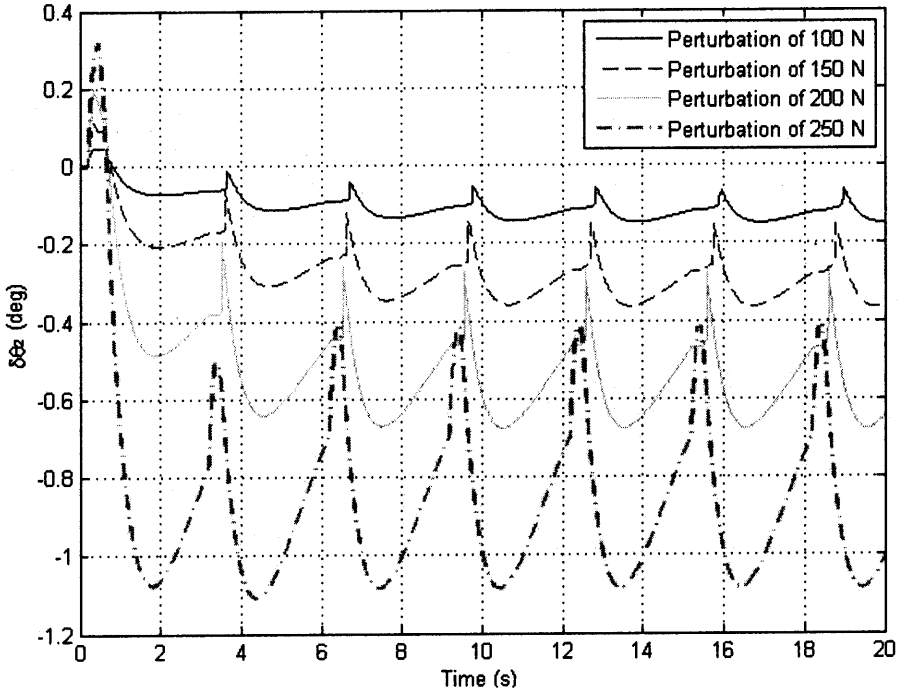

Figure 6-15: $\delta\theta_2$ with the perturbation with amplitude of 100, 150, 200 and 250 (N)

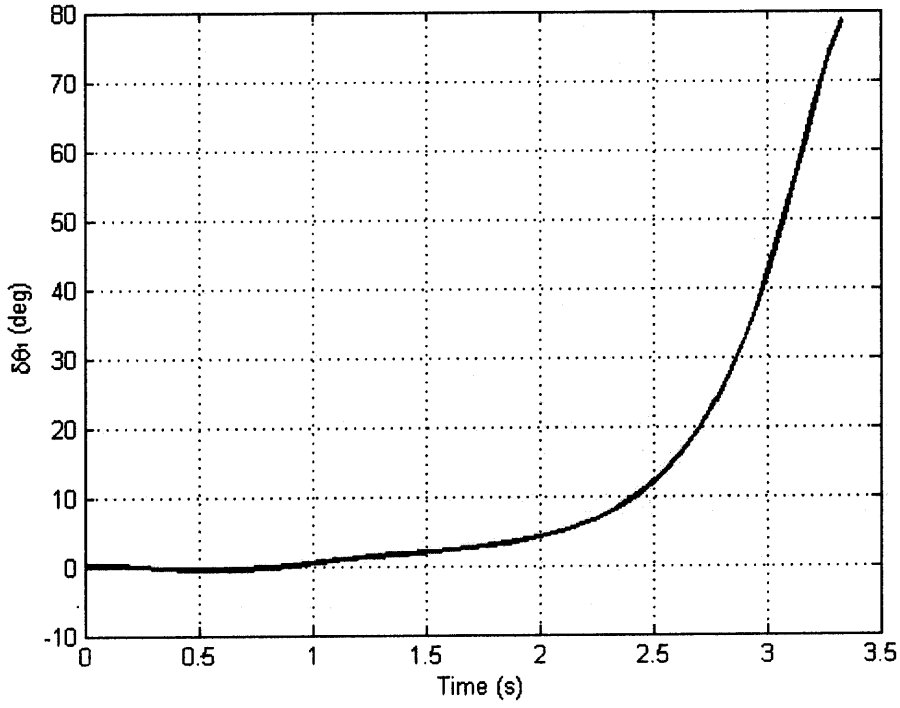

Figure 6-16: $\delta\theta_1$ of the ankle controlled model with the perturbation with amplitude of 310 (N)

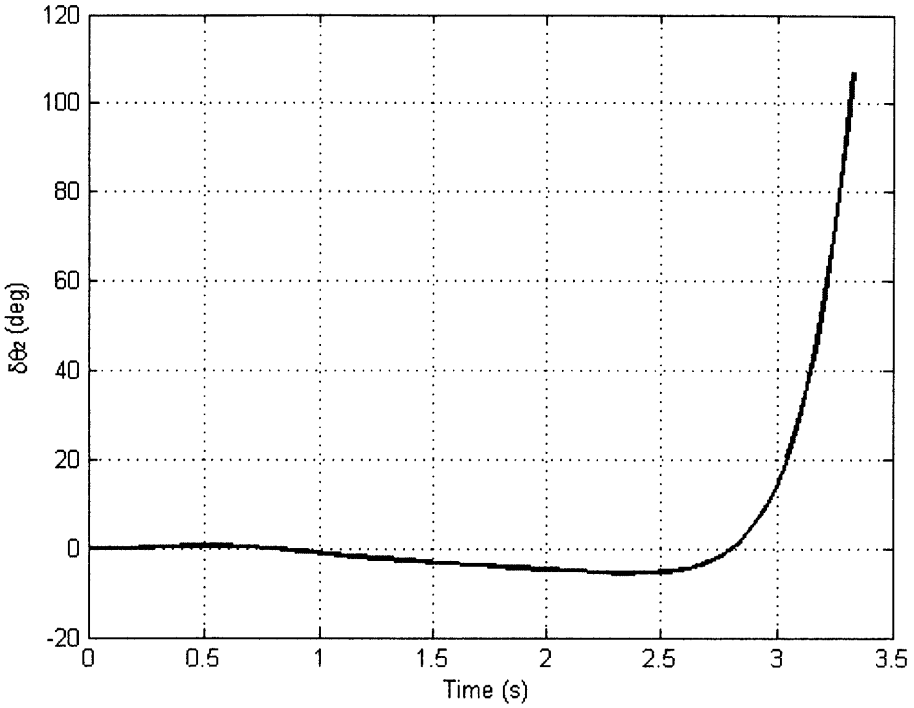

Figure 6-17: $\delta\theta_2$ of the ankle controlled model with the perturbation with amplitude of 310 (N)

Steady State Error versus the Maximal Ankle Torque

In Figure 6-7 and Figure 6-8 there are steady state errors in deviation angle $\delta\theta_1$ and $\delta\theta_2$. The approximate value of the steady state error is below 1 deg. One of the possible ways to reduce this steady state error is allowing larger input torque. Please notice that in Figure 6-11, the ankle torque stays in the saturated value during a significant portion of the overall simulation time. If the necessary torque to recover the posture of zero steady state error is above 10 (N-m), the system cannot achieve the zero steady state error because I confine the input torque in [-10, 10] (N-m).

I verify that the steady state error is influenced by the saturation of the input torque by allowing different maximum value of ankle torque. Figure 6-18 shows the time response of $\delta\theta_1$ with the input torque in [-150, 150] (N-m). Comparing Figure 6-18 with Figure 6-7, it is observed that I obtain less steady state error by allowing larger input torque. However, the model becomes

less realistic without confining ankle torque in reasonable range. This gives an example of a tradeoff between improving the system's performance and being biologically realistic.

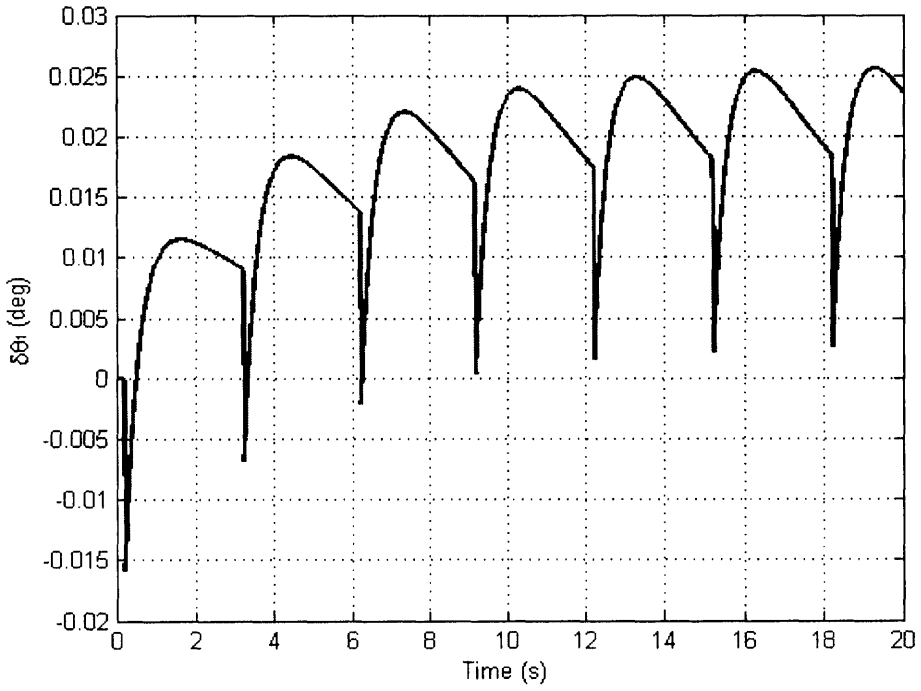

Figure 6-18: Time response of $\delta\theta_1$ of the model with the input torque in [-150, 150] (N-m)

Poles of the Compensated System

The eigenvalues of the matrix (**A** – **BK**) are the poles of the compensated system, which are -3.0027 ± *j*0.0292 and -2.0022 ± *j*0.0734. Note that all poles are now in the left half plane, which guarantees stability

6.6. Frontal Plane Ankle Torque of a Walking Model

In this section, I assess the necessary torque in a frontal plane for a simple model to walk and compare the amount of torque with the case of a standing model. Please see Figure 6-19. An inverted pendulum that has three-dimensional geometry is hinged at the point B, which is a revolute joint, and moving in the x-z plane or the sagittal plane.

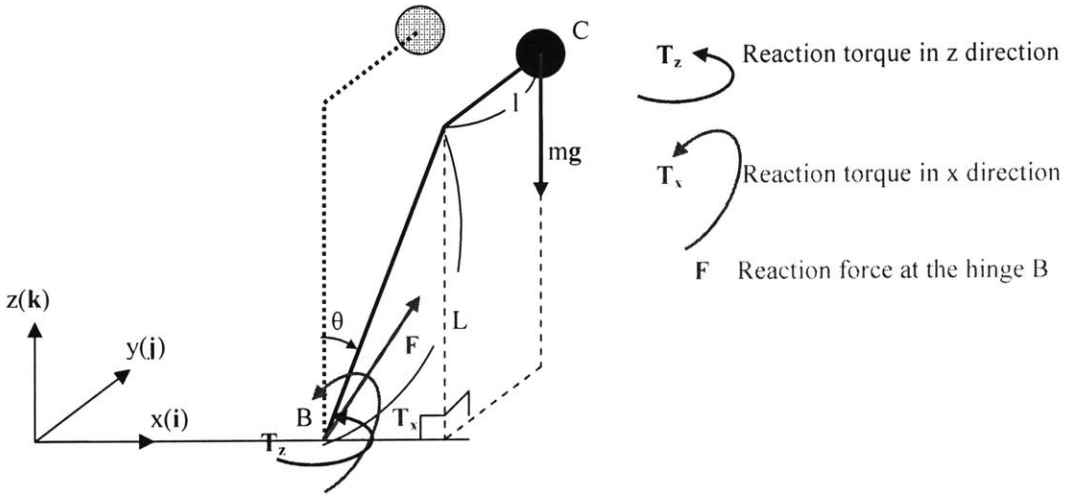

Figure 6-19: The free body diagram of a 3-D inverted pendulum hinged at a revolute joint

Note that point B is a hinge that allows rotation only in y direction or in the sagittal plane. Therefore, there is no applied torque in y direction while reaction torque in x and z direction are nonzero. From the angular momentum principle about point B,

$$\frac{d}{dt}\overrightarrow{H_B} + \overrightarrow{v_B} \times \overrightarrow{P} = \overrightarrow{M_B} = \overrightarrow{r_{BC}} \times m\overrightarrow{g} + \overrightarrow{T_x} + \overrightarrow{T_z}.$$

Using $v_B = 0$,

$$\frac{d}{dt}\overrightarrow{H_B} = \overrightarrow{r_{BC}} \times m\overrightarrow{g} + \overrightarrow{T_x} + \overrightarrow{T_z}. \qquad \text{Eq 6-24}$$

Here,

$$\overrightarrow{H_B} = \overrightarrow{r_{BC}} \times m\overrightarrow{v_{BC}}.$$

Using $\overrightarrow{r_{BC}} = L \sin\theta \mathbf{i} + l\mathbf{j} + L\cos\theta \mathbf{k}$ and $\overrightarrow{v_{BC}} = L\dot{\theta}\cos\theta \mathbf{i} - L\dot{\theta}\sin\theta \mathbf{k}$,

$$\overrightarrow{H_B} = -mLl\,\dot{\theta}\sin\theta \mathbf{i} + mL^2\dot{\theta}\mathbf{j} - mLl\,\dot{\theta}\cos\theta \mathbf{k} .$$

Therefore,

$$\frac{d}{dt}\overrightarrow{H_B} = (-mLl\,\ddot{\theta}\sin\theta - mLl\,\dot{\theta}^2\cos\theta)\mathbf{i} + mL^2\ddot{\theta}\mathbf{j} + (-mLl\,\ddot{\theta}\cos\theta + mLl\,\dot{\theta}^2\cos\theta)\mathbf{k} \quad \text{Eq 6-25}$$

Now, using $\overrightarrow{r_{BC}} = L\sin\theta \mathbf{i} + l\mathbf{j} + L\cos\theta \mathbf{k}$ and $m\vec{g} = -mg\,\mathbf{k}$,

$$(\overrightarrow{r_{BC}} \times m\vec{g}) = -mgl\,\mathbf{i} + mLg\sin\theta \mathbf{j} . \quad \text{Eq 6-26}$$

From Eq 6-24, 6-25 and 6-26,

$$mgl - mLl\,(\ddot{\theta}\sin\theta + \dot{\theta}^2\cos\theta) = T_x , \quad \text{Eq 6-27}$$

$$\ddot{\theta} = \frac{g}{L}\sin\theta \quad \text{and} \quad \text{Eq 6-28}$$

$$-mLl\,\ddot{\theta}\cos\theta + mLl\,\dot{\theta}^2\cos\theta = T_z .$$

From Eq 6-27 and 6-28,

$$mgl - mLl\,(\frac{g}{L}\sin^2\theta + \dot{\theta}^2\cos\theta) = T_x . \quad \text{Eq 6-29}$$

Note that $(\frac{g}{L}\sin^2\theta + \dot{\theta}^2\cos\theta) > 0$ for $-\pi/2 < \theta < \pi/2$. Eq 6-29 implies that with some high speed of the pendulum, T_x can be negative. Physically, if speed is high enough for centrifugal force to overcome gravity, T_x can be negative. I investigate the range of speed when T_x becomes zero or negative. From Eq 6-29,

$$Tx = mgl - mLl\,(\frac{g}{L}\sin^2\theta + \dot{\theta}^2\cos\theta) = ml\cos\theta(g\cos\theta - L\dot{\theta}^2) \le 0 ,$$
$$\Leftrightarrow\ g\cos\theta - L\dot{\theta}^2 \le 0$$

which is exactly the same condition as the condition for the rimless wheel to fly off the ground (2.1.2). Therefore, as long as I confine my interest to the range of $\dot{\theta}$ that keeps the model from

flying off, I can conclude that T_x is positive.

Then, from Eq 6-29 and the fact that $(\frac{g}{L}\sin^2\theta + \dot{\theta}^2\cos\theta) > 0$ for $-\pi/2 < \theta < \pi/2$,

$$0 < Tx < mgl \ ,$$

for $-\pi/2 < \theta < \pi/2$. Please note that the necessary amount of torque for standing equals to *mgl*. Therefore, the above inequality means that for the moving inverted pendulum, the necessary reaction torque in the x direction, which is the frontal torque, is smaller than the necessary torque for the inverted pendulum to stand. Physically, the difference between the frontal torque in both cases is due to the centrifugal force.

The result shows that balancing with nonzero progressive speed needs smaller torque in a frontal plane than balancing with zero speed. Therefore, the result supports the argument that necessary torque in a frontal plane is smaller in walking than in standing with one foot.

6.7. Discussion and Future Work

6.7.1. Discussion

A double inverted pendulum, with a humanlike shape, humanlike inertia, and humanlike stiffness and damping, can be stabilized with control of the torque at a single joint representing an ankle. The system is not only controllable but also can be stabilized even if the amount of torque is bounded within a specific range that is similar to the range of torque a human can apply. The resultant ground reaction force is also bounded in a reasonable range; the studied model can balance without sliding the supporting foot if the friction coefficient of the floor is greater than 0.0183.

The result of this analysis suggests some possibility that a human can achieve stable

posture using ankle torque in a frontal plane alone. This argument can provide a theoretical basis to assess the effectiveness of a rehabilitation strategy for balancing that focuses on the control of the ankles.

For a simple inverted pendulum model, the necessary reaction torque in a frontal plane to move is smaller than necessary reaction torque in a frontal plane to stand. Also, for human locomotion, balancing in walking can be achieved if only the body does not fall before the swing foot becomes the next stance foot. Therefore, the success in balancing with one foot using ankle torque in a frontal plane can also suggest the success in stable walking using dominant ankle torque in a frontal plane and necessary hip actuation only for holding the trunk.

6.7.2. Future Work

As mentioned before, an ankle robot developed by Newman Laboratory at MIT provides simultaneous control of inversion/eversion as well as plantar/dorsiflexion. I aim to make future work so that the analysis can support the design of control of ankle robot more practically.

The controller of the studied double inverted pendulum model is designed using LQR. The success in balancing model supports that the torque control based on LQR can be effective in the control of ankle robot for rehabilitation of balancing in a frontal plane. However, in the double inverted pendulum model, output includes the angle and angular velocity of the upper body. Considering that it is hard for the ankle robot to sense the angle of upper body about hips in a frontal plane, to relate the analysis of the model to the application of ankle robot more closely, I need to investigate whether LQR with output of the angle and angular velocity of ankle alone can achieve balancing. In other words, I might need to consider designing controller with an observer to make the model more applicable for the ankle robot for rehabilitation.

7. Conclusions

7.1. Summary

A rimless wheel on a horizontal floor cannot achieve gait without dissipation of energy. Every step involves a collision that reduces the kinetic energy by a constant fraction determined by the geometry of the wheel. On the other hand, a passive rimless wheel on a horizontal floor does not have any source of mechanical energy. Therefore, a rimless wheel, with a finite angle between spokes, discretely loses its kinetic energy on a horizontal floor, and the kinetic energy of the wheel, in some finite time, come to be less than the minimum value necessary for the wheel to vault over its spokes. Then, the rimless wheel fails to make the next step. As a result, a period-one gait cannot be observed in a rimless wheel on a horizontal floor.

In contrast, a rimless wheel on a slight slope can make a stable period-one gait. A rimless wheel on a slight slope also suffers loss of kinetic energy due to collisions. However, work done by gravity supplies the model with some kinetic energy. If the work done by gravity exactly compensates for the loss of the kinetic energy due to a collision, the rimless wheel yields a period-one gait. The period-one gait can be considered as a fixed point of the Poincaré map representing the stride function. It can be shown that the fixed point is unique, and the fixed point is a stable one. In other words, a rimless wheel on a slight slope can recover its period-one gait regardless of a small perturbation. Physically, the stability of the fixed point is due two facts: one is that the work done by gravity is constant per step, and the other is that the reduction of the kinetic energy due to collision is a constant fraction of its value before the collision.

Constant speed and kinetic energy per step is a necessary condition of a period-one gait. Therefore, energy loss due to collisions should be avoided for a passive walker to make a period-

one gait on a horizontal floor. One way to avoid collisions in steps is to let a model have springy legs. Theoretically, springy legged models that walk in collisionless manners can make lossless period-one gaits. However, the period-one gaits found in this work are unstable fixed points of the stride functions, and the studied springy legged models cannot make period-one gaits if a small perturbation is added.

Motivated by the observation that the stable gait of a rimless wheel on a slight slope is based on two facts of (1) a constant amount of the work done by gravity on each step, which compensates for the loss of kinetic energy; and (2) the reduction of kinetic energy by a constant fraction due to collisions, I established an ankle actuated walker that walks with a collision and a constant amount of energy supplied per step. Like a rimless wheel on a slight slope, the ankle actuated walker has a unique stable fixed point that generates a period-one gait with some proper parameter values; the ankle actuated model can recover the period-one gait regardless of small perturbations.

Balancing of a human in a frontal plane with ankle torque of one foot can be modeled as stabilizing of a double inverted pendulum with torque at a single joint. A double inverted pendulum with a humanlike shape, humanlike inertia, and humanlike stiffness and damping, can be stabilized with control of the torque at a single joint. The stabilization is achieved even if the input torque is bounded within a range of torque a human can apply. An additional analysis shows that for a simple inverted pendulum model, the necessary ankle torque to stand with one joint in a frontal plane is greater than the necessary ankle torque in a frontal plane to balance while moving.

7.2. Discussion and Implications

This study is aimed to better understand the dynamics of passive walkers and to assess the contribution of ankle torque to locomotion and balancing for the development of effective and efficient rehabilitation therapy for locomotion. The study of passive walkers provides not only understanding of the dynamics of bipedal locomotion but also a baseline against which I evaluate the contribution of ankle torque. The two-dimensional analysis of the ankle actuated model on a horizontal plane is aimed to assess the contribution of the ankle torque to locomotion in a sagittal plane. In contrast, the analysis of the double inverted pendulum model controlled at a single joint is aimed to assess the contribution of the ankle torque in a frontal plane to balancing and locomotion.

Through the study of passive walkers, I have confirmed that collisions in bipedal walking necessarily dissipate the kinetic energy. I also investigated two passive walkers walking in a collisionless manner using springy legs and, therefore, walking with no energy cost. Another model has been studied by Mario W. Gomes and Andy L. Ruina [21]. The suggested models, including the springy legged models I analyzed, can generate lossless periodic gaits, but the studied periodic gaits fail to be stable fixed points of the stride functions.

On the other hand, a passive walker that loses its kinetic energy and regain the lost kinetic energy by some external force, such as a rimless wheel on a slope, can generate a stable periodic gait. Related to rehabilitation therapy, the result of the analysis suggests that a slight downhill slope might be used to assist gait rehabilitation. On a slight slope, a patient suffering from neurological or orthopedic injury, for example, might generate a stable periodic gait more easily by virtue of the passive dynamics that the rimless wheel model uses. This may accelerate motor learning of the lower extremities and assist gait rehabilitation.

An ankle actuated walker that loses and regains kinetic energy can be designed to generate

a stable periodic gait like the rimless wheel on a slope. The stable period-one gait of the ankle actuated walker supports the idea that stable walking can be achieved predominantly by ankle torque with negligible hip or knee torque in a sagittal plane. I cannot, though, conclude that stable walking cannot be achieved by actuation of hips or knees. A knee actuated or hip actuated walker might also generate a stable period-one gait by losing and regaining kinetic energy. For example, a study related bipedal walking shows that a hip actuated walker can walk stably on a horizontal floor [22].

However, the stable period-one gait of the ankle actuated walker may be distinguished from the stable gaits of knee or hip actuated walkers. For rehabilitation of locomotion, it would be reasonable to set ankle actuation as the first target to be adjusted or assisted because experimental data show that ankle torque is the most significant source of propulsion in terms of the amount of joint torque [2]. Therefore, in terms of rehabilitation, the analysis showing that a simple passive walker, after actuation through ankle torque in a sagittal plane, can generate a stable periodic gait supports the idea that a rehabilitation strategy focusing on ankle motion in a sagittal plane may be effective. In particular, one possible way to assist a patient to make a stable period-one gait on a horizontal ground is to supply constant energy through a robot equipped at the ankles, assuming that a collision on every step dissipates kinetic energy with a constant or almost constant ratio.

In a frontal plane, a similar argument regarding the contribution of ankle torque to balancing is applicable. Analysis using dynamics shows that a double inverted pendulum, with a humanlike shape, humanlike inertia, and humanlike stiffness and damping, can be stabilized with control of the torque at a single joint representing an ankle. This result suggests a possibility that a human can achieve stable posture by ankle torque alone. Therefore, theoretically, the analysis in this study supports a rehabilitation strategy for balancing that focuses on the control of ankles.

The above argument regarding the ankle control in a frontal plane for balancing can be

extended to locomotion. For a simple inverted pendulum model, analysis using dynamics shows that the frontal plane torque needed to balance while moving is smaller than the frontal plane torque needed to stand. Also, for human locomotion, balancing in a frontal plane during walking only requires the body not to fall before the swing foot becomes the next stance foot. Therefore, the analysis performed also supports the effectiveness of a rehabilitation strategy for locomotion that focuses on the control of an ankle in a frontal plane.

To conclude, a passive model can walk stably only with actuation and control through ankle torque not only in a sagittal plane but also in a frontal plane. This result of the analysis using dynamics supports the rehabilitation strategies for locomotion that focus on ankle motion.

7.3. Future Work

In the study of the springy legged model with a double stance phase, I selected the length of springy legs as the indicator of the completion of a step. This is aimed to make the potential energy of springy legs be constant at every beginning of a step. One of alternatives is a model of which the angle between the legs is always reset as a constant at the beginning of a step. The dynamics of such model is worthy of further investigation, considering that in normal human gait, the angle between two legs is almost constant at every beginning of a step.

I established an ankle actuated model that can make a stable period-one gait in a sagittal plane. However, a knee actuated or hip actuated walker might also generate a stable period-one gait. In particularl, a recent study showed that a hip actuated walker can walk stably on a horizontal floor [22].

One important issue is to compare the behaviors of each "single joint actuated" model. Either an ankle actuated model or a hip actuated model might show behaviors that are closer to the

experimental data of human locomotion than others. To assess the extent to which each bipedal walking model explains the dynamic behavior of human locomotion, it is crucial to allow each model the same simplicity of control algorithm. For example, the ankle actuated model I established in this study automatically stops ankle actuation during the single stance phase. This behavior is consistent with the eletromyograph (EMG) record that shows negligible muscle activity of the swing leg [23, 24]. In contrast, a knee actuated or hip actuated walker might be expected to have another control algorithm beyond a feedforward actuation command to be consistent with this experimental data.

Detailed comparison through analysis of each model is assigned to future work. To assess the accuracy and faithfulness of each model, the same or equivalent simplicity should be allowed. Then, the accuracy of each model should be quantified using comparison with experimental data.

Another important direction of future work for the ankle actuated model is related to the design of controllers for a therapy robot module for the ankle. In the model studied in this thesis, the applied torque is a linear function of ankle angle. However, ankle torque actuation using time rather than angle as the variable may be more convenient considering the practical application of the ankle robot. Therefore, I need to investigate whether the actuation algorithm whose reference variable is time can yield a stable gait of a simple bipedal model. Extended from this investigation, I can analyze the behaviors of the model with various ankle torque profiles.

Finally, in the analysis of the double inverted pendulum, the controller was designed using LQR assuming that the angle and angular velocity of the upper body can also be obtained from any kind of sensor. However, in practical use of a therapy robot module for the ankle, it is hard for the ankle robot to sense the angle of upper body about hips. Therefore, to relate the analysis of the model to the application of ankle robot more closely, I need to investigate whether LQR with output

of the angle and angular velocity of ankle alone can achieve balancing. In other words, I need to check the observability from the ankle alone and design a controller with an observer.

Appendix

A. Existence of Derivative Matrices of the Poincaré Maps

In this section, I show that the Poincaré map representing the stride function of each model is differentiable so that the derivative matrix exists. This argument aims to prove that linearization is valid for the stability analysis of the period-one gaits of the models studied. Before starting the proof, I introduce some relevant terminology and a proven theorem.

Definition A function has smoothness of C^n ($n \geq 0$) when the n^{th} derivative of the function exists and is continuous. For example, a function $f(x) = \begin{cases} 0 (x \leq 0) \\ x (x > 0) \end{cases}$ is C^0 but not C^1 while a function $f(x) = \begin{cases} 0 (x \leq 0) \\ x^2 (x > 0) \end{cases}$ is C^1 and hence C^0 but not C^2.

Theorem Assume that a state vector $\mathbf{x}$ obeys an evolution rule $\dot{\mathbf{x}} = f(\mathbf{x})$. The solution $\mathbf{x}(t; \mathbf{x}_0, t_0)$ is as smooth in $\mathbf{x}_0$ as f is in $(\mathbf{x}, t)$. E.g., if f is C^3 in $(\mathbf{x}, t)$, then $\mathbf{x}(t; \mathbf{x}_0, t_0)$ is C^3 in $(\mathbf{x}_0, t_0)$.

A.1. A rimless Wheel and an Ankle Actuated Model in a Sagittal Plane

Let a collision occur at $t = 0$ and the next collision occur at T_f. With the definitions of $\mathbf{x} = \begin{pmatrix} x_1 \\ x_2 \end{pmatrix} = \begin{pmatrix} \theta \\ \dot{\theta} \end{pmatrix}$ and $\hat{\mathbf{x}} = (x_2) = (\dot{\theta})$, the Poincaré map, $\mathbf{f}$ is summarized schematically as

$$\mathbf{f} : (\hat{\mathbf{x}}_0, t = 0_+) \xrightarrow{\dot{\mathbf{x}} = f(\mathbf{x})} (\hat{\mathbf{x}}, t = T_{f-}) \xrightarrow{Collision} (\hat{\mathbf{x}}, t = T_{f+}),$$

where $f(\mathbf{x}) = \begin{pmatrix} x_2 \\ f_2(x_1) \end{pmatrix}$, which is the corresponding evolution rule of each model, and

$$\mathbf{x}\big|_{t=T_{f+}} = \begin{pmatrix} \theta \\ \dot{\theta} \end{pmatrix}\Big|_{t=T_{f+}} = \begin{pmatrix} -\theta \\ (\cos 2\alpha)\dot{\theta} \end{pmatrix}\Big|_{t=T_{f-}} = \begin{pmatrix} \alpha \\ (\cos 2\alpha)\dot{\theta} \end{pmatrix}\Big|_{t=T_{f-}}.$$

I can obtain an explicit form of **f**. Using a work-energy principle,

$$\frac{1}{2}mv_0^2 + W = \frac{1}{2}mv_1^2,$$

where $v_0 = v(t = 0_+)$, $v_1 = v(t = T_{f-})$, and W is the work done by an external force. For the rimless wheel on a slight slope, $W = 2mgl\sin\alpha\sin\gamma$, and for the ankle actuated walker $W = \frac{1}{2}k(\frac{\pi}{2} + \alpha)^2$. For both cases, W is a constant, and $v_1 = \sqrt{v_0^2 + \frac{2W}{m}}$.

The whole map of $\mathbf{f} : (\hat{\mathbf{x}}_0, t = 0_+) \xrightarrow{\dot{\mathbf{x}} = f(\mathbf{x})} (\hat{\mathbf{x}}, t = T_{f-}) \xrightarrow{Collision} (\hat{\mathbf{x}}, t = T_{f+})$ becomes

$$\dot{\theta}(t = T_{f+}) = -\frac{\cos 2\alpha}{l}\sqrt{l^2\dot{\theta}_{0+}^2 + \frac{4mgl\sin\alpha\sin\gamma}{m}} = \mathbf{f}(\hat{\mathbf{x}}_0, t = 0_+) = \mathbf{f}(\dot{\theta}_{0+})$$

for the rimless wheel on a slope and

$$\dot{\theta}(t = T_{f+}) = -\frac{\cos 2\alpha}{L}\sqrt{L^2\dot{\theta}_{0+}^2 + \frac{k}{m}(\frac{\pi}{2} + \alpha)^2} = \mathbf{f}(\hat{\mathbf{x}}_0, t = 0_+) = \mathbf{f}(\dot{\theta}_{0+})$$

for the ankle actuated model in a sagittal plane, where $\dot{\theta}_{0+} = \dot{\theta}(t = 0_+)$. In each explicit form, the map **f** is differentiable with respect to $\hat{\mathbf{x}}_0$, which means that the derivative matrix of the map of each model exists.

A.2. Springy legged models

I will show that the Poincaré map is C^1 in state variables in the case of the model with double stance phase. In the case of the model without double stance, proof can be done similarly.

I consider a map representing one step as a combination of two maps. The first part is the map $\mathbf{f}_1$ whose input and output are the reduced state vectors at the beginning and the end of one step respectively. The second part is the map $\mathbf{f}_2$ whose input and output are the reduced state vectors at the end of one step and the beginning of the next step respectively.

T_{ss} is the time when a step ends. The combination of $\mathbf{f}_1$ and $\mathbf{f}_2$ makes the whole map corresponding to the Poincaré map whose input and output are the reduced state vectors at $t = 0_+$ and $t = T_{ss+}$ respectively, or

$$\mathbf{f} = \mathbf{f}_2 \circ \mathbf{f}_1 : (\hat{\mathbf{x}}_0, t = 0_+) \rightarrow (\hat{\mathbf{x}}, t = T_{ss-}) \xrightarrow{\text{continuity of velocity}} (\hat{\mathbf{x}}, t = T_{ss+}).$$

With some reasonable assumptions and the introduced theorem above, I can state that the first map $\mathbf{f}_1$ is smooth enough to be C^1 in $\hat{\mathbf{x}}_0$. Hereafter, I refer to this fact as ⓐ. I will depend on fact ⓐ to complete the proof.

Please see Figure A - 1. Let η be the value of $-\theta$ at $t = T_{ss-}$. To be faithful to the Poincaré section I selected, I need the length of the new stance leg l_n to be the unloaded leg length l_0 at $t = T_{ss+}$. Then, φ at $t = T_{ss+}$, which I define as β hereafter, and the new stride distance s are determined by geometry because I know the values of l_2 at $t = T_{ss-}$, which is l^*, and $-\theta$, which is η. To summarize, at $t = T_{ss-}$, $-\theta = \eta$, and $l_2 = l^*$ while at $t = T_{ss+}$, $\varphi = \beta$, and $l_n = l_0$.

Using the geometry and continuity of the velocity vector at $t = T_{ss}$,

$$x_3\big|_{t=T_{ss+}} = \varphi\big|_{t=T_{ss+}} = \beta = \cos^{-1}\left(\frac{l^*}{l_0}\cos\eta\right) = \cos^{-1}\left(\frac{l^*}{l_0}\cos(-\theta\big|_{t=T_{ss-}})\right), \text{ and} \quad \text{Eq A} - 1$$

$$\left.\begin{pmatrix} x_2 \\ x_4 \end{pmatrix}\right|_{t=Tf+} = \begin{pmatrix} \dot{l}_n \\ \dot{\varphi} \end{pmatrix} = \begin{pmatrix} -\sin\beta & -l_0\cos\beta \\ \cos\beta & -l_0\sin\beta \end{pmatrix}^{-1} \left.\begin{pmatrix} \dot{l}_2(\sin\eta) - l^*\dot{\theta}(\cos\eta) \\ \dot{l}_2(\cos\eta) + l^*\dot{\theta}(\sin\eta) \end{pmatrix}\right|_{t=Tss-} \quad \text{. Eq A} - 2$$

By ⓐ, η is at least C^1 in $\hat{\mathbf{x}}_0$. Therefore, it is obvious that β or $x_3|_{t=Tss+}$ is at least C^1 in $\hat{\mathbf{x}}_0$ from Eq A–1. Also, by ⓐ, $\dot{l}_2$ at $t = T_{ss-}$ is at least C^1 in $\hat{\mathbf{x}}_0$. Therefore, $x_2|_{t=Tss+}$ and $x_4|_{t=Tss+}$ are also at least C^1 in $\hat{\mathbf{x}}_0$ from Eq A–2.

Therefore, map of $\mathbf{f} = \mathbf{f}_2 \circ \mathbf{f}_1 : (\hat{\mathbf{x}}_0, t = 0_+) \rightarrow (\hat{\mathbf{x}}, t = T_{ss-}) \xrightarrow{\text{continuity of velocity}} (\hat{\mathbf{x}}, t = T_{ss+})$ is at least C^1 in $\hat{\mathbf{x}}_0$. This guarantees the existence of the derivative matrix of the Poincaré map.

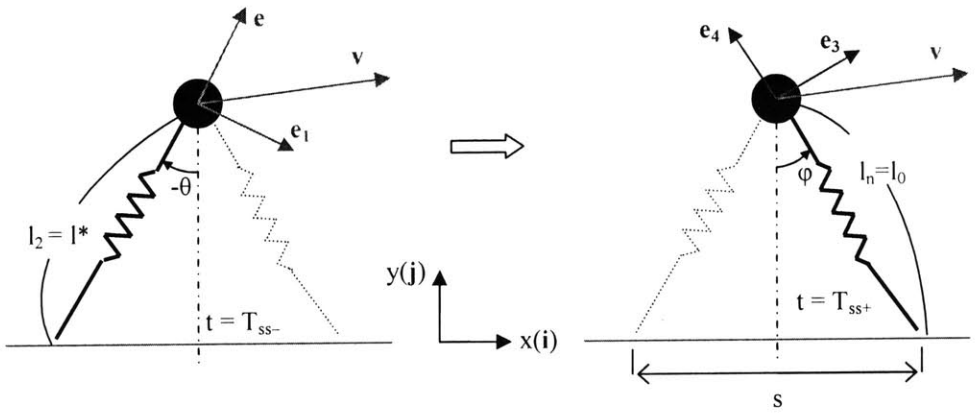

Figure A - 1

B. Source Codes

I attach detailed source codes for numerical simulation. Source codes for evolution rules, Poincaré map and finding eigenvalues of the derivative matrix of the Poincaré map of each model analyzed in chapter 2,3,4 and 5 are included in this section. Source codes for linearization of the equation of motion of the double inverted pendulum are also attached.

B.1. A Rimless Wheel Model in a Vertical Plane

Equation of Motion

```
%=========================================================================
% Equation of motion or evolution rule of the swing phase, which is
% equivalent with an inverted pendulum motion
%=========================================================================

function dx = f(t,x)

g = 9.81; gamma = 0.1; l = 1;

dx = zeros(2,1);

dx(1) = x(2);
dx(2) = g/l*sin(x(1) - gamma);
```

Poincaré Map of the Stride Function

```
%=========================================================================
% Poincare map of the rimless wheel on a slight slope
%=========================================================================

function x2f = PM(x20)

tf = 10;                          % Enough time to complete one step
l = 1; g = 9.81; m = 10;          % Parameter values
gamma = 0.1;                      % Slope angle
alpha = pi/8;                     % Half of an angle between two legs

x10 = alpha; x20bc = x20;         % Initial value of state variables before
                                  % collision
x20ac = x20bc*cos(2*alpha);       % Initial value of the angular velocity
                                  % after collision
x0 = [x10, x20ac];                % Initial state vector after collision
```

```
options = odeset('RelTol',1e-8,'AbsTol',[1e-8 1e-8]);
[T,x] = ode45(@f, [0 tf], x0, options);      % Solve the predefined equation
                                             % of motion

id = min(find (x(:,1) < - alpha));    % Find index that makes x(1) = -alpha
Tf = T(id-1) + (T(id) - T(id-1))*(-alpha - x(id-1,1))/(x(id,1) - x(id-1,1));
                                      % Define the time when a step ends
x2f =  x(id-1,2) + (x(id,2) - x(id-1,2))*(Tf - T(id-1))/(T(id) - T(id-1));
                        % x(2) at the end of a step, which is the output of the map
```

Time Response of the State Variables

```
%=========================================================================
% This code shows the time response of each state variables for a rimless
% wheel motion with a specific initial velocity
%=========================================================================
clear all; close all;

tf = 10;                          % Enough time to complete one step

l = 1; g = 9.81; m = 10;          % Parameter values
gamma = 0.1;                      % Slope angle
alpha = pi/8;                     % Half of an angle between two legs

eps = -0.4;                       % Arbitrary deviation from the value of the
                                  % fixed point of the stride function

v0 = sqrt(4*g*l*sin(alpha)*sin(gamma)/(1 - (cos(2*alpha))^2)) + eps;
% Initial speed of interest = Initial speed of for the fixed point of Poincare
% map + arbitrary deviation

%----------------------------Solving Equation of Motion--------------------
x10 = alpha; x20bc = - v0/l;  % Initial value of state variables before collision
x20ac = x20bc*cos(2*alpha);   % Initial value of the angular velocity after
                              % collision
x0 = [x10, x20ac];            % Initial state vector after collision

options = odeset('RelTol',1e-8,'AbsTol',[1e-8 1e-8]);
[T,x] = ode45(@f, [0 tf], x0, options);  % Solve the predefined equation of motion
%-------------------------------------------------------------------------
%----------------------------Define the end of one step--------------------
id = min(find (x(:,1) < - alpha));     % Find index that makes x(1) = -alpha
Tf = T(id-1) + (T(id) - T(id-1))*(-alpha - x(id-1,1))/(x(id,1) - x(id-1,1));
% Define the time when a step ends
x2f =  x(id-1,2) + (x(id,2) - x(id-1,2))*(Tf - T(id-1))/(T(id) - T(id-1));
% x(2) at the end of a step, which is the output of the map
error = x2f - x20bc;
%-------------------------------------------------------------------------

for (i = 1:id)
   time(i) = T(i);
   z(i,1) = x(i,1);
   z(i,2) = x(i,2);
end
```

```
figure(2);
subplot(2,1,1); plot(time, z(:,1),'r'); grid on;
xlabel('time (s)'); ylabel('\theta (rad)');
subplot(2,1,2); plot(time, z(:,2),'g'); grid on;
xlabel('time (s)'); ylabel('d\theta/dt (rad/s)');
```

Eigenvalues of the Derivative Matrix of the Poincaré Map

```
%=========================================================================
% Stability analysis using the eigenvalues of the derivative matrix of the
% Poincare Map
%=========================================================================

clear all; close all;


n = 10;                          % Number of mapping

l = 1; g = 9.81; m = 10;         % Parameter values
gamma = 0.1;                     % Slope angle
alpha = pi/8;                    % Half of an angle between two legs

v0f = sqrt(4*g*l*sin(alpha)*sin(gamma)/(1 - (cos(2*alpha))^2));
                                 % Initial speed for the fixed point of Poincare Map
x2fixed = -v0f/l;
x2v = x2fixed-0.3:0.01:x2fixed+0.3;

for (i = 1:length(x2v))
   x2f(i) = PM(x2v(i));          % Use the predefined function PM, which represents
                                 % the Poincare map of the stride function
end

deriv_M = gradient(x2f, 0.01);       % Derivative matrix of the Poincare map

id = find(x2v == x2fixed);

eigen = deriv_M(id);             % The eigenvalue of the Poincare map
```

Behavior of a Small Neighborhood of the Fixed Point of the Poincaré Map

```
%=========================================================================
% Stability analysis by investigating the behavior of a small neighborhood
% of the fixed point of the Poincare map
%=========================================================================

clear all; close all;

n = 10;                          % Number of mapping

l = 1; g = 9.81; m = 10;         % Parameter values
gamma = 0.1;                     % Slope angle
alpha = pi/8;                    % Half of an angle between two legs
```

```
eps = 0.1;                          % Unit of deviation from the fixed point

v0f = sqrt(4*g*l*sin(alpha)*sin(gamma)/(1 - (cos(2*alpha))^2));
                                    % Initial speed for the fixed point of Poincare Map
x2fixed = -v0f/l;

for (j = 1:7)

v0 = v0f + eps*(j-4);               % Various Initial speed

x20(1) = -v0/l;

    for (i = 1:n)
       x2f(i) = PM(x20(i));
       error(i,j) = x2f(i) - x2fixed;        % Deviation from the fixed point
       x20(i+1) = x2f(i);
    end
end

figure(1);
plot(error(:,1),'k'); hold on;
plot(error(:,2),'--b'); hold on;
plot(error(:,3),'-.c'); hold on;
plot(error(:,4),'g'); hold on;
plot(error(:,5),':b'); hold on;
plot(error(:,6),'--m'); hold on;
plot(error(:,7),'r'); hold on;
legend('\epsilon = -0.3','\epsilon = -0.2','\epsilon = -0.1','\epsilon =
0','\epsilon = 0.1','\epsilon = 0.2','\epsilon = 0.3')
grid on;
xlabel('Number of mapping'); ylabel('d\theta/dt - (d\theta/dt)_0 (rad/s)');
```

B.2. A Springy Legged Model without Double Stance

Equation of Motions

```
%=========================================================================
% Equation of motion or evolution rule of the system
%=========================================================================

function dx = f(t,x)

g = 9.81; m = 10; k = 1000; lo = 1;

dx = zeros(4,1);
dx(1) = x(2);
dx(2) = x(1)*x(4)^2 - g*cos(x(3)) - k/m*(x(1)-lo);
dx(3) = x(4);
dx(4) = -1/x(1)*(2*x(2)*x(4)) + g/x(1)*sin(x(3));
```

Poincaré Map of the Stride Function

```
%=========================================================================
% Poincare map of the springy legged model without double stance phase
%=========================================================================

function [x2f, x3f, x4f] = PM(x20, x30, x40)

t = 2;
lo = 1; g = 9.81; m = 10;      % Parameter values
alpha = pi/8;                  % Half of an angle between two legs

x10 = lo;                      % The anchor indicating the end of a step

x0 = [x10, x20, x30, x40];     % Initial state vector

options = odeset('RelTol',1e-6,'AbsTol',[1e-6 1e-6 1e-6 1e-6]);
[T,x] = ode45(@f, [0 t], x0, options);       % Solve the eq of motions

id = min(find (x(:,1)>lo));    % Index that makes x1 = lo

Tf = T(id-1) + (T(id) - T(id-1))*(lo - x(id-1,1))/(x(id,1) - x(id-1,1));
                                                    % Time when a step ends
x1_f =  x(id-1,1) + (x(id,1) - x(id-1,1))*(Tf - T(id-1))/(T(id) - T(id-1));
                                                    % Final value of x1
x2_f =  x(id-1,2) + (x(id,2) - x(id-1,2))*(Tf - T(id-1))/(T(id) - T(id-1));
                                                    % Final value of x2
x3_f =  x(id-1,3) + (x(id,3) - x(id-1,3))*(Tf - T(id-1))/(T(id) - T(id-1));
                                                    % Final value of x3
x4_f =  x(id-1,4) + (x(id,4) - x(id-1,4))*(Tf - T(id-1))/(T(id) - T(id-1));
                                                    % Final value of x4

x3f = -x3_f;

b = [(x2_f*sin(x3f) - x1_f*x4_f*cos(x3f)), (x2_f*cos(x3f) +
x1_f*x4_f*sin(x3f))]';
A = [(-sin(x3f)), (-x1_f*cos(x3f)); (cos(x3f)), (-x1_f*sin(x3f))];

z = A\b;

x2f = z(1);
x4f = z(2);
```

Calculating the Normalized Norm of Error Vector ξ

```
%=========================================================================
% This function returns
% [1] the proper initial velocity which minimizes the norm of
% (x(desired) - x(actual)) locally at the end of a step and
% [2] the minimal norm or the error.
% Input of this function is the initial estimates of initial condition
%=========================================================================

function ff = func1(y)

t = 1;
alpha =  pi/8;
```

```
g = 9.81; m = 10; k = 1000; lo = 1; li = lo;

v0 = y(1);              % Define initial condition from the input of func1()
beta = y(2);            % Define initial condition from the input of func1()

%-------------------------------------------------------------------------
% Perform the procedure of "springy_leg_specific.m to solve the ODE with
% each initial condition
%-------------------------------------------------------------------------

x10 = li; x20 = -1*v0*sin(alpha - beta); x30 = alpha; x40 = -1*v0*cos(alpha -
beta)/li;
x0 = [x10, x20, x30, x40];

options = odeset('RelTol',1e-6,'AbsTol',[1e-6 1e-6 1e-6 1e-6]);
[T,x] = ode45(@f, [0 t], x0, options);

id = min(find (x(:,1)>lo));          % Index that makes x1 = lo

Tf = T(id-1) + (T(id) - T(id-1))*(lo - x(id-1,1))/(x(id,1) - x(id-1,1));
                                                    % Time when a step ends
x1f =  x(id-1,1) + (x(id,1) - x(id-1,1))*(Tf - T(id-1))/(T(id) - T(id-1));
                                                    % Final value of x1
x2f =  x(id-1,2) + (x(id,2) - x(id-1,2))*(Tf - T(id-1))/(T(id) - T(id-1));
                                                    % Final value of x2
x3f =  x(id-1,3) + (x(id,3) - x(id-1,3))*(Tf - T(id-1))/(T(id) - T(id-1));
                                                    % Final value of x3
x4f =  x(id-1,4) + (x(id,4) - x(id-1,4))*(Tf - T(id-1))/(T(id) - T(id-1));
                                                    % Final value of x4

%-------------------------------------------------------------------------
% Desired value of each state variable at the end of the step to make
% periodic gait
%-------------------------------------------------------------------------
x1f_d = li;
x2f_d = v0*sin(alpha + beta);
x3f_d = -alpha;
x4f_d = -1*v0/li*cos(alpha + beta);

ff = norm([x2f/x2f_d-1, x3f/x3f_d-1, x4f/x4f_d-1]);    % Return the norm of error
```

Find a Fixed Point of the Poincaré map and Visualize the Resultant Motion

```
%=========================================================================
% This function finds the proper initial velocity which minimizes
% the norm of (x(desired) - x(actual)) locally at the end of a step,
% and then, show the response of this optimal initial velocity
%=========================================================================

clear all; close all;

v00 =1.5; beta0 = 0;        % Set the initial value where I'll start optimization
ic0 = [v00, beta0];
[ic,ffval] = fminsearch(@func1,ic0);    % Find the optimal initial condition which
generates periodic gait
```

```
t = 1;                  % Set enough time first
alpha =  pi/8;          % Two times alpha means the angle between two legs
g = 9.81; m = 10; k = 1000; lo = 1; li = lo; % Parameter value

v0 = ic(1);             % Plug in the optimal initial condition
beta = ic(2);           % Plug in the optimal initial condition

x10 = li; x20 = -1*v0*sin(alpha - beta); x30 = alpha; x40 = -1*v0*cos(alpha -
beta)/li;
x0 = [x10, x20, x30, x40];

options = odeset('RelTol',1e-6,'AbsTol',[1e-6 1e-6 1e-6 1e-6]);
[T,x] = ode45(@f, [0 t], x0, options);     % Solve the nonlinear eqs of motion

id = min(find (x(:,1)>lo)); % Index that makes x1 = lo

Tf = T(id-1) + (T(id) - T(id-1))*(lo - x(id-1,1))/(x(id,1) - x(id-1,1));
                                                    % Time when a step ends
x1f =  x(id-1,1) + (x(id,1) - x(id-1,1))*(Tf - T(id-1))/(T(id) - T(id-1));
                                                    % Final value of x1
x2f =  x(id-1,2) + (x(id,2) - x(id-1,2))*(Tf - T(id-1))/(T(id) - T(id-1));
                                                    % Final value of x2
x3f =  x(id-1,3) + (x(id,3) - x(id-1,3))*(Tf - T(id-1))/(T(id) - T(id-1));
                                                    % Final value of x3
x4f =  x(id-1,4) + (x(id,4) - x(id-1,4))*(Tf - T(id-1))/(T(id) - T(id-1));
                                                    % Final value of x4



for (i = 1:id-1)
   time(i) = T(i);
   z(i,1) = x(i,1);    % Length of a springy leg
   z(i,2) = x(i,2);    % Time derivative of length of a springy leg
   z(i,3) = x(i,3);    % Angle
   z(i,4) = x(i,4);    % Time derivative of angle
end

time(id) = Tf;
z(id,1) = x1f;    % Length of a springy leg
z(id,2) = x2f;    % Time derivative of length of a springy leg
z(id,3) = x3f;    % Angle
z(id,4) = x4f;    % Time derivative of angle

figure(1);
subplot(2,2,1); plot(time, z(:,1),'r'); grid on;
xlabel('Time (s)'); ylabel('l (m)');
subplot(2,2,2); plot(time, z(:,2),'g'); grid on;
xlabel('Time (s)'); ylabel('dl/dt (m/s)');
subplot(2,2,3); plot(time, z(:,3)); grid on;
xlabel('Time (s)'); ylabel('\theta (rad)');
subplot(2,2,4); plot(time, z(:,4),'c'); grid on;
xlabel('Time (s)'); ylabel('d\theta/dt (rad/s)');
```

Eigenvalues of the Derivative Matrix of the Poincaré Map

```
%=========================================================================
% Finds the eigenvalues of the Derivative Matrix of the Poincare Map
%=========================================================================

clear all; close all;

v00 =1.5; beta0 = 0;   % Set the initial value where I'll start optimization
ic0 = [v00, beta0];
[ic,ffval] = fminsearch(@func1,ic0);
               % Find the optimal initial condition which generates periodic gait

alpha =  pi/8;          % Two times alpha means the angle between two legs
lo = 1; li = lo;        % Parameter value

v0 = ic(1);             % Plug in the optimal initial condition
beta = ic(2);           % Plug in the optimal initial condition

x10 = li; x20 = -1*v0*sin(alpha - beta); x30 = alpha; x40 = -1*v0*cos(alpha -
beta)/li;

x2v = x20-0.03:0.01:x20+0.03;
x3v = x30-0.03:0.01:x30+0.03;
x4v = x40-0.03:0.01:x40+0.03;

N = length(x2v);

for (i = 1:N)
    for (j = 1:N)
        for (k = 1:N)
            [x2f(i,j,k), x3f(i,j,k), x4f(i,j,k)] = PM(x2v(i), x3v(j), x4v(k));
        end
    end
end

[D22, D23, D24] = gradient(x2f, x2v, x3v, x4v);
[D32, D33, D34] = gradient(x3f, x2v, x3v, x4v);
[D42, D43, D44] = gradient(x4f, x2v, x3v, x4v);

io = find(x2v == x20);
jo = find(x3v == x30);
ko = find(x4v == x40);

d22 = D22(io, jo, ko); d23 = D23(io, jo, ko); d24 = D24(io, jo, ko);
d32 = D32(io, jo, ko); d33 = D33(io, jo, ko); d34 = D34(io, jo, ko);
d42 = D42(io, jo, ko); d43 = D43(io, jo, ko); d44 = D44(io, jo, ko);

D = [d22, d23, d24; d32, d33, d34; d42, d43, d44];
                              % D = Derivative Matrix of Poincare Map at fixed pt

lambda = eig(D);
```

Behavior of a Small Neighborhood of the Fixed Point of the Poincaré Map

```
%=========================================================================
% Stability Analysis by the behavior of a small neighborhood of the fixed
% point of the Poincare map
%=========================================================================

clear all; close all;

v00 =1.5; beta0 = 0;        % Set the initial value where I'll start optimization
ic0 = [v00, beta0];
[ic,ffval] = fminsearch(@func1,ic0);    % Find the optimal initial condition which
generates periodic gait

t = 1;                  % Set enough time first
alpha =  pi/8;          % Two times alpha means the angle between two legs
g = 9.81; m = 10; k = 1000; lo = 1; li = lo; % Parameter value

v0 = ic(1);             % Plug in the optimal initial condition
beta = ic(2);           % Plug in the optimal initial condition

x10 = li; x20 = -1*v0*sin(alpha - beta); x30 = alpha; x40 = -1*v0*cos(alpha -
beta)/li;
x0 = [x10, x20, x30, x40];

n = 4;                  % No. of mapping

eps = 0.01;             % Unit of deviation

% Fixed point of Poincare Map
x2fixed = x0(2);
x3fixed = x0(3);
x4fixed = x0(4);

for (j = 1:7)

x20(1) = x2fixed + eps*(j-4);        % Initial speed
x30(1) = x3fixed;
x40(1) = x4fixed;

error(1,j) = norm([(x20(1)/x2fixed - 1)]);

   for (i = 1:n)
       [x2f(i), x3f(i), x4f(i)] = PM(x20(i), x30(i), x40(i));
       error(i+1,j) = norm([(x2f(i)/x2fixed - 1), (x3f(i)/x3fixed - 1),
(x4f(i)/x4fixed -1)]);
       x20(i+1) = x2f(i); x30(i+1) = x3f(i); x40(i+1) = x4f(i);
   end
end


figure(2);
plot(error(:,1),'k'); hold on;
plot(error(:,2),'--b'); hold on;
plot(error(:,3),'-.c'); hold on;
plot(error(:,4),'g'); hold on;
plot(error(:,5),':b'); hold on;
plot(error(:,6),'--m'); hold on;
```

```
plot(error(:,7),'r'); hold on;
legend('\epsilon = -0.03','\epsilon = -0.02','\epsilon = -0.01','\epsilon =
0','\epsilon = 0.01','\epsilon = 0.02','\epsilon = 0.03')
grid on;
xlabel('Number of mapping'); ylabel('Norm of \xi');
```

B.3. A Springy Legged Model with Double Stance

Equation of Motions

```
%=========================================================================
% Equation of motion or evolution rule of double stance phase
%=========================================================================

function dx = fd(t,x)

g = 9.81; m = 10; k = 1000; lo = 1; s = 0.75;

dx = zeros(4,1);
dx(1) = x(2);
dx(2) = x(1)*x(4)^2 - g*cos(x(3)) - k/m*((x(1)-lo) + (x(1) - s*sin(x(3))) -
lo*(x(1) - s*sin(x(3)))/sqrt(s^2 + x(1)^2 - 2*s*x(1)*sin(x(3))));
dx(3) = x(4);
dx(4) = -1/x(1)*(2*x(2)*x(4)) + g/x(1)*sin(x(3)) - k/m*s*cos(x(3))*(lo/sqrt(s^2 +
x(1)^2 - 2*s*x(1)*sin(x(3))) - 1);


%=========================================================================
% Equation of motion or evolution rule of double stance phase
% considering stride length s as a parameter value that is constant during
% one step but can vary discretely per step number
%=========================================================================

function dx = fdpm(t,x)

g = 9.81; m = 10; k = 1000; lo = 1;

dx = zeros(4,1);
dx(1) = x(2);
dx(2) = x(1)*x(4)^2 - g*cos(x(3)) - k/m*((x(1)-lo) + (x(1) - x(5)*sin(x(3))) -
lo*(x(1) - x(5)*sin(x(3)))/sqrt(x(5)^2 + x(1)^2 - 2*x(5)*x(1)*sin(x(3))));
dx(3) = x(4);
dx(4) = -1/x(1)*(2*x(2)*x(4)) + g/x(1)*sin(x(3)) -
k/m*x(5)*cos(x(3))*(lo/sqrt(x(5)^2 + x(1)^2 - 2*x(5)*x(1)*sin(x(3))) - 1);
dx(5) = 0;      % x(5) = si, which is not a state variable but a varying
                % parameter: a step stride length
```

```
%=========================================================================
% Equation of motion or evolution rule of single stance phase
%=========================================================================

function dy = fs(t,y)

g = 9.81; m = 10; k = 1000; lo = 1;

dy = zeros(4,1);
dy(1) = y(2);
dy(2) = y(1)*y(4)^2 - g*cos(y(3)) - k/m*(y(1)-lo);
dy(3) = y(4);
dy(4) = -1/y(1)*(2*y(2)*y(4)) + g/y(1)*sin(y(3));
```

Poincaré Map of the Stride Function

```
%=========================================================================
% Poincare Map of the springy legged model with double stance phase
%=========================================================================

function [sf, x2f, x3f, x4f] = PM(si, x20, x30, x40)

td = 0.3;       % Enough time to complete double stance phase
ts = 1;         % Enough time to complete one step
lo = 1;

li = lo;
x10 = li;
x50 = si;
l10 = sqrt(x10^2 + si^2 - 2*si*x10*sin(x30));
% Initial values of l1 -- the anchor indicating the end of a step


%-------------------------------------------------------------------------
%------------------------ Double stance phase ----------------------------

x0 = [x10, x20, x30, x40, x50];
% Initial state vector -- Note that x5 is not a state variable, but a varying
% parameter -  a stride length

options1 = odeset('RelTol',1e-8,'AbsTol',[1e-8 1e-8 1e-8 1e-8 1e-8]);
[T,x] = ode45(@fdpm, [0 td], x0, options1);  % Solve the predefined equation of
                                             % motion
%-------------------------------------------------------------------------

%------------------------ Single stance phase ----------------------------

l1 = sqrt(x(:,1).^2 + si^2 - 2*si*x(:,1).*sin(x(:,3))); % Values of l1
id = min(find (l1 > lo));                               % Index that makes l1 = lo
Tds = T(id-1) + (T(id) - T(id-1))*(lo - l1(id-1))/(l1(id) - l1(id-1));
                              % Define the time when double stance phase ends

y10 =  x(id-1,1) + (x(id,1) - x(id-1,1))*(Tds - T(id-1))/(T(id) - T(id-1));
                        % Initial value of l2 for single stance phase
y20 =  x(id-1,2) + (x(id,2) - x(id-1,2))*(Tds - T(id-1))/(T(id) - T(id-1));
                        % Initial value of d(l2)/dt for single stance phase
```

```
y30 =  x(id-1,3) + (x(id,3) - x(id-1,3))*(Tds - T(id-1))/(T(id) - T(id-1));
                        % Initial value of theta for single stance phase
y40 =  x(id-1,4) + (x(id,4) - x(id-1,4))*(Tds - T(id-1))/(T(id) - T(id-1));
                        % Initial value of d(theta)/dt for single stance phase

y0 = [y10, y20, y30, y40];          % Initial state vector for single stance phase
options2 = odeset('RelTol',1e-8,'AbsTol',[1e-8 1e-8 1e-8 1e-8]);
[T_s,y] = ode45(@fs, [Tds ts], y0, options2);       % Solve the predefined
                                                    % equation of motion


id_s = max(find (y(:,1) < l10));                    % Index that makes y1 = l10
Tss = T_s(id_s) + (T_s(id_s+1) - T_s(id_s))*(y(id_s,1) - l10)/(y(id_s,1) -
y(id_s+1,1));                                  % Define the time when a step ends

y1f =  y(id_s,1) + (y(id_s+1,1) - y(id_s,1))*(Tss - T_s(id_s))/(T_s(id_s+1) -
T_s(id_s));                    % Final value of l2
y2f =  y(id_s,2) + (y(id_s+1,2) - y(id_s,2))*(Tss - T_s(id_s))/(T_s(id_s+1) -
T_s(id_s));                    % Final value of d(l2)/dt
y3f =  y(id_s,3) + (y(id_s+1,3) - y(id_s,3))*(Tss - T_s(id_s))/(T_s(id_s+1) -
T_s(id_s));                    % Final value of theta
y4f =  y(id_s,4) + (y(id_s+1,4) - y(id_s,4))*(Tss - T_s(id_s))/(T_s(id_s+1) -
T_s(id_s));                    % Final value of d(theta)/dt
%-------------------------------------------------------------------------

%---- Transition from end of one step to the beginning of the next step ---

sf = y1f*sin(-y3f) + sqrt(li^2 - (y1f*cos(-y3f))^2);
x3f = acos((y1f*cos(-y3f))/li);

b = [(y2f*sin(-y3f) - y1f*y4f*cos(-y3f)), (y2f*cos(-y3f) + y1f*y4f*sin(-y3f))]';
A = [(-sin(x3f)), (-li*cos(x3f)); (cos(x3f)), (-li*sin(x3f))];

z = A\b;

x2f = z(1);
x4f = z(2);
%-------------------------------------------------------------------------
%-------------------------------------------------------------------------
```

Calculating the Normalized Norm of Error Vector ξ

```
%=========================================================================
% This function returns
% [1] the locally optimal initial velocity that minimizes the norm of
% ((desired x for a periodic gait) - (solved x)) at the end of one step and
% [2] the minimal norm or the error.
% Input of this function is the initial estimates of initial condition
%=========================================================================

function ff = func(y)

td = 0.3;               % Enough time to complete double stance
ts = 2;                 % Enough time to complete one step

s = 0.75;               % Step stride length
```

```
g = 9.81; m = 10; k = 1000; lo = 1;          % Parameter values
delta = 0.1;

li = lo; alpha = asin(s/2/li) + delta;       % Initial value of theta and li

v0 = y(1);              % Define initial condition from the input of func()
beta = y(2);            % Define initial condition from the input of func()

gamma = atan(s/lo/cos(alpha) - tan(alpha));


%-------------------------------------------------------------------------
% Perform the procedure of solving the predefined ODE set with each initial
% condition
%-------------------------------------------------------------------------

%-------------------------------------------------------------------------
%------------------------ Double stance phase ----------------------------

x10 = li; x20 = -v0*sin(alpha - beta); x30 = alpha; x40 = -v0*cos(alpha -
beta)/li;
                                        % Initial value of state variables
x0 = [x10, x20, x30, x40];              % Initial state vector

l10 = sqrt(x10^2 + s^2 - 2*s*x10*sin(x30));
                % Initial values of l1 -- the anchor indicating the end of a step

options = odeset('RelTol',1e-8,'AbsTol',[1e-8 1e-8 1e-8 1e-8]);
[T,x] = ode45(@fd, [0 td], x0, options);  % Solve the predefined equation of
motion
%-------------------------------------------------------------------------

%------------------------ Single stance phase ----------------------------
l1 = sqrt(x(:,1).^2 + s^2 - 2*s*x(:,1).*sin(x(:,3)));   % Values of l1
id = min(find (l1 > lo));      % Index that makes l1 = lo
Tds = T(id-1) + (T(id) - T(id-1))*(lo - l1(id-1))/(l1(id) - l1(id-1));
                               % Define the time when double stance phase ends

y10 =  x(id-1,1) + (x(id,1) - x(id-1,1))*(Tds - T(id-1))/(T(id) - T(id-1));
                          % Initial value of l2 for single stance phase
y20 =  x(id-1,2) + (x(id,2) - x(id-1,2))*(Tds - T(id-1))/(T(id) - T(id-1));
                          % Initial value of d(l2)/dt for single stance phase
y30 =  x(id-1,3) + (x(id,3) - x(id-1,3))*(Tds - T(id-1))/(T(id) - T(id-1));
                          % Initial value of theta for single stance phase
y40 =  x(id-1,4) + (x(id,4) - x(id-1,4))*(Tds - T(id-1))/(T(id) - T(id-1));
                          % Initial value of d(theta)/dt for single stance phase

y0 = [y10, y20, y30, y40];     % Initial state vector for single stance phase
[T_s,y] = ode45(@fs, [Tds ts], y0, options);
                               % Solve the predefined equation of motion


id_s = min(find (y(:,3) < -gamma));  % Index that makes y3 = -gamma
Tss = T_s(id_s-1) + (T_s(id_s) - T_s(id_s-1))*(y(id_s-1,3)+gamma)/(y(id_s-1,3) -
y(id_s,3));                    % Define the time when a step ends

y1f =  y(id_s-1,1) + (y(id_s,1) - y(id_s-1,1))*(Tss - T_s(id_s-1))/(T_s(id_s) -
T_s(id_s-1));                  % Final value of l2
y2f =  y(id_s-1,2) + (y(id_s,2) - y(id_s-1,2))*(Tss - T_s(id_s-1))/(T_s(id_s) -
```

```
T_s(id_s-1));                  % Final value of d(l2)/dt
y3f = y(id_s-1,3) + (y(id_s,3) - y(id_s-1,3))*(Tss - T_s(id_s-1))/(T_s(id_s) -
T_s(id_s-1));                  % Final value of theta
y4f = y(id_s-1,4) + (y(id_s,4) - y(id_s-1,4))*(Tss - T_s(id_s-1))/(T_s(id_s) -
T_s(id_s-1));                  % Final value of d(theta)/dt

%-------------------------------------------------------------------------
%-------------------------------------------------------------------------


%-------------------------------------------------------------------------
% Desired value of each state variable at the end of the step to make a
% periodic gait
%-------------------------------------------------------------------------

x1f = l10;
x2f = v0*sin(gamma + beta);
x3f = -gamma;
x4f = -v0/x1f*cos(gamma + beta);

ff = norm([y1f/x1f-1, y2f/x2f-1, y4f/x4f-1]);
              % Return the minimum of the norm of the normalized error vector
```

Find a Fixed Point of the Poincaré map and Visualize the Resultant Motion

```
%=========================================================================
% This function returns the locally optimal initial velocity that minimizes
% the norm of ((desired x for a periodic gait) - (solved x)) at the end of
% one step, and then, shows the response of this optimal initial velocity.
%=========================================================================

clear all; close all;

v00 = 1.5; beta0 = 0.04;       % Set the initial estate from which optimization
                               % starts
ic0 = [v00, beta0];
[ic,ffval] = fminsearch(@func,ic0);
             % Find the optimal initial condition that generates a periodic gait


td = 0.3;       % Enough time to complete double stance
ts = 2;         % Enough time to complete one step

s = 0.75;       % Step stride length
g = 9.81; m = 10; k = 1000; lo = 1;          % Parameter values
delta = 0.1;

li = lo; alpha = asin(s/2/li) + delta;       % Initial value of theta and li
gamma = atan(s/lo/cos(alpha) - tan(alpha));

v0 = ic(1);     % Plug in the optimal initial condition
beta = ic(2);   % Plug in the optimal initial condition
```

```
%-------------------------------------------------------------------------
%------------------------ Double stance phase ----------------------------

x10 = li; x20 = -v0*sin(alpha - beta); x30 = alpha; x40 = -v0*cos(alpha -
beta)/li;                       % Initial value of state variables
x0 = [x10, x20, x30, x40];    % Initial state vector

options = odeset('RelTol',1e-8,'AbsTol',[1e-8 1e-8 1e-8 1e-8]);
[T,x] = ode45(@fd, [0 td], x0, options);     % Solve the predefined equation
                                             % of motion
%-------------------------------------------------------------------------

%------------------------ Single stance phase ----------------------------
l1 = sqrt(x(:,1).^2 + s^2 - 2*s*x(:,1).*sin(x(:,3)));       % Values of l1
id = min(find (l1 > lo));                                % Index that makes l1 = lo
Tds = T(id-1) + (T(id) - T(id-1))*(lo - l1(id-1))/(l1(id) - l1(id-1));
                        % Define the time when double stance phase ends

y10 =  x(id-1,1) + (x(id,1) - x(id-1,1))*(Tds - T(id-1))/(T(id) - T(id-1));
                        % Initial value of l2 for single stance phase
y20 =  x(id-1,2) + (x(id,2) - x(id-1,2))*(Tds - T(id-1))/(T(id) - T(id-1));
                        % Initial value of d(l2)/dt for single stance phase
y30 =  x(id-1,3) + (x(id,3) - x(id-1,3))*(Tds - T(id-1))/(T(id) - T(id-1));
                        % Initial value of theta for single stance phase
y40 =  x(id-1,4) + (x(id,4) - x(id-1,4))*(Tds - T(id-1))/(T(id) - T(id-1));
                        % Initial value of d(theta)/dt for single stance phase

y0 = [y10, y20, y30, y40];    % Initial state vector for single stance phase
[T_s,y] = ode45(@fs, [Tds ts], y0, options);
                              % Solve the predefined equation of motion

id_s = min(find (y(:,3) < -gamma));          % Index that makes y3 = -gamma
Tss = T_s(id_s-1) + (T_s(id_s) - T_s(id_s-1))*(y(id_s-1,3)+gamma)/(y(id_s-1,3) -
y(id_s,3));                                  % Define the time when a step ends

y1f =  y(id_s-1,1) + (y(id_s,1) - y(id_s-1,1))*(Tss - T_s(id_s-1))/(T_s(id_s) -
T_s(id_s-1));                                % Final value of l2
y2f =  y(id_s-1,2) + (y(id_s,2) - y(id_s-1,2))*(Tss - T_s(id_s-1))/(T_s(id_s) -
T_s(id_s-1));                                % Final value of d(l2)/dt
y3f =  y(id_s-1,3) + (y(id_s,3) - y(id_s-1,3))*(Tss - T_s(id_s-1))/(T_s(id_s) -
T_s(id_s-1));                                % Final value of theta
y4f =  y(id_s-1,4) + (y(id_s,4) - y(id_s-1,4))*(Tss - T_s(id_s-1))/(T_s(id_s) -
T_s(id_s-1));                                % Final value of d(theta)/dt
%-------------------------------------------------------------------------
%-------------------------------------------------------------------------



%-------------------- Reconstructing the whole step ----------------------
for (i = 1:id-1)
   time(i) = T(i);
   z(i,1) = x(i,1);    % Length of a springy leg
   z(i,2) = x(i,2);    % Time derivative of length of a springy leg
   z(i,3) = x(i,3);    % Angle
   z(i,4) = x(i,4);    % Time derivative of the angle
   test_time(i) = T(i);
   test_l1(i) = l1(i);
end
```

```
for (i = id:id+id_s-2)
    time(i) = T_s(i-id+1);
    z(i,1) = y(i-id+1,1);    % Length of a springy leg
    z(i,2) = y(i-id+1,2);    % Time derivative of length of a springy leg
    z(i,3) = y(i-id+1,3);    % Angle
    z(i,4) = y(i-id+1,4);    % Time derivative of angle
end

time(id+id_s-1) = Tss;
z(id+id_s-1,1) = y1f;
z(id+id_s-1,2) = y2f;
z(id+id_s-1,3) = y3f;
z(id+id_s-1,4) = y4f;
%-------------------------------------------------------------------------------



%------------------------ Check periodicity --------------------------------

% Desired value of each state variable at the end of the step to make a
% periodic gait

x1f = l1(1);
x2f = v0*sin(gamma + beta);
x3f = -gamma;
x4f = -v0/x1f*cos(gamma + beta);

% check the norm of normalized error (check the periodicity)
ff = norm([y1f/x1f-1, y2f/x2f-1, y4f/x4f-1]);
%-------------------------------------------------------------------------------



%---------------------------- Visualization ----------------------------------
%------------------ Plotting state variables versus time -------------------
% Plotting l1
figure(1)
plot(test_time, test_l1); grid on;
xlabel('Time (s)'); ylabel('l\fontsize{6}1 \fontsize{10}(m)');

% Plotting state variables
figure(2);
subplot(2,2,1); plot(time, z(:,1),'r'); grid on;
xlabel('Time (s)'); ylabel('l\fontsize{6}2 \fontsize{10}(m)');
subplot(2,2,2); plot(time, z(:,2),'g'); grid on;
xlabel('Time (s)'); ylabel('dl\fontsize{6}2\fontsize{10}/dt (m/s)');
subplot(2,2,3); plot(time, z(:,3)); grid on;
xlabel('Time (s)'); ylabel('\theta (rad)');
subplot(2,2,4); plot(time, z(:,4),'c'); grid on;
xlabel('Time (s)'); ylabel('d\theta/dt (rad/s)');
%-------------------------------------------------------------------------------

%--------------Plotting the motion in Cartesian coordinate-----------------

xm = s + z(:,1).*cos(z(:,3) + pi/2);
ym = z(:,1).*sin(z(:,3)+ pi/2);

%Trajectory
figure(3);
```

```
trajectory = plot(xm, ym, ':');
set(trajectory, 'LineWidth',3);
xlabel('x(m)'); ylabel('y(m)');
xlim([0 2*s]); ylim([0 lo]);
grid on;
hold on;
mark = plot(xm(id),ym(id), 'or');
set(mark,'MarkerSize',14, 'LineWidth',4);
legend('Trajectory of m','The end of double stance phase');


%Animation
figure(4)
n = length(time);
for (j = 1:n)
    h = plot(xm(j), ym(j), 'o');
    set(h,'MarkerSize',18);
    title('Motion');
    xlim([0 2*s]); ylim([0 lo]);
    xlabel('x(m)'); ylabel('y(m)');
    grid on;
    M(j) = getframe;
end

movie2avi(M, 'motion_realtime','fps',500);
movie2avi(M, 'motion_slowtime','fps',20);
%-------------------------------------------------------------------------
%-------------------------------------------------------------------------

%--------------------------Average speed ---------------------------------
n = length(time);
speed = (xm(n) - xm(1))/(time(n) - time(1));
%-------------------------------------------------------------------------
```

Eigenvalues of the Derivative Matrix of the Poincaré Map

```
%=========================================================================
% Finds the eigenvalues of the Derivative Matrix of the Poincare Map
%=========================================================================

clear all; close all;

v00 =3; beta0 = 0;     % Set the initial estate from which optimization starts

ic0 = [v00, beta0];
[ic,ffval] = fminsearch(@func,ic0);
       % Find the optimal initial condition which generates a periodic gait

v0 = ic(1);            % Plug in the optimal initial condition
beta = ic(2);          % Plug in the optimal initial condition

s0 = 0.75;             % Initial step stride length
g = 9.81; m = 10; k = 1000; lo = 1;          % Parameter values
delta = 0.1;
```

```
li = lo;                % Initial value of leg length
alpha = asin(s0/2/li) + delta;              % Initial value of theta

x10 = li; x20 = -v0*sin(alpha - beta); x30 = alpha; x40 = -v0*cos(alpha -
beta)/li;               %Initial value of state variables

x2v = x20-0.03:0.01:x20+0.03;
x3v = x30-0.03:0.01:x30+0.03;
x4v = x40-0.03:0.01:x40+0.03;

N = length(x2v);

for (i = 1:N)
    for (j = 1:N)
        for (k = 1:N)
            [sf, x2f(i,j,k), x3f(i,j,k), x4f(i,j,k)] = PM(s0, x2v(i), x3v(j),
x4v(k));
        end
    end
end

[D22, D23, D24] = gradient(x2f, x2v, x3v, x4v);
[D32, D33, D34] = gradient(x3f, x2v, x3v, x4v);
[D42, D43, D44] = gradient(x4f, x2v, x3v, x4v);

io = find(x2v == x20);
jo = find(x3v == x30);
ko = find(x4v == x40);

d22 = D22(io, jo, ko); d23 = D23(io, jo, ko); d24 = D24(io, jo, ko);
d32 = D32(io, jo, ko); d33 = D33(io, jo, ko); d34 = D34(io, jo, ko);
d42 = D42(io, jo, ko); d43 = D43(io, jo, ko); d44 = D44(io, jo, ko);

D = [d22, d23, d24; d32, d33, d34; d42, d43, d44];
                                % D = Derivative Matrix of Poincare Map at fixed pt

lambda = eig(D);                % Eigenvalues of D
```

Behavior of a Small Neighborhood of the Fixed Point of the Poincaré Map

```
%=========================================================================
% Stability analysis by investigating the behavior of the small
% neighborhood of the fixed point of the Poincare map
%=========================================================================

clear all; close all;

td = 0.3;       % Enough time to complete double stance
ts = 1;         % Enough time to complete one step
n = 30;         % Number of mapping

v00 = 3; beta0 = 0;         % Set the initial value where I'll start optimization
ic0 = [v00, beta0];
[ic,ffval] = fminsearch(@func,ic0);   % Find the optimal initial condition that
                                      % generates a periodic gait
```

```
v0 = ic(1);     % Plug in the optimal initial condition
beta = ic(2);   % Plug in the optimal initial condition



s0 = 0.75;      % Initial step stride length
g = 9.81; m = 10; k = 1000; lo = 1;   % Parameter values
delta = 0.1;
eps = 0.01;

li = lo;        % Initial value of leg length
alpha = asin(s0/2/li) + delta;        % Initial value of theta

x10 = li; x20 = -v0*sin(alpha - beta); x30 = alpha; x40 = -v0*cos(alpha -
beta)/li;                             % Initial value of state variables
x0 = [x10, x20, x30, x40];            % Initial state vector

x2fixed = x0(2);
x3fixed = x0(3);
x4fixed = x0(4);

for (j = 1:7)

x20(1) = x2fixed + eps*(j-4);         % Various initial speed
x30(1) = x3fixed;
x40(1) = x4fixed;
si(1) = s0;

error(1,j) = norm([(x20(1)/x2fixed - 1)]);

   for (i = 1:n)
       [sf(i), x2f(i), x3f(i), x4f(i)] = PM(si(i), x20(i), x30(i), x40(i));
       error(i+1,j) = norm([(x2f(i)/x2fixed - 1), (x3f(i)/x3fixed - 1),
(x4f(i)/x4fixed -1)]);
       si(i+1) = sf(i); x20(i+1) = x2f(i); x30(i+1) = x3f(i); x40(i+1) = x4f(i);
   end
end

for (i = 0:n)
       error(i+1,4) = ffval;% Eliminate residual errors from numerical simulation
end

figure(2);

plot(error(:,1),'k'); hold on;
plot(error(:,2),'--b'); hold on;
plot(error(:,3),'-.c'); hold on;
plot(error(:,4),'g'); hold on;
plot(error(:,5),':b'); hold on;
plot(error(:,6),'--m'); hold on;
plot(error(:,7),'r'); hold on;

legend('\epsilon = -0.03','\epsilon = -0.02','\epsilon = -0.01','\epsilon =
0.01','\epsilon = 0.02','\epsilon = 0.03')
grid on;
xlabel('Number of mapping'); ylabel('Norm of \xi');
xlim([0 32]);
```

B.4. An Ankle Actuated Model in a Vertical Plane

Equation of Motion

```
%=========================================================================
% Equation of motion or evolution rule of double stance phase
%=========================================================================

function dx = fd(t,x)

g = 9.81; m = 10; k = 8; L = 1; l = 0.2; alpha = pi/6;

dx = zeros(2,1);


s = 2*L*sin(alpha);
phi = atan(L*cos(x(1))/(s - l - L*sin(x(1))));
psi = acos((2*s*l - s^2 + 2*(s-l)*L*cos(pi/2 - x(1)))/(2*L*l));
a = sqrt( L^2 + l^2 - 2*L*l*cos(psi));
gamma = acos((a^2 + l^2 - L^2)/(2*a*l));
Fa = k*(pi - psi)/l/sin(gamma);


dx(1) = x(2);
dx(2) = 1/(m*L)*(m*g*sin(x(1)) - Fa*(sin(x(1))*sin(phi) + cos(x(1))*cos(phi)));


%=========================================================================
% Equation of motion or evolution rule of single stance phase
%=========================================================================

function dx = fs(t,x)

g = 9.81; L = 1;

dx = zeros(2,1);
dx(1) = x(2);
dx(2) = g/L*sin(x(1));
```

Poincaré Map of the Stride Function

```
%=========================================================================
% Poincare Map of the ankle actuated model in a sagittal plane
%=========================================================================

function x2f = PM(x20)

td = 2;      % Enough time for completion of a double stance
ts = 5;      % Enough time for completion of a step

g = 9.81; m = 10; k = 8; L = 1; l = 0.2; alpha = pi/6;  % Parameter values
s = 2*L*sin(alpha);           % Stride length
```

```
%------------------------ Double stance phase -----------------------------

x10 = alpha; x20bc = x20;      % Initial value before collision
x20ac = x20bc*cos(2*alpha);    % Initial value after collision
x0 = [x10, x20ac];             % Initial state vector

options = odeset('RelTol',1e-6,'AbsTol',[1e-6 1e-6]);
[T,x] = ode45(@fd, [0 td], x0, options);  % Solve the eq of motions
x = real(x);
%--------------------------------------------------------------------------

%------------------------ Single stance phase -----------------------------

theta_ds = asin((L^2 + (s-l)^2 - (l+L)^2)/(2*(s-l)*L));
id = min(find (x(:,1) < theta_ds));

Tds = T(id-1) + (T(id) - T(id-1))*(theta_ds - x(id-1,1))/(x(id,1) - x(id-1,1));
                                          % Time when double stance phase ends
y10 =  x(id-1,1) + (x(id,1) - x(id-1,1))*(Tds - T(id-1))/(T(id) - T(id-1));
                      % Initial value of theta for single stance phase
y20 =  x(id-1,2) + (x(id,2) - x(id-1,2))*(Tds - T(id-1))/(T(id) - T(id-1));
                      % Initial value of d(theta)/dt for single stance phase

y0 = [y10, y20];       % Initial state vector for single stance phase
[T_s,y] = ode45(@fs, [Tds ts], y0, options); % Solve the eq of motions
%--------------------------------------------------------------------------

%------------------------ The whole step ----------------------------------
id_s = min(find (y(:,1) < - alpha)); % Index that makes theta = -alpha
Tss = T_s(id_s-1) + (T_s(id_s) - T_s(id_s-1))*(y(id_s-1,1)+alpha)/(y(id_s-1,1) -
y(id_s,1));    % Time at the end of one step in case of periodic motion
x2f =  y(id_s-1,2) + (y(id_s,2) - y(id_s-1,2))*(Tss - T_s(id_s-1))/(T_s(id_s) -
T_s(id_s-1));  % Final value of d(theta)/dt
%--------------------------------------------------------------------------
```

Time Response of the State Variables

```
%==========================================================================
% This code shows the time response of each state variables for specific
% initial velocity
%==========================================================================

clear all; close all;

td = 2;      % Enough time for completion of a double stance
ts = 5;      % Enough time for completion of a step

g = 9.81; m = 10; k = 8; L = 1; l = 0.2; alpha = pi/6;   % Parameter values
s = 2*L*sin(alpha);


eps = 0;
v0 = sqrt(k*((pi/2 + alpha)^2)/m/(1 - (cos(2*alpha))^2)) + eps;
                      % v0 = initial speed for fixed point of Poincare Map
```

```
%----------------------- Double stance phase ----------------------------

x10 = alpha; x20bc = - v0/L;          % Initial value before collision
x20ac = x20bc*cos(2*alpha);           % Initial value after collision
x0 = [x10, x20ac];                    % Initial state vector

options = odeset('RelTol',1e-6,'AbsTol',[1e-6 1e-6]);
[T,x] = ode45(@fd, [0 td], x0, options);     % Solve the equation of motion
x = real(x);
%------------------------------------------------------------------------

%----------------------- Single stance phase ----------------------------

theta_ds = asin((L^2 + (s-l)^2 - (l+L)^2)/(2*(s-l)*L));
id = min(find (x(:,1) < theta_ds));

Tds = T(id-1) + (T(id) - T(id-1))*(theta_ds - x(id-1,1))/(x(id,1) - x(id-1,1));
                                      % Time when double stance phase ends
y10 =  x(id-1,1) + (x(id,1) - x(id-1,1))*(Tds - T(id-1))/(T(id) - T(id-1));
                      % Initial value of theta for single stance phase
y20 =  x(id-1,2) + (x(id,2) - x(id-1,2))*(Tds - T(id-1))/(T(id) - T(id-1));
                      % Initial value of d(theta)/dt for single stance phase

y0 = [y10, y20];      % Initial state vector for single stance phase
[T_s,y] = ode45(@fs, [Tds ts], y0, options); % Solve the equation of motion
%------------------------------------------------------------------------

%----------------------- The whole step ---------------------------------
id_s = min(find (y(:,1) < - alpha));          % Index that makes theta = -alpha
Tss = T_s(id_s-1) + (T_s(id_s) - T_s(id_s-1))*(y(id_s-1,1)+alpha)/(y(id_s-1,1) -
y(id_s,1));           % Time at the end of one step in case of periodic motion
y2f =  y(id_s-1,2) + (y(id_s,2) - y(id_s-1,2))*(Tss - T_s(id_s-1))/(T_s(id_s) -
T_s(id_s-1));         % Final value of d(theta)/dt
%------------------------------------------------------------------------



for (i = 1:id-1)
   time(i) = T(i);
   z(i,1) = x(i,1);    % Angle
   z(i,2) = x(i,2);    % Time derivative of angle
end

for (i = id:id+id_s-2)
   time(i) = T_s(i-id+1);
   z(i,1) = y(i-id+1,1);    % Angle
   z(i,2) = y(i-id+1,2);    % Time derivative of angle
end

time(id+id_s-1) = Tss;
z(id+id_s-1,1) = -alpha;
z(id+id_s-1,2) = y2f;


figure(1);

subplot(2,1,1); plot(time, z(:,1)); grid on;
```

```
xlabel('time (s)'); ylabel('\theta (rad)');
subplot(2,1,2); plot(time, z(:,2),'c'); grid on;
xlabel('time (s)'); ylabel('d\theta/dt (rad/s)');

ff = abs(y2f) - abs(x20bc);

Fn_min = m*g*cos(-alpha) - m*(L*y2f)^2/L;
```

Eigenvalues of the Derivative Matrix of the Poincaré Map

```
%=========================================================================
% Stability Analysis by investigating the eigenvalues of
% the Derivative Matrix of the Poincare Map
%=========================================================================

clear all; close all;

g = 9.81; m = 10; k = 8; L = 1; l = 0.2; alpha = pi/6;      % Parameter values

v0f = sqrt(k*((pi/2 + alpha)^2)/m/(1 - (cos(2*alpha))^2));
                      % v0 = initial speed for fixed point of Poincare Map

x2fixed = -v0f/L;

x2v = x2fixed-0.3:0.01:x2fixed+0.3;

for (i = 1:length(x2v))
   x2f(i) = PM(x2v(i));
end

deriv_M = gradient(x2f, 0.01);

id = find(x2v == x2fixed);

eigen = deriv_M(id);
```

Behavior of a Small Neighborhood of the Fixed Point of the Poincaré Map

```
%=========================================================================
% Stability Analysis by investigating the behavior of a small neighborhood
% of the fixed point of the Poincare map
%=========================================================================

clear all; close all;


n = 5;          % No. of mapping

g = 9.81; m = 10; k = 8; L = 1; l = 0.2; alpha = pi/6;      % Parameter values

eps = 0.1;

v0f = sqrt(k*((pi/2 + alpha)^2)/m/(1 - (cos(2*alpha))^2));
               % v0f = initial speed for fixed point of Poincare Map
```

```
x2fixed = -v0f/L;

for (j = 1:7)

v0 = v0f + eps*(j-4);          % Initial speed

x20(1) = -v0/L;

    for (i = 1:n)
        x2f(i) = PM(x20(i));
        error(i,j) = x2f(i) - x2fixed;
        x20(i+1) = x2f(i);
    end
end

figure(1);
plot(error(:,1),'k'); hold on;
plot(error(:,2),'--b'); hold on;
plot(error(:,3),'-.c'); hold on;
plot(error(:,4),'g'); hold on;
plot(error(:,5),':b'); hold on;
plot(error(:,6),'--m'); hold on;
plot(error(:,7),'r'); hold on;
legend('\epsilon = -0.3','\epsilon = -0.2','\epsilon = -0.1','\epsilon =
0','\epsilon = 0.1','\epsilon = 0.2','\epsilon = 0.3')
grid on;
xlabel('Number of mapping'); ylabel('d\theta/dt - (d\theta/dt)_0 (rad/s)');
```

B.5. Balancing Using Ankle Torque in a Frontal Plane

Finding A and B Matrix using Linearization after Differentiating Equations of Motion

```
clear all; close all;

syms('theta0', 'theta1', 'theta2', 'theta1_prime', 'theta2_prime', 'J1', 'J2',
'alpha', 'gamma', 'T', 'm1', 'm2', 'g', 'rAC1', 'rC1B', 'rAB', 'rBC2', 'k', 'b');


% Equation 14
LHS_14_theta1_twoprime_coef = J1 - m1*rAC1*rC1B*cos(alpha+gamma) +
m1*rAB*rAC1*cos(gamma) + m2*rAB^2;

LHS_14_theta2_twoprime_coef = m2*rAB*rBC2*cos(theta1 + gamma - theta2);

RHS_14 = (T - m1*g*rC1B*sin(theta1+alpha+gamma) + (m1+m2)*g*rAB*sin(theta1+gamma)
+ k*(theta2-theta1-theta0) + b*(theta2_prime-theta1_prime) +
(m1*rAB*rAC1*sin(gamma))*theta1_prime^2 - [m2*rAB*rBC2*sin(theta1+gamma-
theta2)]*theta2_prime^2);


% Equation 15
LHS_15_theta1_twoprime_coef = m2*rAB*rBC2*cos(theta1+gamma-theta2);
```

```
LHS_15_theta2_twoprime_coef = J2+m2*rBC2^2;

RHS_15 = m2*rAB*rBC2*sin(theta1+gamma-theta2)*theta1_prime^2 +
rBC2*m2*g*sin(theta2) - k*(theta2-theta1-theta0) - b*(theta2_prime-theta1_prime);


% Equations to be linearized
theta1_twoprime = [RHS_14 -
LHS_14_theta2_twoprime_coef*RHS_15/LHS_15_theta2_twoprime_coef] /
[LHS_14_theta1_twoprime_coef -
LHS_14_theta2_twoprime_coef*LHS_15_theta1_twoprime_coef/LHS_15_theta2_twoprime_co
ef];

theta2_twoprime = [RHS_14 -
LHS_14_theta1_twoprime_coef*RHS_15/LHS_15_theta1_twoprime_coef] /
[LHS_14_theta2_twoprime_coef -
LHS_14_theta1_twoprime_coef*LHS_15_theta2_twoprime_coef/LHS_15_theta1_twoprime_co
ef];


% A matrix
diff_theta1_twoprime_theta1 = diff(theta1_twoprime, theta1);

diff_theta1_twoprime_theta1_prime = diff(theta1_twoprime, theta1_prime);

diff_theta1_twoprime_theta2 = diff(theta1_twoprime, theta2);

diff_theta1_twoprime_theta2_prime = diff(theta1_twoprime, theta2_prime);

diff_theta2_twoprime_theta1 = diff(theta2_twoprime, theta1);

diff_theta2_twoprime_theta1_prime = diff(theta2_twoprime, theta1_prime);

diff_theta2_twoprime_theta2 = diff(theta2_twoprime, theta2);

diff_theta2_twoprime_theta2_prime = diff(theta2_twoprime, theta2_prime);


A = [0 1 0 0; diff_theta1_twoprime_theta1 diff_theta1_twoprime_theta1_prime
diff_theta1_twoprime_theta2 diff_theta1_twoprime_theta2_prime; 0 0 0 1;
diff_theta2_twoprime_theta1 diff_theta2_twoprime_theta1_prime
diff_theta2_twoprime_theta2 diff_theta2_twoprime_theta2_prime];


% B Matrix
diff_theta1_twoprime_T = diff(theta1_twoprime, T);

diff_theta2_twoprime_T = diff(theta2_twoprime, T);


B = [0; diff_theta1_twoprime_T; 0; diff_theta2_twoprime_T];

% Change symbols to real numbers
% Multiple Substitutions.    subs(cos(a)+sin(b),{a,b},{sym('alpha'),2}) returns
cos(alpha)+sin(2)
% Symbols are 'theta0', 'theta1', 'theta2', 'theta1_prime', 'theta2_prime', 'J1',
'J2', 'alpha', 'gamma', 'T', 'm1', 'm2', 'g', 'rAC1', 'rC1B', 'rAB', 'rBC2', 'k',
'b'
A_value = subs(A, {theta0, theta1, theta2, theta1_prime, theta2_prime, J1, J2,
```

```
alpha, gamma, T, m1, m2, g, rAC1, rC1B, rAB, rBC2, k, b}, {0.41451, 0 ,-0.56524,
0, 0, 6.107, 3.744, 0.1974, 0.21711, 0, 44, 40, 9.81, 0.4966, 0.54545, 1.0198,
0.4, 86.556, 1})
% A_value_simple = simple(A_value)

B_value = subs(B, {theta0, theta1, theta2, theta1_prime, theta2_prime, J1, J2,
alpha, gamma, T, m1, m2, g, rAC1, rC1B, rAB, rBC2, k, b}, {0.41451, 0 ,-0.56524,
0, 0, 6.107, 3.744, 0.1974, 0.21711, 0, 44, 40, 9.81, 0.4966, 0.54545, 1.0198,
0.4, 86.556, 1});
B_double = double(B_value)
```

Investigating Controllability and Designing Controller

```
clear all; close all;

A = [0    1.0000        0        0;
     9.2676   -0.0472    0.7404    0.0472;
     0        0        0    1.0000;
     -2.0263    0.1524    3.6751   -0.1524];

B = [     0;
     0.0220;
          0;
    -0.0252];

C = [1 0 0 0;
     0 0 1 0];

D = zeros(2,1);

Controllability = ctrb(A,B);
r = rank(Controllability);

Q = eye(4);
R = eye(1);

sys = ss(A,B,C,D);
h = tf(sys);

[K,S,e] = lqr(sys,Q,R);
```

SimMechanics Model

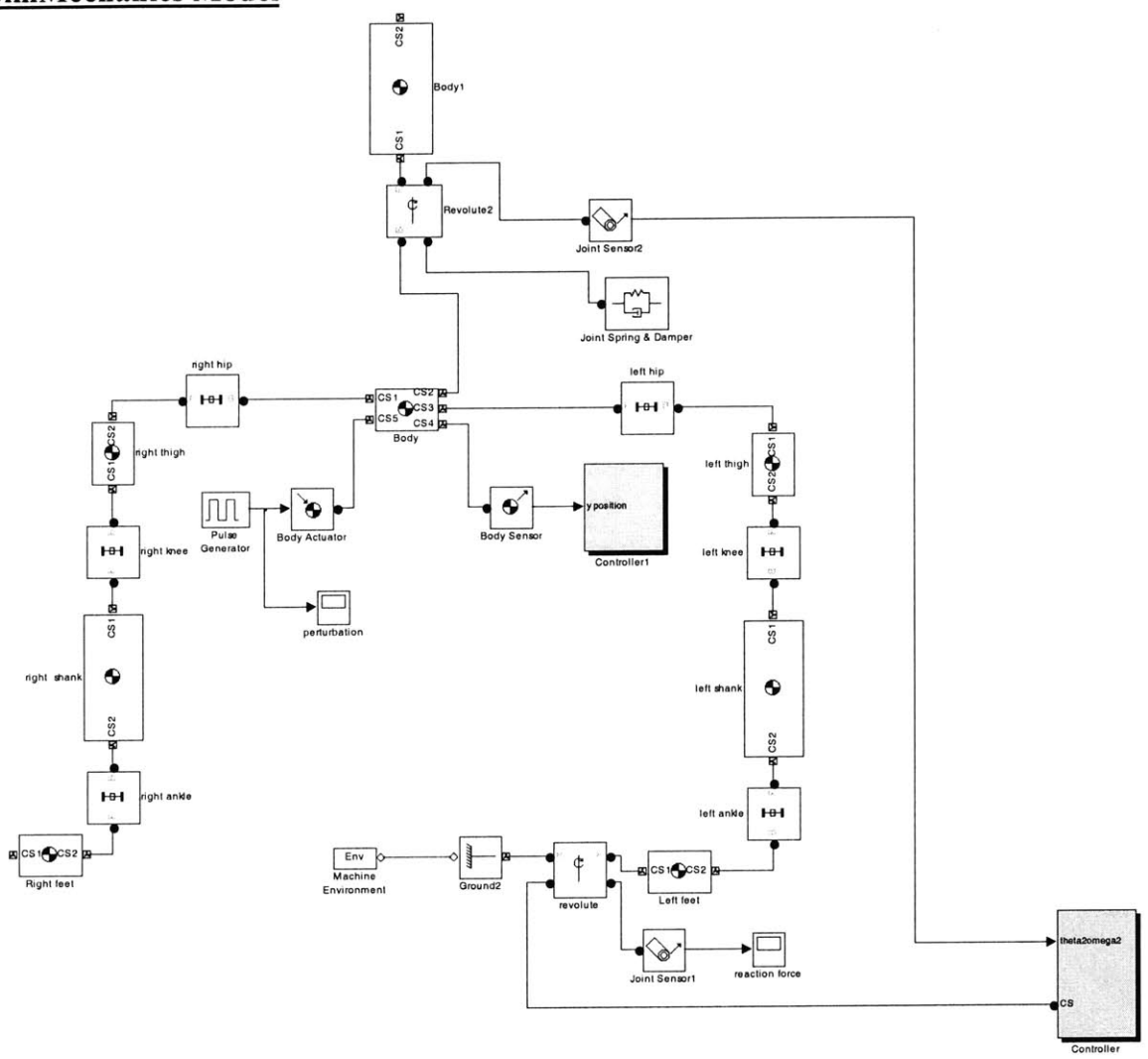

The Geometry of the Simulated Model

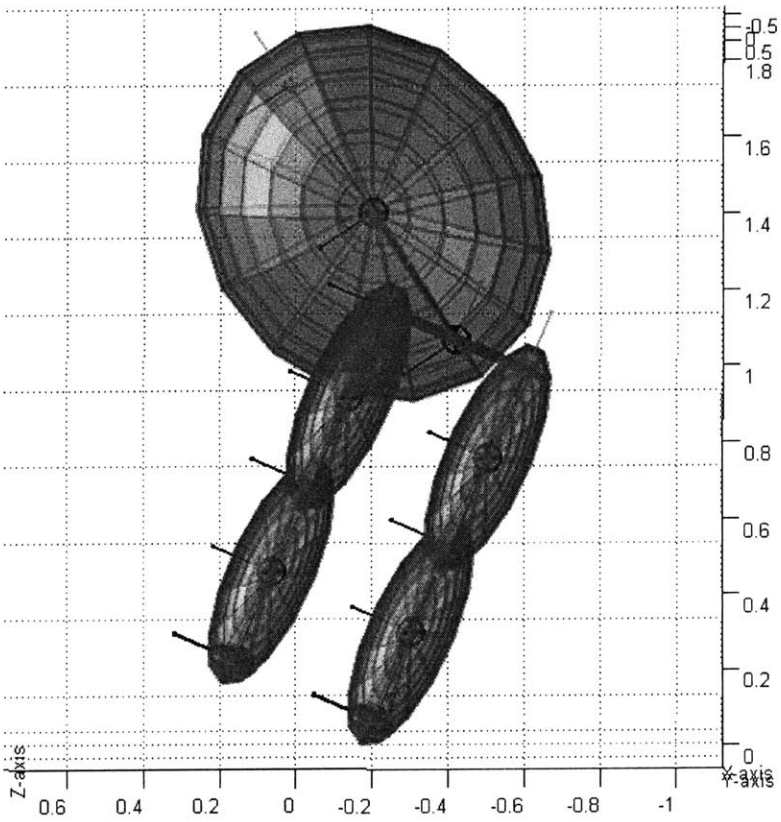

References

[1] A. E. Wall and J. M. Hidler, "Alterations in EMG patterns during robotic assisted walking," Springfield, MA, United States, 2004.

[2] J. Perry, *Gait Analysis*: SLAK Incorporated, 1992.

[3] D. A. Winter, *The Biomechanics and Motor Control of Human Gait*. Waterloo, Ontarion, Canada: University of Waterloo Press, 1987.

[4] S. Collins, A. Ruina, R. Tedrake, and M. Wisse, "Efficient bipedal robots based on passive-dynamic walkers," *Science*, vol. 307, pp. 1082-1085, 2005.

[5] S. P. Buerger, J. J. Palazzolo, H. I. Krebs, and N. Hogan, "Rehabilitation robotics: Adapting robot behavior to suit patient needs and abilities," Boston, MA, United States, 2004.

[6] H. I. Krebs, N. Hogan, M. L. Aisen, and B. T. Volpe, "Effect of learning and training in the post-acute stroke phase," Atlanta, GA, USA, 1996.

[7] H. Igo Krebs, N. Hogan, M. L. Aisen, and B. T. Volpe, "Robot-aided neurorehabilitation," *IEEE Transactions on Rehabilitation Engineering*, vol. 6, pp. 75-87, 1998.

[8] K. A. Jugenheimer, N. Hogan, and H. I. Krebs, "A robot for hand rehabilitation: A continuation of the MIT-MANUS neuro-rehabilitation workstation," Pittsburgh, PA, United States, 2001.

[9] D. J. Williams, H. I. Krebs, and N. Hogan, "A robot for wrist rehabilitation," Istanbul, Turkey, 2001.

[10] J. W. Wheeler, H. I. Krebs, and N. Hogan, "An ankle robot for a modular gait rehabilitation system," Sendai, Japan, 2004.

[11] T. McGeer, "Passive dynamic walking," *International Journal of Robotics Research*, vol. 9, pp. 62-82, 1990.

[12] J. Guckenheimer and P. Holmes, *Nonlinear Oscillations, Dynamical Systems, and Bifurcations of Vector Fields*, vol. 42. New York: Springer, 1983.

[13] M. J. Coleman, A. Chatterjee, and A. Ruina, "Motions of a rimless spoked wheel: A simple three-dimensional system with impacts," *Dynamics and Stability of Systems*, vol. 12, pp. 139-159, 1997.

[14] A. Ruina, "Nonholonomic stability aspects of piecewise holonomic systems," Calgary, Alta., Canada, 1998.

[15] J. I. Neimark and N. A. Fufaev, *Dynamics of Nonholonomic Systems*, vol. 33. Providence, Rhode Island: American Mathematical Society, 1972.

[16] P. L. Weiss, R. E. Kearney, and I. W. Hunter, "Position dependence of ankle joint dynamics. II. Active mechanics," *Journal of Biomechanics*, vol. 19, pp. 737-51, 1986.

[17] M. Mihelj, Z. Matjacic, and T. Bajd, "Ankle stiffness in response to disturbance in sagittal plane," Atlanta, GA, USA, 1999.

[18] R. A. Ottaviani, J. A. Ashton-Miller, and E. M. Wojtys, "Inversion and Eversion Strengths in the Weightbearing Ankle of Young Women," *The American Journal of*

Sport Medicine vol. 29, pp. 219-225, 2001.

[19] N. P. Whitehead, J. E. Gregory, D. L. Morgan, and U. Proske, "Passive mechanical properties of the medial gastrocnemius muscle of the cat," *Journal of Physiology*, vol. 536.3, pp. 893–903, 2001.

[20] J. Jeka, K. Oie, G. Schoner, T. Dijkstra, and E. Henson, "Position and Velocity Coupling of Postural Sway to Somatosensory Drive," *J Neurophysiol*, vol. 79, pp. 1661-1674, 1998.

[21] M. W. Gomes and A. L. Ruina, "A Wallking Model with No Energy Cost," 2004.

[22] M. Wisse, "Three additions to passive dynamic walking; actuation, an upper body, and 3D stability," Santa Monica, CA, United States, 2004.

[23] E. G. Gray and J. V. Basmajian, "Electromyography and cinematography of leg and foot (normal and flat) during walking," *The Anatomical Record*, vol. 161, pp. 1-15, 1968.

[24] T. A. McMahon, *Muscles, Reflexes, and Locomotion*. Princeton, NJ: Princeton University Press, 1984.